

STUDIES ON THE FORMATION OF DNA-LIPID COMPOSITES

By

Ms VIDYA RAMAKRISHNAN

PHYSICAL CHEMISTRY DIVISION
NATIONAL CHEMICAL LABORATORY
PUNE 411 008
INDIA

OCTOBER 2002

**STUDIES ON THE FORMATION OF
DNA-LIPID COMPOSITES**


**THESIS SUBMITTED TO
THE UNIVERSITY OF PUNE
FOR THE DEGREE OF
DOCTOR OF PHILOSOPHY
IN
CHEMISTRY**

BY

Ms VIDYA RAMAKRISHNAN

**PHYSICAL CHEMISTRY DIVISION
NATIONAL CHEMICAL LABORATORY
PUNE -411 008
INDIA**

OCTOBER 2002



Dedicated
to my
Family
and
Teachers

CERTIFICATE

This is to certify that the work discussed in the thesis entitled “**STUDIES ON THE FORMATION OF DNA–LIPID COMPOSITES**” by **Ms Vidya Ramakrishnan** for the degree of philosophy in chemistry was carried out under my supervision in the Physical Chemistry Division of National Chemical Laboratory, Pune. Such material as has been obtained by other sources has been duly acknowledged in this thesis. To best of my knowledge, the present work or any part thereof, has not been submitted to any other university for the award of any other degree or diploma

Date:

Dr. Murali Sastry

Place: Pune

(Research Co-guide)

CERTIFICATE

This is to certify that the work discussed in the thesis entitled “ **STUDIES ON THE FORMATION OF DNA–LIPID COMPOSITES**” by **Ms Vidya Ramakrishnan** for the degree of philosophy in chemistry was carried out under my supervision. As per my suggestions, the thesis work was carried out in the Physical Chemistry Division of National Chemical Laboratory, Pune. Such material as has been obtained by other sources has been duly acknowledged in this thesis. To best of my knowledge, the present work or any part thereof, has not been submitted to any other university for the award of any other degree or diploma.

Date:

Prof. S.F. Patil

Place: Pune

(Research Guide)

Acknowledgements

I wish to record my deep sense of gratitude to my research guide, Prof. S.F.Patil, Vice Chancellor, Bharati Vidya Peeth, Pune (former head of chemistry department, University of Pune) for his constant support and encouragement during the course of my research work.

I am greatly indebted to my co-guide, Dr. Murali Sastry, Physical Chemistry Division, National Chemical Laboratory, Pune for his inspiring guidance and critical evaluation at every phase of this dissertation. His tireless enthusiasm was always a source of inspiration. His constant support was invaluable and went a long way towards the completion of this thesis.

Words fail me in expressing my sincere thanks to you, mother, for your help and encouragement, towards the completion of this thesis. My special thanks to my dear husband and my loving daughter; Akshatha, who were extremely patient and tolerant towards my erratic hours of work and their continued support has seen me through my thesis. I owe my very special thanks to my aunt and uncle who were always there when I needed them the most. My sincere thanks to my in-laws who have helped me in some way or the other.

It gives me great pleasure to thank Dr. K.N.Ganesh, head, organic synthesis division, National Chemical Laboratory, for his valuable suggestions and making all the facilities available for the DNA characterization.

I wish to thank Dr.P.Ganguly and Dr. S.K.Date, former and present Heads, Physical Chemistry Division, for their constant support and encouragement.

I also wish to thank Prof Mali and Prof. Rao, former and present Heads, Chemistry Department, University of Pune, for their constant support and encouragement. I also wish to place on record my sincere thanks to Drs. (Ms) Joshi, and Rajurkar for all their support.

My sincere thanks to Dr. Gopinathan for the FTIR characterization.

A very special mention of thanks goes to Mrunalini Pattarkine (Leena), my friend and former colleague at NCL for a sound briefing on the subject and getting me familiarized with all sophisticated characterization techniques. My heartfelt thanks to my friend and colleague, Moneesha D'Costa, for her untiring and continued support during my thesis work. Her timely help and friendship shall always be remembered. Thank-you.

My heartfelt thanks to my senior, Anand Gole, who has gone out of his way in getting me familiarized with all the lab facilities and making me feel at home during my initial days of Ph.D. I would like to take this opportunity to thank all my lab mates who have helped me in all possible ways and have been my extended family during the tenure of my work at NCL. Thank-you, Ashavani, Saikat, Sumant, Debabrat, Chinmay Damle, Kannan, Shankar, Anita, Chinmay Soman, Madhu, Neeta, Jaspreet. A special mention of thanks to my friends . Thank-you Priya, Pallavi, Reddy, Rohini, Dinesh.

Working under a single roof, it was a pleasant company of Ms. S. Adyanthaya who has always helped me in one-way or the other. I would also like to thank Ms Anita for all the help and support she gave me.

I owe a very special thanks to Dr. (Ms) Vasantha Shivaramakrishnan and her family for all their continued support and constant encouragement.

I'm grateful to Dr P. Ratnaswamy and Dr. S. Sivaram, former and present directors of NCL, Pune for giving me the opportunity to work in this institute and making all the facilities available for my research work.

My thanks are duly acknowledged to CSIR, New Delhi for their valuable support in the form of a Senior Research Fellowship.

TABLE OF CONTENTS		Page Nos
CHAPTER I: Introduction		1
1.1.	Molecular Craftwork With DNA	2
1.2.	Brief Structure Of DNA/PNA	4
1.3.	Forces Responsible For Stabilizing DNA/PNA	12
1.4.	DNA-Lipid Studies (need for immobilization)	13
1.5.	The Method Described In This Thesis	17
1.6.	References	19
 CHAPTER II: Experimental Techniques		 24
2.1.	Introduction	25
2.2.	Thermal Evaporation Of Fatty Lipids	26
2.3.	Synthesis Of Oligonucleotides and PNA Oligomers	27
2.4.	Langmuir-Blodgett (LB) Technique	29
2.5.	Quartz Crystal Microgravimetry	31
2.6.	Uv- Visible Spectroscopy	34
2.7.	Uv-Melting (T_M) Studies	35
2.8.	Fluorescence Spectroscopy	37
2.9.	Fourier Transform Infrared Spectroscopy (FTIR)	38
2.10.	X-ray Photoelectron Spectroscopy (XPS)	41
2.11.	Circular Dichroism (CD)	42
2.12.	Ellipsometry	44
2.13.	Contact angle measurements	47
2.14.	References	47

CHAPTER III: Immobilization and Hybridization		51
of DNA at the air - water interface		
3.1.	Introduction	52
3.2.	DNA Hybridization At Air-Water Interface	53
3.3.	Pressure-Area Isotherms and QCM measurements	57
3.4.	Fluorescence Studies	60
3.5.	FTIR Studies	62
3.6.	UV-Melting Studies	63
3.7.	Polarized UV-Vis Spectroscopy	63
3.8.	Conclusions	65
3.9.	Salt induced Hybridization of DNA by sequential immobilization of Oligonucleotides in the presence of ODA Monolayers at the air-water interface.	65
3.10.	Immobilization of pre-formed DNA (dsDNA) hybrids (with/without salt) complexed with ODA monolayers at the air-water interface	73
3.11.	Salt induced Hybridization of DNA by Sequential and pre-formed Immobilization of Oligonucleotides in the presence of DOTAP monolayers at the Air-Water Interface	75
3.12.	Conclusion	78
3.13.	Summary	78
3.14.	References	79
CHAPTER IV: Studies related to the hybridization of encapsulated DNA in cationic lipid films		82
4.1.	Introduction	83
4.2.	Entrapment and <i>in-situ</i> hybridization of DNA in thermally evaporated cationic fatty lipid films	83

4.3.	Quartz Crystal Microgravimetry	85
4.4.	Contact Angle Measurement	91
4.5.	Test Of Hybridization : Fluorescence Studies	92
4.6.	DNA Structural Studies	94
4.7.	XPS Studies	95
4.8.	UV-Melting Measurements	97
4.9.	Conclusions	98
4.10.	Studies Related To The Electrostatic Entrapment and Thermal Stability of Pre-formed DNA Duplexes of Different Lengths Within Thermally Evaporated Cationic Lipid Films	98
4.11.	Summary	102
4.12.	References	103
	CHAPTER V: Formation of PNA-DNA Hybrids with Octadecylamine molecules	106
5.1.	Introduction	107
5.2.	Sequential Entrapment Of PNA and DNA in Lipid Bilayers Stacks	109
5.3.	Quartz Crystal Microgravimetry	111
5.4.	UV-melting (T_M) Studies	113
5.5.	Conclusions	114
5.6.	PNA-DNA Hybridization at the Air-Water Interface with Langmuir Monolayers	114
5.7.	Pressure-Area Isotherms and QCM Measurements	116
5.8.	UV-melting studies of LB films of ODA-DNA- PNA	119
5.9.	Conclusion	121
5.10.	Summary of the Work	121
5.11.	References	122

	CHAPTER VI: Phase transfer of DNA by interaction with cationic surfactant molecules at the liquid / liquid interface	125
6.1.	Introduction	126
6.2.	UV-visible Measurements	129
6.3.	Fluorescence Studies	131
6.4.	UV – Melting Measurements	134
6.5.	FTIR Studies	135
6.6.	Chemical Analysis from XPS	136
6.7.	Conclusions	138
6.8.	References	139
	CHAPTER VII: Conclusions	140
7.1.	Summary of the Whole Work	141
7.2.	Future Prospects (application of the present work)	142

LIST OF PUBLICATIONS

CHAPTER I

INTRODUCTION

It's one small step for DNA, one vast leap for nanotechnology.

-----Professor Nadrian Seeman
BBC News Online.

This chapter begins with some introductory remarks on the magnitude and significance of interdisciplinary kind of work in today's research. A general overview on structural aspects of DNA and its analogues (PNA) are also discussed. The need and importance of DNA-lipid interactions is mentioned. Furthermore, the different protocols used for the immobilization of DNA and PNA is also discussed in this chapter. The chapter ends with the description on the method employed for the immobilization of DNA/PNA for the thesis work.

1.1. MOLECULAR CRAFTWORK WITH DNA

Deoxyribonucleic acids (DNA) are important as a source of biological information depending on the base sequences. Studies utilizing DNA as *programmable assemblers* is a young and rapidly increasing research field located at the crossroads of material research, nanosciences and molecular nanobiotechnology.¹ There are currently several fields driving towards the creation and use of nucleic acids for both biological and non-biological applications. These converging areas: (i) the miniaturization of biosensors and biochips into the nanometer scale regime, (ii) the fabrication of nanoscale objects that can be placed in intracellular locations for monitoring and modifying cell function, (iii) the replacement of silicon devices with nanoscale molecular based computational systems, and (iv) the application of biopolymers in the formation of novel nanostructured materials with unique optical and transport properties.

The high predictable hybridization chemistry of DNA, the ability to completely control the length and content of oligonucleotides and the wealth of enzymes which is a complete toolbox of high specific bimolecular reagents, such as endonucleases, ligases and other DNA modifying enzymes that allow the processing of DNA material with atomic precision and accuracy on Angstrom level, make the use of DNA as an attractive candidate for all the above mentioned applications.

As an example, the work of Seeman et al indicates that DNA can be used to synthesize nanostructured scaffoldings,^{2c,d} surface architecture,^{2c,f} and even nanomechanical devices.^{2a, b} Seeman and co-workers were the first to exploit DNA's molecular recognition properties to design complex mesoscopic structures solely on DNA.^{2g,h} They prepared branched junctions that serve as building blocks for more complex two and three dimensional DNA structures.^{2a, b}

DNA-Based computation appears at this time to be the simplest way of implementing molecular computation.³ The idea is to use the vast numbers of molecules present in a solution to perform many operations in parallel. There are many different ways that this can be realized, one of the most popular being, computation by algorithmic self-assembly process.^{3b} It is possible to do computation by self-assembly of DNA tiles indicating that it is

possible to use DNA components to do algorithmic assembly, in addition to periodic assembly.

Mirkin et al ^{4e} and other workers ⁵ have demonstrated that superstructures of bioconjugates of DNA formed with gold nanoparticles could be formed by hybridization of complementary base sequences in the gold surface bound DNA molecules. From a more fundamental point of view, Mirkin et al have used this strategy to critically study the role of interparticle separation and aggregate size on the optical properties of DNA –modified colloidal Gold solution.^{4c} This strategy can be used for simple and economically viable sensors in biomedical diagnostics, for example for the detection of nucleic acids from pathogenic organism. Several analytical applications that allow the detection of nucleic acids in homogenous solutions have already been reported.^{4 a- b, 6} Mirkin et al have developed new methods for the constructing and evaluating two-dimensional molecular based nanostructures. This effort involves the use of scanning probe instruments (AFM and STM) to generate well-defined patterns of soft molecule -based materials. These structures allow us to ask and answer key questions in the area of molecule-based electronics and nanotechnology.^{4d}

One aspect of nanoscale self-assembly that remains relatively unexplored is the organization of nanoparticles into predefined, topologically intricate structures. An attractive alternative to the more popular lithographic⁷ and masking⁸ procedures to achieve nanoparticle patterning is the use of biological templates for assembling nanoparticles.⁹ DNA molecules, in particular, are being investigated as exciting templates for the assembly of nanoparticles and generation of quantum wires.¹⁰ The cylindrical double-helical structure of DNA molecules together with capability of the negatively charged DNA phosphate groups to bind metal cations/charged nanoparticles make them ideal templates for growing nanowires by stringing together metal nanoparticles.^{10a-c} The formation of rings of nanoparticles using circular plasmid DNA^{10a} and DNA-streptavidin “nanocircle” conjugates¹¹ is an exciting application with considerable potential for development.

One more area that has progressed by leaps and bounds is the field of gene therapy. Success of gene therapy is largely dependent on the development of carrier system(s) capable of delivering genes into the target cells. Among the different delivery strategies, cationic – lipid based gene carriers have recently gained great interest as non-viral vectors in cell fusion studies.¹²

The future development of joint venture between biotechnology and material science will profit from the rapid current advances in chemistry as a central science. In addition, the current genome and proteome research will also be beneficial for this field, since it provides data that will allow us to produce even more suitable bio components.

We are not very far from the fabled autonomous nanomachines that heal wounds and perform surgery in living organism.

"All of the DNA-based self-assembly molecules we have created before now are static. Now it's time to have control over the motion, not just the shape. The ultimate uses of this new molecule will be in the analytical, in the laboratory, and also technological. Ultimately we will be able to make small nanomachines that can do molecular manufacturing and then step up to nanorobots."

----- **Prof. N.C. Seeman**

Scientists in New York (Seeman et al) have created a nanometer-sized moving arm from synthetic DNA. This kind of mechanical device, which operates on a molecular scale, is seen as the precursor for nano-robots, which will manufacture or repair molecules, possibly within the human body.¹³ The new device, reported in Nature, has two rigid DNA arms linked by a special piece of DNA. This helix in this special piece winds in the usual direction, right-handed.

1.2 BRIEF STRUCTURE OF DNA/PNA

1.2.1 DISCOVERY OF DNA:

The idea that genetic material is nucleic acid had its roots in the discovery of transformation by Griffith in 1928.¹⁴ Frederick Griffith, a British microbiologist who discovered a phenomenon called transformation—meaning an alteration of hereditary characteristics—in the *Streptococcus pneumoniae* bacterium. Griffith's work paved the way for later experiments, which proved that deoxyribonucleic acid (DNA) is the material within cells that passes on genetic traits. *He is considered by some to be the father of molecular biology.*

During the 1940s, American geneticist Oswald T. Avery sought to determine the nature of the transforming substance proposed by Griffith.

“When alcohol reaches a concentration of about 9/10 volume, there separates out a fibrous substance which on stirring, the mixture wraps itself about the glass rod like thread on a spool and the other impurities stay behind as a granular precipitate. The fibrous material is redissolved and the process repeated several times. In short, this substance is highly reactive and on elementary analysis confirms very closely to the theoretical values of pure DNA (who could have guessed it).”

---- Oswald Avery, 1944

Together with his colleagues, Colin MacLeod and Maclyn MacCarty, Avery proved that it was DNA, not other potential contenders such as ribonucleic acid (RNA) or protein, that caused the R strain to acquire the virulent characteristics of the S strain and to transmit those characteristics to subsequent generations of bacteria. This result led to further experiments in the 1950s that clearly established DNA as hereditary material. *Thus these two experiments proved that DNA is the genetic material.*

Deoxyribonucleic Acid (DNA), genetic material of all cellular organisms and most viruses. DNA carries the information needed to direct *protein synthesis* and *replication*. Protein synthesis is the production of the proteins needed by the cell or virus for its activities and development. Replication is the process by which DNA copies itself for each descendant cell or virus, passing on the information needed for protein synthesis. In most cellular organisms, DNA is organized on chromosomes located in the nucleus of the cell.

1.2.2. COMPONENTS OF DNA

A molecule of DNA consists of two *chains*, strands composed of a large number of chemical compounds, called nucleotides, linked together to form a chain. These chains are arranged like a ladder that has been twisted into the shape of a winding staircase, called a double helix. Each nucleotide consists of three units:

- 1) A pentose sugar (a five carbon sugar in ring form)
- 2) A nitrogenous base (purine or pyrimidine base)
- 3) An esterified phosphoric acid moiety.

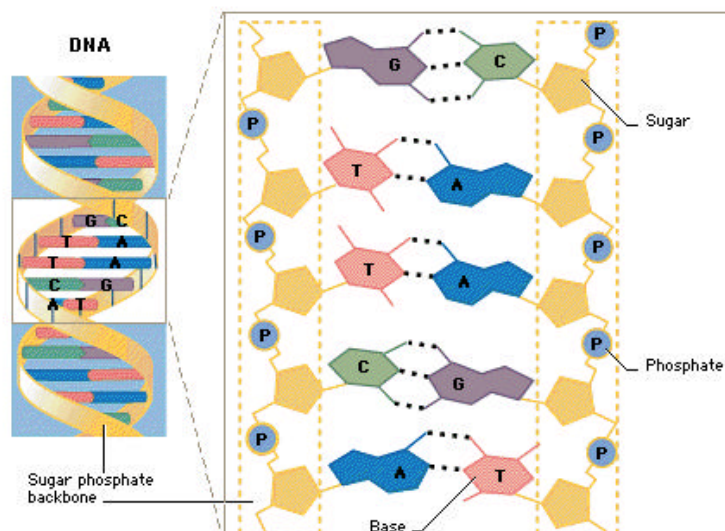


Figure 1.2.2.1: A DNA molecule consisting of a ladder, formed of sugars and phosphates, and four nucleotide bases: adenine (A), thymine (T), cytosine (C), and guanine (G).

The sugar is either ribose or deoxyribose, distinguishing the nucleic acid into two major groups. Ribonucleic acid (RNA) has its sugar D-ribose in the furanose configuration, whereas DNA, as its name implies, has D- 2-deoxyribose, also, in the furanose configuration.

The nitrogenous bases fall into two types, namely purines and pyrimidines. Pyrimidines have a six- membered ring; purines have fused five – and six – membered rings. Each nucleic acid contains four types of base. The four bases are adenine (A), guanine (G), (purines) and thymine (T), and cytosine (C) (pyrimidines).

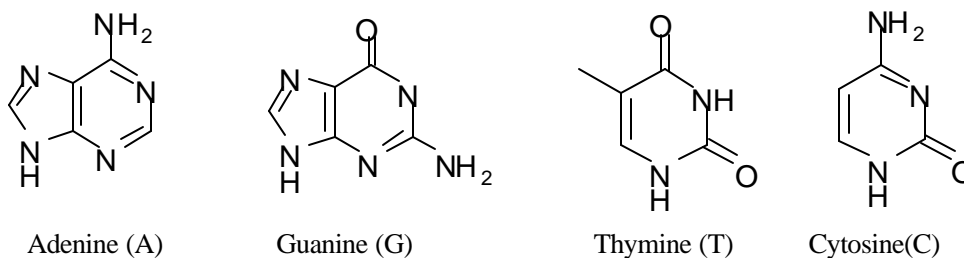


Figure. 1.2.2.2. Diagram showing the nitrogenous bases in nucleic acids. The purines, adenine (A) and guanine (G) and the pyrimidines, thymine (T) and cytosine (C) are depicted in the figure.

A base linked to a sugar is called a **nucleoside** ; when a phosphate group is added, the base –sugar –phosphate is called a **nucleotide**. Nucleotides provide the building blocks from which nucleic acids are constructed. The deoxyribose molecule occupies the center position in

the nucleotide, flanked by a phosphate group on one side and a base on the other. The phosphate group of each nucleotide is also linked to the deoxyribose of the adjacent nucleotide in the chain. The 5' position of one pentose ring is connected to the 3' position of the next pentose ring via a phosphate group. It is conventional to write nucleic acid sequences in the 5' - 3' direction – that is, from the 5' at the left to the 3' at the right. The terminal nucleotide at one end of the chain has a free 5' group; the terminal nucleotide at the other end has a free 3' group.

1.2.3. DNA IS A DOUBLE HELIX

The observation that the bases are present in different amounts in the DNA's of different species led to the concept that the *sequence of bases is the form in which genetic information is carried*.

In 1953 American biochemist James D. Watson and British biophysicist Francis Crick published the first description of the structure of DNA. Their model proved to be so important for the understanding of protein synthesis, DNA replication, and mutation that they were awarded the 1962 Nobel Prize for physiology or medicine for their work.



Photograph 1.2.3.1: Picture showing James Watson, *left*, and Francis Crick, *right*, describing the structure of the DNA molecule as a double helix, somewhat like a spiral staircase with many individual steps.

Three notions converged in the construction of the double helix model for DNA by Watson and Crick :

- X-ray diffraction data showed that DNA has the form of a regular helix, making a complete turn every 3.4 nm, with a diameter of 2nm. Since the distance between adjacent nucleotides is 3.4 nm, there must be 10 nucleotides per turn.
- The density of DNA suggests that the helix must contain two polynucleotide chains. The constant diameter of the helix can be explained if the bases in each chain face inward and are restricted so that a purine is always opposite a pyrimidine.
- Irrespective of the actual amounts of each base, the proportion of G is always the same as the proportion of C in DNA, and the proportion of A is always the same as that of T. Thus the composition of any DNA can be described by the proportion of its bases that is G+C, which ranges from 26% to 74% for different species.

J.Watson and F.Crick reconciled the properties of uniform structure and diverse genetic function when they conceived their now well –known model for DNA structure, *the most influential model of a biological molecule ever constructed.*

The nucleotides in one DNA strand have a specific association with the corresponding nucleotides in the other DNA strand. Because of the chemical affinity of the bases, nucleotides containing adenine are always paired with nucleotides containing thymine, and nucleotides containing cytosine are always paired with nucleotides containing guanine. The complementary bases are joined to each other by weak chemical bonds called hydrogen bonds.

Watson and Crick proposed that the two polynucleotide chains in the double helix associate by hydrogen bonding between the nitrogenous bases.

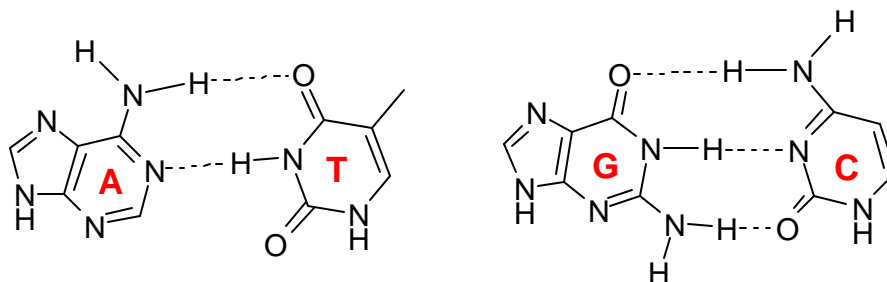


Figure.1.2.3.1. Diagram showing the complementary base pairing involving the formation of two hydrogen bonds between A and T and of three hydrogen bonds between G and C. No other pairs form in DNA.

Fig. 1.2.3.1 demonstrates that, in their usual forms, Guanine (G) can hydrogen bond specifically only with Cytosine (C) while Adenine (A) can hydrogen bond specifically only with Thymine (T). These reactions are described as **base pairing** and the paired bases (G with C, or A with T) are said to be **complementary**.

The model requires the two polynucleotide chains to run in opposite directions (antiparallel), as illustrated in fig 1.2.3.2. Looking along the helix, therefore, one strand runs in the 5'-3' direction and the other strand runs in 3'-5' direction.

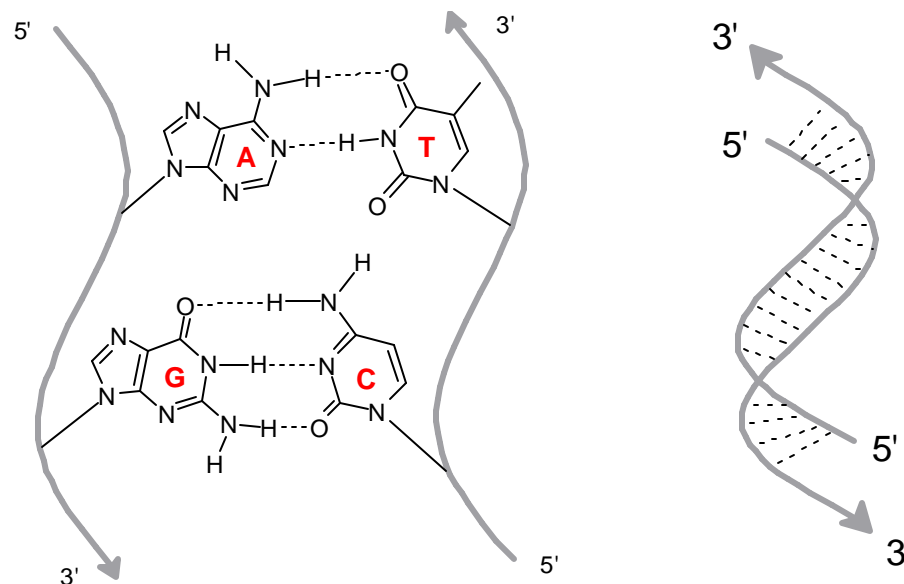


Figure.1.2.3.2. : Diagram showing the two polynucleotide chains running in opposite directions (antiparallel). One strand runs in the 5'-3' direction and the other strand runs in 3'-5' direction.

The sugar – phosphate backbone is on the outside and carries negative charges on the phosphate groups. The bases lie on the inside. They are flat structures, lying in pairs perpendicular to the axis of the helix. Proceeding along the helix, bases are stacked above one another, in a sense like a pile of plates.

1.2.4. CHEMICAL STRUCTURE OF PEPTIDE NUCLEIC ACID (PNA)

Since the investigation of oligonucleotides as potential therapeutics that target nucleic acids was initiated,¹⁵ the search for nucleic acid mimetics with improved properties such as strengthened binding affinity to complementary nucleic acids, increased biological stability and improved cellular uptake has accelerated rapidly. Also, studies of DNA analogues and mimics help us to understand more on the structure, stability and molecular recognition properties of DNA. In the last few years, attempts to optimise the properties of oligonucleotides have resulted in the synthesis and analyses of a huge variety of new oligonucleotides derivatives with modification to the phosphate group, the ribose or the nucleobase.¹⁶

In a pioneering report, Nielsen and co-workers demonstrated that the entire sugar-phosphate backbone in DNA could be replaced by an N-(2-aminoethyl) glycine based polyamine structure and that the DNA bases could be attached to the peptide backbone yielding a class of molecules known as peptide nucleic acids (PNA).¹⁷

PNA was originally designed and developed as a mimic of a DNA-recognizing, major-groove-binding, triplex forming oligonucleotide.^{17d-f} The concept was to mimic an oligonucleotide binding to double stranded DNA via Hoogsteen base pairing in the major groove.¹⁷ Thus the nucleobases of DNA were retained, but the deoxyribose phosphodiester backbone of DNA was replaced by a pseudo-peptide backbone that according to computer building was homomorphous with the DNA backbone.

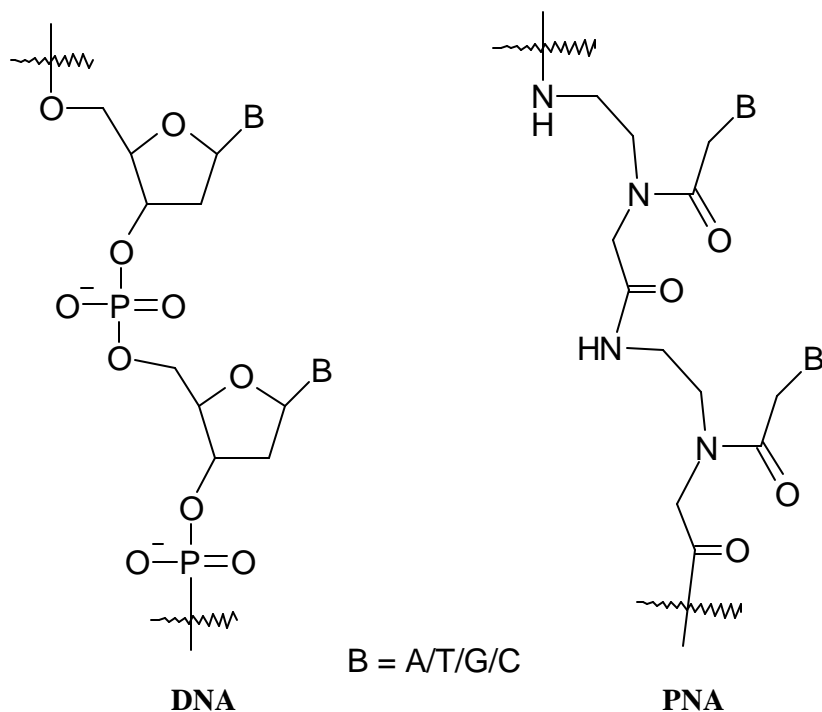


Figure .1.2.4.1. Chemical structures of a DNA molecule and a PNA molecule.

The structure of PNA is remarkably simple consisting of repeating N-(2-aminoethyl)-glycine units linked by amide bonds. The purines (A,G) and pyrimidine (C,T) bases are attached to the backbone through methylene carbonyl linkages. Unlike DNA or DNA analogs, PNA do not contain any pentose sugar moieties or phosphate groups. By convention, PNAs are depicted like peptides, with the N-terminus at the first (left) position and the C-terminus at the right. The backbone of PNA is acyclic, achiral and neutral. PNAs can bind to complementary nucleic acids in both antiparallel and parallel orientation.

However, the antiparallel orientation is strongly preferred, and the parallel duplex has shown to have a different structure.

Three-dimensional structures have been determined for the major families of PNA families. Two duplex structures, a hexamer PNA-RNA duplex¹⁸ and an octamer PNA-DNA duplex¹⁹ were solved by NMR methods while a decamer PNA₂-DNA²⁰ triplex and a PNA-RNA duplex²¹ were solved by X-ray crystallography. These structures clearly demonstrated that the PNA has the flexibility enabling adaptation to the A- and B-form helices preferred by RNA or DNA. These results clearly show that PNA prefers to adopt a helical conformation named the 'P' form that is distinctly different from other nucleic acid helices.^{20,21} The 'P' form is a much wider helix (28 Å) and more slowly winding helix (18 base pair pitch).

1.2.4.2. CHEMICAL AND PHYSICAL PROPERTIES OF PNA

Chemical Stability:

With the exception of the nucleobases, PNAs and DNA have no functional groups in common as a result of which the chemical stability is completely different for both the molecules. DNA depurinates on treatment with strong acids while PNAs are completely acid stable. PNAs are also sufficiently stable to weak bases.^{15a}

Binding Affinity:

The neutral character of the PNA backbone is an important feature that has many consequences. One of the most impressive is the high binding affinity of PNA to complementary DNA sequences. The strongest binding affinity is to PNA itself.^{15a}

Duplex Formation:

PNAs obey the Watson-Crick base pairing rules on hybridization with complementary DNA and RNA.²² As mentioned in the above section; in contrast to DNA they can, however bind in both the parallel and antiparallel orientation, whereby the PNA C-terminus corresponds to the 3' end, and the N-terminus to the 5' end of normal oligonucleotides. The antiparallel orientation is favored. Antiparallel PNA . DNA hybrids are considerably more stable than the corresponding DNA-DNA complexes.

Ionic Strength:

The stability of PNA-DNA duplexes is almost unaffected by the ionic strength of the medium in contrast to the behavior of DNA double helical structures.²³ In a careful study by Tomac et al.,^{23b} the melting transition temperature (T_m) of DNA-DNA hybrids was shown to increase considerably with increasing salt concentration (0.01 to 0.5M NaCl), whereas the T_m of PNA-DNA duplexes is almost identical at 0.5 M. The contrasting effect of ionic strength on duplex formation can be explained by the association of counter ions in the case of DNA-DNA duplex formation and by the displacement of counter ions in the case PNA-DNA hybrid formation.

Biological aspects of PNA:

Although numerous reports have appeared on translation inhibition by antisense oligonucleotides, there are remarkably few studies of PNA oligomers as antisense agents.²⁴ PNAs exhibit high resistance to Dnases and proteinases making them highly biostable.

Consequently, these favorable properties of PNA have attracted wide attention in medicinal chemistry for development of gene therapeutic (antisense and antigene) drugs²⁶ and in molecular diagnostics.^{17a} Potential therapeutic applications for PNAs arise from their biological properties described above. The sequence – specific inhibition of replication (antigene agents), transcription and translation (antisense agents) could be potentially exploited for therapeutic applications. The excellent hybridization properties of PNA has allowed the development of several techniques for isolation and detection of nucleic acids for analysis in genetic diagnostics.²⁷

1.3. FORCES RESPONSIBLE FOR STABILIZING DNA/PNANoncovalent interactions stabilize DNA:

All nucleic acid helices are stabilized by hydrogen bonding and base stacking interactions.^{14, 28} A single stranded nucleic acid can form a stable single stranded helix without any base pairing partners if its nucleotide bases are proficient at stacking. Double and Triple stranded helices (which can be formed either intra- or intermolecularly) are stabilized both by base stacking and by hydrogen bonding.

The base pairs contribute to the thermodynamic stability of the double helix in two ways. Energy is released by the formation of base pairs and by interaction between adjacent base pairs.

- ❖ Hydrogen bonding between the bases in each pair releases energy corresponding to 3 bonds per G. C pair and 2 bonds per A. T pair.
- ❖ Hydrophobic base – stacking results from interactions between the electron systems of the stacked base pairs. Each base pair is involved in two such interactions, one with the other base pair on each side.

Hydrogen bonding:

Hydrogen bonding can be considered chiefly an electrostatic interaction between an acidic proton and a good electron donor. Hydrogen bonding is only of the two most important interactions, which stabilizes the double helical structure. Recognition of natural DNA usually requires complementary hydrogen –bonding groups.

Base Stacking:

It has been recognized for some time that base stacking is as crucial to stabilization of DNA helices as hydrogen bonding is. Aromatic π π stacking occurs largely between bases

within one strand of the helix, although because of the helical twist there is also a contribution of stacking between bases in opposite strands of a duplex. *What specific interactions contribute to base stacking?* Although quite a number of theoretical analyses of base stacking have been carried out, very few experimental studies of stacking in nucleic acids exist. Several factors, including dispersion forces, dipole-induced dipole interactions,²⁹ solvophobic effects, and electrostatics all may play a role in base stacking and only recently has the relative importance of these factors begun to be experimentally examined in duplex DNA.³⁰

Electrostatic Effects:

Aside from hydrogen bonding, by far the most important electrostatic factor in DNA helix formation is the repulsion of negative charge on phosphate between strands forming a double (or higher) helix. This is largely an enthalpic effect, which becomes a destabilizing factor in the final complex (depending on ionic strength).³¹ A number of molecular strategies for lowering this repulsion in DNA have been realized in recent years; for example, an oligonucleotide could be modified to carry an uncharged^{17f} or even a positively charged backbone,³² thus leading to lowered or eliminated electrostatic repulsion or even attraction between the oligonucleotide and its target.

1.4. DNA-LIPID STUDIES (need for immobilization)

1.4.1. NEED FOR DNA-LIPID STUDIES

There are few areas of biomedical research that have moved so rapidly or have so completely captured the imagination of the scientific community as the field of gene therapy.^{33, 34} Gene therapy can be defined as the introduction of nucleic acids into cells for the purpose of altering the course of a medical condition or disease.³⁵ The progress in this field has been incremental. This phenomenal success surely reflects the enormous potential of this approach for correction of genetic disease. Success of gene therapy is largely dependent on the development of carrier system(s) capable of delivering genes into the target cells.

Vehicles for Gene transfer: The major classes of vehicles for gene transfer are:

1. Viral Vectors
2. Non-Viral Vectors

Some researchers believe that viruses will be most successful because they have evolved for millions of years to become efficient vesicles for transferring genetic material into cells. But results from both preclinical and clinical studies show that although viral vectors are very efficient in transferring genes into cells, they suffer from many problems. Viral vectors all induce an immunological response to some degree & may have safety risks (such as insertional mutagenesis & toxicity problems). Furthermore their capacity is limited & large-scale production may be difficult to achieve.

Non-viral vectors have become a reliable, alternate vehicle for targeting specific genes into cells due to their lack of immunogenicity, potential for tissue – specific targeting, relative safety and ease of large-scale production. There are three methods of non-viral DNA transfer. Namely:

- Plasmid DNA
- Liposome
- Molecular conjugates

Among the different delivery strategies, cationic – lipid based gene carriers have recently gained great interest as non-viral vectors in cell fusion studies.¹²

1. 4. 2. CATIONIC LIPID BASED GENE CARRIERS

Cationic lipid based gene carriers represent a multicomponent, self-assembly system that forms supramolecular structure through electrostatic interactions between negatively charged DNA molecules and positively charged cationic lipids. Much attention has been paid recently to the effects of buffer and ionic strengths upon the binding of DNA with cationic lipids, since these complexes can serve as efficient agents for transfection of eukaryotic cells.³⁶ Synthesis and structure-activity relationships of novel cationic lipids for DNA transfer have received much attention recently.³⁷ Cationic lipid complexes have been widely used for the delivery of genes into mammalian cells and currently they are also being tested for clinical trials.^{37b}

Transfection Process: The cationic lipid complexes play a role in each step of the transfection process. The stage in which the lipid and DNA dissociate is not yet clear.

- ❖ The first step in the transfection is the formation of DNA –lipid complex.
- ❖ Entry of the DNA –lipid complex into cells (mainly by endocytosis, fusion, and incorporation through membrane pores).
- ❖ The last step in the transfection process is the entry of DNA-lipid complex into the nucleus and the expression of the DNA.

Among the different cationic lipid gene carriers, lipoplexes, which are formed spontaneously between cationic liposomes and negatively charged nucleic acids are commonly used for gene and oligonucleotide delivery in vitro and in vivo.¹² Entrapment of DNA in cationic liposomes has important application in the development of non-viral DNA vectors in gene therapy.¹² Studies related to the interactions between DNA and synthetic cationic liposomes have recently received much attention in terms of understanding the physicochemical properties.³⁸

1.4.3. DIFFERENT PROTOCOLS FOR DNA IMMOBILIZATION

As entrapment of DNA in cationic liposomes has important applications in gene therapy, the immobilization of DNA in different matrixes and on planar supports has become a prime topic of current research. The immobilization of DNA on a two dimensional solid surface is

of great interest to researchers all over the globe for its numerous application in various fields.³⁹ Various routes have been employed for the immobilization of DNA have been described on planar supports.

Assembly at the air-water interface with Langmuir monolayers :

The immobilized DNA on monolayers contributes to better understanding of DNA drug interactions and also studying molecular recognition procedures.^{39a} The DNA -lipid LB films would serve as molecular devices for one-dimensional electron transfer and conduction along stacked base pairs.⁴⁰

Langmuir monolayers of lipid molecules have frequently been used as models to understand the organization and function of biological membranes.⁴¹ Molecular recognition between signal peptides and receptor proteins are a basic feature of many biological processes. *Kunitake et al* have observed molecular recognition of aqueous Dipeptides at multiple hydrogen bonding sites of mixed monolayers at the air-water interface.⁴²

Studies on DNA immobilization at the air-water interface have thus far concentrated on electrostatic complexation of preformed double-helical DNA molecules with cationic lipid Langmuir monolayers.⁴³ Electrostatic forces have been used as driving force for the complex formation. One such example is the complex of the cationic lipid and the DNA molecule.^{43d} *Okahata et al* have studied the orientation of DNA strands along the dipping direction of LB film.^{43c} It was confirmed by X- ray diffraction patterns and polarization spectra that the dye-intercalated DNA strands were aligned along the dipping direction in the LB films. Yet, in another study, *Kago et al* have observed the fine structure of the lipid-DNA complex at the air-water interface by X- ray Reflectometry.^{43a} Base pairing between the monolayer forming amphiphilic nucleobases with water soluble bases at the air-water interface might be a driving force of molecular organization termed as molecular recognition directed self- assembly. *Shimomura et al* have reported the tailoring of two- dimensional DNA- mimetic molecular organization at the air-water interface.⁴⁰ They have used fluorescence microscopic imaging for how nucleobase amphiphiles are organized to two- dimensional (2-D) molecular assemblies at the air-water interface. *Kunitake*⁴⁴ and other workers⁴⁰ have stated that molecular recognition of small molecules based on hydrogen bond formation could be observed at the lipid surface but could not be observed in bulk solution. Through elegant QCM measurements, Okahata and co-workers have recently shown that alkylated monolayer forming nucleobases recognize linear oligonucleotides introduced into the subphase.⁴⁵ Hydrogen bonding between complementary bases (alkylated-A and linear oligonucleotide-T molecules) leads to the recognition at the air-water interface while such a hydrogen-bonding is not possible in the bulk of the subphase.⁴⁵

By self assembled monolayers (SAMs) of thiols:

Higashi et al have reported the attachment to terminally functionalized self-assembled monolayers (SAMs) via electrostatic⁴⁶ and intercalation interactions.^{39a} *Steel et al*⁴⁷ have compared electrostatic binding of small redox molecules to DNA in solution with DNA immobilized on alkanethiol modified gold surfaces^{47a} and have also reported electrochemical quantification on DNA immobilized on thiolated DNA on gold surfaces.^{47b} *Wang et al* have immobilized thiol-derivatized PNA (peptide nucleic acids) on gold surfaces.^{47c} *Tarlov et al*⁴⁸ have also used alkanethiol self-assembly methods to fabricate DNA-probe modified gold surfaces with known and reproducible probe coverages that exhibit high hybridization activity. Studies on surface coverage and orientation of DNA molecules immobilized onto preformed alkanethiol SAMs was conducted by *Huang et al*.⁴⁹

Onto Quartz Crystal Oscillators:

Immobilization of oligonucleotides by self assembly process onto quartz crystal oscillators has been recently demonstrated.⁵⁰ *Caruso et al* have immobilized two 30-mer oligonucleotides, one biotinylated (biotin-DNA) and the other having a mercaptohexyl group at the 5' phosphate end onto modified gold surfaces to study hybridization of nucleic acids for sensor development using a QCM.^{50c} *Okahata et al* have extensively used QCM technique for immobilization and hybridization of 10-30mer oligonucleotides immobilized on QCM.^{50b,d}

Recent advances in biosensor technology have contributed significantly to our understanding of the mechanisms of molecular recognition process. In this regard, *Yang et al* have carried out surface plasmon resonance studies of DNA Polymerases binding to Template/ Primer DNA duplexes immobilized on supported lipid monolayers.⁵¹

On Polystyrene Micro spheres:

Some other methods include single molecule analysis of DNA immobilized on polystyrene micro spheres described by *Balasubramanian et al*.⁵²

Methods for immobilization of PNA :

The immobilization of analogues of DNA (namely PNA) in different matrixes has of late; attracted wide attraction of researchers around the globe. Some of the methods include use of cationic liposomes or lipids as carriers for PNA-DNA hybrids which has important applications in the development of nonviral vectors in gene therapy.^{26a} Recently, the air-water interface has been used to study interaction of biomolecules with Langmuir monolayers as a means of modeling cellular delivery of DNA/PNA across biological membranes in gene therapy.^{17a, 12c}

1.5. THE METHOD DESCRIBED IN THIS THESIS

In this thesis, formation of DNA hybrids in thermally evaporated cationic lipid films⁵³ and with Langmuir monolayers is demonstrated.⁵⁴ Also, we have looked at the immobilization and hybridization of DNA and PNA (a DNA mimic) in cationic lipid bilayers⁵⁵ and with Langmuir monolayers⁵⁶ at the air-water interface. Hybridization and phase transfer of DNA molecules with cationic surfactant at liquid-liquid interface is also discussed in this thesis.⁵⁷

The thesis consists of seven chapters. Chapter one is an introduction to the thesis and gives a brief review about the importance and applications of DNA in various fields, introducing some basics of DNA, forces involved in stabilizing DNA strands, need for immobilization of DNA/PNA within lipid bilayers and at the air-water interface with cationic monolayers and different protocols currently in vogue for DNA/PNA immobilization.

In chapter two, experimental techniques such as thermal evaporation of fatty lipids using vacuum deposition unit, the Langmuir-Blodgett technique, Quartz Crystal Microgravimetry (QCM), UV-visible Spectroscopy, UV-melting studies (T_M), Fourier Transform Infrared Spectroscopy (FTIR), Fluorescence Spectroscopy, X-ray photoemission spectroscopy (XPS), Circular dichroism (CD), Ellipsometry, Contact Angle measurements, that are used for characterization of the DNA/PNA-lipid composite films have been discussed in detail. The physical principles on which the different techniques are based and their application to understanding various aspects of formation of the composite films have been outlined.

The third chapter discusses the hybridization of DNA by sequential electrostatic and hydrogen-bonding immobilization of single-stranded complementary oligonucleotides at the air-water interface with cationic Langmuir monolayers. The complexation of the single-stranded DNA molecules with octadecylamine (ODA) Langmuir monolayers was followed in time by monitoring the pressure-area isotherms. Langmuir-Blodgett (LB) films of the ODA-DNA complex were formed on different substrates and characterized using quartz-crystal microgravimetry (QCM), Fourier transform infrared spectroscopy (FTIR), polarized-UV-vis and fluorescence spectroscopy as well as thermal melting studies. These measurements clearly showed that hybridization of the complementary single-stranded DNA molecules had occurred at the air-water interface leading to the characteristic double-helical structure. Furthermore, it was observed that the DNA molecules in the LB films were oriented parallel to the substrate withdrawal direction. Effect of salt on the hybridization of DNA by sequential immobilization of oligonucleotides at the air-water interface in the presence of ODA/DOTAP monolayers is also demonstrated in this chapter.

The fourth chapter deals with the encapsulation of double stranded DNA (dsDNA) and *in-situ* hybridization of complementary single stranded DNA (ssDNA) molecules in a fatty lipid matrix. The immobilization of DNA is accomplished by simple immersion of a thermally evaporated octadecylamine film (ODA) in the DNA solution at close to physiological pH. The diffusion of the DNA molecules into the cationic lipid film is dominated by attractive electrostatic interaction between the negatively charged phosphate backbone of the DNA molecules and the protonated amine molecules in the thermally evaporated film and has been quantified using quartz crystal microgravimetry (QCM). Fluorescence studies of DNA-ODA films obtained by sequential immersion of the ODA matrix in the complementary single strand DNA solutions using ethidium bromide intercalator clearly showed that the hybridization of the DNA single strands had occurred within the lipid matrix. Furthermore, fluorescence studies of the preformed dsDNA-ODA biocomposite film indicated DNA encapsulation without distortion to the native double helix structure. The DNA-fatty lipid composite films would serve as model systems for understanding DNA-membrane interactions as well as in the study of DNA-drug/protein interactions. In this chapter, we have also looked at the electrostatic entrapment and thermal stability of pre-formed DNA duplexes of different lengths within thermally evaporated cationic lipid films. In addition, the specificity of base pairing within a sequence was also studied.

Chapter five deals with the formation of PNA-DNA hybrids within lipid bilayers and also with Langmuir monolayers at the air-water interface. In this chapter sequential immobilization and *in-situ* hybridization of single stranded DNA and complementary PNA molecules in thermally evaporated fatty amine films and at the air-water interface with cationic Langmuir monolayers is demonstrated. Quartz crystal microgravimetry and UV-melting analysis of the films of ODA-PNA-DNA hybrids formed by both the methods of immobilization clearly showed that the sequential immobilization process had resulted in hybridization of the complementary single-stranded DNA molecules with PNA at the air-water interface and within lipid bilayer stacks. The specificity of base pairing in the DNA-PNA complexes with the ODA monolayers and within the ODA matrix was also studied by introduction of a single mismatch in the DNA sequence.

Chapter six describes the hybridization of complementary single-stranded DNA molecules at the interface between water and hexane containing cationic fatty lipid molecules (ODA). During vigorous shaking of the biphasic mixture, the individual DNA single strands are bound electrostatic ally to ODA molecules at the water-hexane interface following which they hybridize into the double helical structure. The binding of the cationic lipid molecules to the DNA double helices renders them hydrophobic and results in the phase transfer of the

DNA molecules into the organic phase. Pre-formed DNA double helical structures could also be phase transferred by this method without distortion to the duplex structure. The surfactant-stabilized hybridized DNA molecules could be formed as thin films on suitable substrates by simple solution casting. The protocol described herein is much simpler and more versatile than the Bligh and Dyer extraction procedure currently used for hydrophobizing DNA. It is expected to facilitate the generation of DNA-lipid complexes and the design of lipid-based DNA carrier systems in gene therapy.

Chapter seven summarizes the work presented in the thesis and compares the protocols developed by us with those currently in vogue on the immobilization and hydrophobization of DNA. The thesis ends with a brief discussion of possible avenues of future research.

1.6. REFERENCES

- (1) Niemeyer, C.M. *Angew.Chem.Int.Edn.* **2001**, *40*, 4128.
- (2) a) Sha, R.; Liu, F.; Bruist, M. Seeman, N.C. *Biochemistry* **1999**, *38*, 2832; b) Mao, C.; Sun, W. Seeman, N.C. *J. Am.Chem.Soc.* **1999**, *121*, 5437; c) Liu, F.; Sha, R. Seeman, N.C. *J. Am. Chem. Soc.* **1999**, *12*, 917; d) Seeman, N. C. *Angew.Chem.Int.Edn.* **1998**, *37*, 3220; e) Yang, X.; Wenzler, L.A.; Qi, J.; Li, X.; Seeman, N.C. *J. Am.Chem.Soc.* **1998**, *120*, 9779; f) Winfree, F.; Liu F.; Wenzler, L.A.; Seeman, N.C.; *Nature* **1998**, *394*, 539; g) Seeman, N.C. *Acc.Chem.Res.* **1997**, *30*, 357; h) Seeman, N.C.; Zhang, Y.; Chen, J.; *J.Vac.Sci.Technol.A.* **1994**, *12*, 1895.
- (3) a) Condon, A.; Rozenberg, G.; Springer Verlag, Berlin Heidelberg, lecture notes in computer science, **2001**, *173*, 2054; b) Mao, C.; LaBean, T.; Reif, J.H.; Seeman, N.C.; *Nature* **2000**, *407*, 493; c) Liu, F.; Wang, H.; Seeman, N.C. *Nanobiology* **1999**, *4*, 257.
- (4) a) Mirkin, C.A.; *Inorg Chem.* **2000**, *39*, 2258; b) Reynolds, R.; Mucic, R.C.; Mirkin, C.A.; Letsinger, R.L.; *J.Am.Chem Soc.* **2000**, *122*, 3795; c) Storhoff, J.J.; Mirkin, C.A.; Letsinger, R.L.; Schatz, G.C.; *J.Am.Chem.Soc.* **2000**, *122*, 4640; d) Mirkin, C.A.; Piner, R.D.; Zhu, J.; Xu, F.; Hong, S.; *Science* **1999**, *283*, 661; e) Mirkin, C.A.; Letsinger, R.L.; Mucic, R.C.; Storhoff, J.J. *Nature* **1996**, *382*, 607.
- (5) Alvisatos, A.P.; Johsson, K.P.; Peng, X.; Wilson, T.E.; Loweth, C.J.; Bruchez, M.P.; Jr.; Schultz, P.G.; *Nature* **1996**, *382*, 609.
- (6) a) Dubertret, B.; Calame, M.; Libehaber, A, J.; *Nat.Biotechnol*, **2001**, *19*, 365; b) Storhoff, J.J.; Elghanian, R.; Mucic, R.C.; Mirkin, C.A.; Letsinger, R.; L. *J. Am. Chem.*

- Soc.* **1998**, *I20*, 1959; c) Elghanian, R.; Storhoff, J.J.; Mucic, R.C.; Letsinger, R.L.; Mirkin, C.A.; *Science* **1997**, *277*, 1078.
- (7) a) He, H.X.; Zhang, H.; Li, Q.G.; Zhu, T.; Li, S.F.Y.; Liu, Z.F. *Langmuir* **2000**, *16*, 3846; b) Aizenberg, J.; Braun, P.V.; Wiltzius, P. *Phys.Rev.Lett* **2000**, *84*, 2997 .
- (8) Sastry, M.; Gole, A.; Sainkar, S.R. *Langmuir* **2000**, *16*, 3553.
- (9) a) Mukherjee, P.; Ahmad, A.; Mandal, D. ; Senapati, S.; Khan, M.I. Sainkar, S.R. Ramani, R. Parischa, R. ; Ajayakumar, P.V.; Alam, M.; Sastry, M. Kumar, R. *Angew.Chem.Int.Ed.* **2001**. *40*, 3585; b) Sleytr, U.B. Messner, P. Pum, D. Sara, M. *Angew.Chem.Int.Ed.* **1999**, *38*, 1034; c) Shenton, W.; Douglas, T.; Young, M. ; Stubbs, G.; Mann, S. *Adv.Mater.* **1999**, *11*, 253; d) Shenton, W. Pum, D.; Sleytr, Band, U.; Mann, S. *Nature* **1997**, *389*, 585.
- (10) a) Sastry, M.; Kumar, A.; Datar, S.; Dharmadhikari, C.V. Ganesh, K.N. *Appl.Phys.Lett.* **2001**, *78*, 2943; b) Richter, J.; Seidel, R.; Kirsch, R.; Mertig, M.; Pompe, W.; Plaaschke, H.K. *Adv.Mater* **2000**, *12*, 507; c) Braun, E.; Eichen, Y.; Sivan, U. Ben-Yoseph, G. *Nature* **1998**, *391*, 75; d) Cofer, J.L.; *J.Cluster Sci.* **1997**, *8*, 159; f) Cofer, J.L.; Bigham, S.R.; Pinizzotto, R.F. Yang, H. *Nanotechnology* **1992**, *3*, 69.
- (11) Niemeyer, C.M.; Adler, M.; Gao, S. Chi, L. *Angew.Chem.Int.Ed.* **2000**, *39*, 2967.
- (12) a) Hirsch-Lerner, D., Barenholz, Y. *Biochim. Biophys. Acta.* **1999**, *1461*, 47; b) Lasic, D.D.; *Trends Biotechnol.* **1998**, *16*, 307; c) Radler, J.O.; Koltover, I.; Jamieson, A.; Salditt, T.; Safinya, C. R. *Langmuir* **1998** , *14*, 4272; d) Radler, J.O.; Koltover, I.; Salditt, T.; Safinya, C. R. *Science* **1997**, *275*, 810.
- (13) Yan, H.; Zhang, X.; Shen, Z.; Seeman, N.C. A Robust DNA Mechanical Device Controlled by Hybridization Topology, *Nature* **2002**, *415*, 62.
- (14) GENES V by Benjamin Lewin, Oxford University Press, **1994**.
- (15) a) Uhlmann , E.; Peyman , A.; Breipohl , G.; Will, D.W. *Angew .Chem .Int . Ed. Engl.* **1998**, *37*, 2796; b) Crooke , S.T.; Bennett, C.F. *Annu.Rev.Pharmacol.Toxicol.* **1996**, *36*, 107; c) Thuong , N.T; Helene, C. *Angew .Chem .Int . Ed. Engl.* **1993**, *32*, 666.
- (16) Uhlmann, E.; Peyman, A.; Breipohl , G.; Will, D.W. Encyclopedia of Cancer, Vol. 1 (Ed: J.R.Bertino), Academic Press, San Diego, CA, **1997**, 64.
- (17) a) Nielsen, P.E. *Curr.Opin.Biol.* **2001**, *12*, 16; b) Nielsen, P.E. *Acc.Chem.Res.* **1999**, *32*, 624; c) Nielsen, P.E.; Haaima, G. *Chem.Soc.Rev.* **1997**, *73*; d) Egholm, M.; Buchardt, O.; Nielsen, P.E.; Berg, R.H. *J.Am.Chem.Soc.* **1992**, *114*, 1895; e) Egholm M.; Buchardt, O.; Nielsen, P.E.; Berg, R.H. *J.Am.Chem.Soc.* **1992**, *114*, 9677; f) Nielsen, P.E.; Egholm M.; Berg, R.H.; Buchardt, O. *Science* **1991**, *254*, 1497.
- (18) Brown, S. C.; Thomson, S.A.; Veal, A.J.; Davis, D.G. *Science* **1994**, *265*, 777.

- (19) Eriksson, M.; Nielsen, P.E. *Nat. Struct. Biol.* **1996**, *3*, 410.
- (20) Betts, L.; Josey, J.A.; Veal, J.M.; Jordan, S.R.A. *Science* 1995, *270*, 1838.
- (21) Rasmussen, H.; Kastrup, J.S.; Nielsen, J.S.; Nielsen, J.N.; Nielsen, J.M.; Nielsen, P.E. *Nat. Struct. Biol* **1997**, *4*, 98.
- (22) Egholm, M.; Buchardt, O.; Christensen, L.; Behrens, C.; Freier, S.M.; Driver, D.A.; Berg, R.H.; Kim, S.K.; Norden, B.; *Nature* **1993**, *365*, 566.
- (23) a) Giesen, U.; Kleider, W.; Berding, C.; Geiger, A.; Orum, H.; Nielsen, P.E.; *Nucleic Acids. Res.* **1998**, *26*, 5004; b) Tomac, S.; Sarkar, M.; Ratilainen, T.; Wittung, P.; Nielsen, P.E. *J.Am.Chem.Soc.* **1996**, *118*, 1996.
- (24) a) Doyle, D. F.; Braasch, D. A.; Simmons, C.G.; Janowski, B.A.; Corey, D.R. *Biochemistry* **2001**, *40*, 53. b) Hamilton, S.E.; Simmons, C.G.; Kathiriyai, I.S.; Corey, D.R. *Chemistry and Biology* **1999**, *6*, 343.
- (25) Demidov, V.; Potaman, V.N.; Frank-Kamenetskii, M.D.; Buchardt, O.; Egholm M.; Nielsen, P.E. *Biochem.Pharmacol.* **1994**, *48*, 1309.
- (26) a) Nastruzzi, C.; Cortesi, R.; Esposito, E.; Gambari, R.; Borgatti, M.; Bianchi, N.; Feriotto, G.; Mischiati, C. *J. Controlled Release*, **2000**, *68*, 237; b) Hamilton, S.E.; Simmons, C.G.; Kathiriyai, I.S.; Corey, D.R. *Chemistry and Biology* **1999**, *6*, 343; c) Larsen, J.H.; Bentin, T.; Nielsen, P.E. *Biochim.Biophys.Acta.* **1999**, *1489*, 159; d) Hyrup, B.; Nielsen, P.E. *Bioorg.Med.Chem.* **1996**, *4*, 5; e) Nielsen, P.E.; Egholm M.; Berg, R.H.; Buchardt, O. *Trends Biotech.* **1993**, *11*, 384.
- (27) Nielsen, P.E.; Egholm M. : Peptide Nucleic Acid (PNA). Protocols and applications. Horizon Scientific Press, Norfolk, **1999**.
- (28) Kool, E.T. *Chem. Rev.* **1997**, *97*, 1473.
- (29) Newcomb, L.F.; Gellman, S.H. *J.Am.Chem.Soc.* **1994**, *116*, 4993.
- (30) Guckian, K.; Schweitzer, B.A.; Ren, X.F.; Sheils, C.J.; Paris, P.L.; Tahmassebi, D.C.; Kool, E.T. *J.Am.Chem.Soc.* **1996**, *118*, 8182.
- (31) Manning, G.S.Q. *Rev.Biophys.* **1978**, *11*, 179.
- (32) Hashimoto, H.; Nelson, M.G.; Switzer, C. *J. Org. Chem.* **1993**, *58*, 4194.
- (33) a) Huang, L.; Li, S. *Annu. Rev. Biophys. Biomol. Struct.* 2000, *29*, 27; b) Huang, L. *Gene Ther.* 2000, *7*, 731; c) Miller, A. D. *Angew Chem.Int. Ed.Engl.* 1998, *37*, 1768.
- (34) a) Lin, A.L. *J.Drug. Targt.* 2000, *8*, 13; b) Whitecome, D.; Newton, C.R.; Little, S. *Curr. Opin.Biotech.* 1998, *9*, 602.
- (35) Kay, M. A; Liu, D.; Hoogerbrugge, P. M. *Proc. Natl. Acad.Sci.USA* **1997**, *94*, 12744.
- (36) a) Raspaud, E.; Pitard, B.; Durand, D.; Chariol, A. O.; Pelta, J.; Byk, G.; Scherman, D.; Livolant, F. *J. Phys. Chem. B.* **2001**, *105*, 5291; b) Kennedy, M.T.; Pozharski, E.V.;

- Rakhmanova, V. A.; MacDonald, R.C. *Biophys. J.* **2000**, *78*(3), 1620; c) Silva, M.B.; Kuhn, P. S.; Lucena, L. S. *Physica A.* **2001**, *296* (1-2), 31.
- (37) a) Wang, Y.; Dubin, P.L.; Zhang, H. *Langmuir* **2001**, *17*, 1670; b) Byk, G.; Dubertet, C.; Eseriou, V.; Fredric, M.; Jaslin, G.; Rangara, R.; Pitard, B.; Crouzet, J.; Wils, P.; Schwartz, B.; Scherman, D. *J.Med. Chem.* **1998**, *41*, 224; c)
- (38) Kikuchi, I.S.; Carmona-Ribeiro, A.M. *J.Phys. Chem.B* . **2000**, *104*, 2829.
- (39) a) Higashi, N.; Inoue, T.; Niwa, M. *J.Chem.Soc., Chem.Commun.* **1997**, 1507; b) Xu, X.H.; Yang, H.C.; Mallouk, T.E.; Bard, A.J. *J. Am. Chem. Soc.* **1994**, *116*, 836; c) Weisenhorn, A.L.; Egger, M.; Ohnessorge, F.; Gould, S.A.C.; Heyn, S.P.; Hansma, H.G.; Sinsheimer, R.L.; Gaub, H.E.; Hansma, P.K. *Langmuir* **1991**, *7*, 8.
- (40) Shimomura, M.; Nakamura, F.; Ijio, K.; Taketsuna, H.; Tanaka, M.; Nakamura, H.; Hasebe, K. *J. Am. Chem. Soc.* **1997**, *119*, 2341.
- (41) Ahlers, M.; Muller, W.; Reichert, A.; Ringsdorf, H.; Venzmer, J. *Angew. Chem. Int. Ed. Engl.* **1990**, *29*, 1269.
- (42) Cha, X.; Ariga, K.; Kunitake, T. *J.Am. Chem. Soc.* **1996**, *118*, 9545.
- (43) a) Kago, K.; Matsuoka, H.; Yoshitome, R.; Yamaoka, H.; Ijio, K.; Shimomura, M. *Langmuir* **1999**, *15*, 5193; b) Vijayalakshmi, R.; Dhathathreyan, A.; Kanthimathi, M.; Subramanian, V.; Nair, B.U.; Ramasami, T. *Langmuir* **1999**, *15*, 2898; c) Okahata, O.; Kobayashi, T.; Tanaka, K. *Langmuir* **1996**, *12*, 1326; d) Ijio, K.; Shimomura, M.; Tanaka, M.; Nakamura, H.; Hasebe, K. *Thin Solid Films* **1996**, *284*, 780.
- (44) Sasaki, D.Y.; Kurihara, K.; Kunitake, T. *J.Am.Chem.Soc.* **1991**, *113*, 9685.
- (45) Ebara, Y.; Mizutani, K.; Okahata, Y. *Langmuir* **2000**, *16*, 2416.
- (46) Higashi, N.; Takahashi, M.; Niwa, M. *Langmuir* **1999**, *15*, 111.
- (47) a) Steel, A. B.; Herne, T. M.; Tarlov, M. J. *Bioconjugate. Chem.* **1999**, *10*, 419; b) Steel, A. B.; Herne, T. M.; Tarlov, M. J. *Anal.Chem.* **1998**, *70*, 4670; c) Wang, J.; Nielsen, P.E.; Jiang, M.; Cai, X.; Fernandez, J.R.; Grant, D.H.; Ozsoz, M.; Begleiter, A.; Mowat, M. *Anal.Chem.* **1997**, *69*, 5200.
- (48) Tarlov, M.J.; Herne, T.M. *J. Am.Chem.Soc.* **1997**, *119*, 8916.
- (49) Huang, E.; Zhou, F.; Deng, L. *Langmuir* **2000**, *16*, 3272.
- (50) a) Zhou, X. C.; Huang, L.Q.; Li, S. F.Y. *Biosens. Bioelectron.* **2001**, *16*(1-2), 85; b) Okahata, Y.; Kawase, M.; Niikura, K.; Ohtake, F.; Furusawa, H.; Ebara, Y. *Anal. Chem.* **1998**, *70*, 1288; c) Caruso, F.; Rodda, E.; Furlong, D.N. *Anal.Chem.* **1997**, *69*, 2043; d) Matsuura, K.; Ebara, Y.; Okahata, Y. *Langmuir* **1997**, *13*, 814.
- (51) Tsoi, P. Y.; Yang, J.; Sun, Y.T.; Sui, S.F.; Yang, M. *Langmuir* **2000**, *16*, 6590.
- (52) Osborne, M.A.; Furey, W.S.; Klenerman, D.; Balasubramanian, S. *Anal.Chem.* **2000**, *72*, 3678.

- (53) Sastry, M.; Ramakrishnan, V.; Pattarkine, M.; Ganesh, K.N. *J.Phys.Chem.B* **2001**, *105*, 4409.
- (54) Sastry, M.; Ramakrishnan, V.; Pattarkine, M.; Gole, A.; Ganesh, K.N. *Langmuir* **2000**, *16*, 9142.
- (55) Ramakrishnan, V.; Sable, M.; D'Costa, M.; Ganesh, K.N.; Sastry, M. *J. Chem. Soc. Chem. Commun.* **2001**, 2622.
- (56) Ramakrishnan, V.; D'Costa, M.; Ganesh, K.N.; Sastry, M. *Langmuir* **2002**, *18*, 6307.
- (57) Sastry, M.; Kumar, A.; Pattarkine, M.; Ramakrishnan, V.; Ganesh, K.N. *J. Chem. Soc. Chem. Commun.* **2001**, 1434.

CHAPTER II

EXPERIMENTAL

TECHNIQUES

The different experimental techniques used during the course of the present work are discussed in this chapter

2.1 INTRODUCTION

This thesis aims at the study of DNA/PNA-lipid interactions within cationic lipid matrices as well as at the air-water interface with Langmuir monolayers. We have also looked at the hybridization; hydrophobization and phase transfer of DNA by interaction with cationic surfactant molecules at the liquid/liquid interface. The sequential electrostatic and hydrogen-bonding immobilization of single-stranded complementary oligonucleotides at the air-water interface with cationic Langmuir monolayers was monitored by was followed in time by monitoring the pressure-area isotherms. Langmuir-Blodgett (LB) films of the ODA-DNA complex were formed on different substrates and characterized using quartz-crystal microgravimetry (QCM), Fourier transform infrared spectroscopy (FTIR) and fluorescence spectroscopy as well as thermal melting (T_m) studies. These measurements clearly showed that hybridization of the complementary single-stranded DNA molecules had occurred at the air-water interface leading to the characteristic double-helical structure. Furthermore, it was observed that the DNA molecules in the LB films were oriented parallel to the substrate withdrawal direction from polarized-UV-vis spectroscopy.

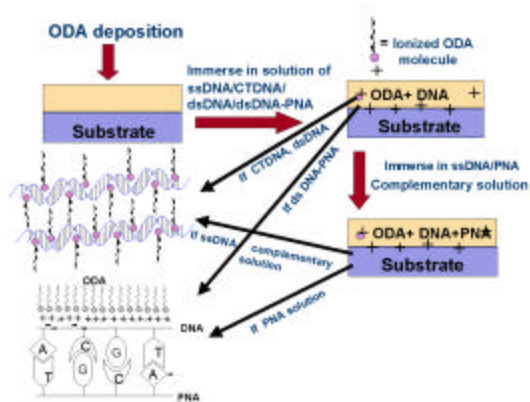
The encapsulation of double-stranded DNA (dsDNA) and *in-situ* hybridization of complementary single-stranded DNA (ssDNA) molecules in a fatty lipid matrix is accomplished by simple immersion of a thermally evaporated octadecylamine film (ODA) in the DNA solution at close to physiological pH has been quantified using quartz crystal microgravimetry (QCM). The substantial incorporation of the DNA molecules in the lipid matrix was further confirmed from contact angle measurements, which indicated a hydrophobic surface. Enhanced fluorescence from the ethidium bromide molecules in the DNA-ODA films obtained confirmed the hybridization of the DNA single strands in the ODA films. Furthermore, fluorescence studies of the preformed dsDNA-ODA biocomposite film indicated DNA encapsulation without distortion to the native double helix structure. The DNA biocomposite films have been further characterized with Fourier Transform Infrared (FTIR) and X-ray Photoelectron Spectroscopy (XPS) measurements.

The DNA-PNA hybrids formed within ODA film were characterized by QCM and UV-melting studies. The study of DNA-PNA immobilization and hybridization with Langmuir monolayers at the air-water interface has been monitored by recording pressure-area isotherms, QCM and melting measurements.

The process of hybridization, phase transfer and thermal stability of the surfactant-stabilized DNA double helical molecules has been studied using UV-vis spectroscopy, fluorescence spectroscopy with ethidium bromide as the intercalator, infrared spectroscopy, UV melting transition and X-ray photoemission spectroscopy measurements.

2.2 THERMAL EVAPORATION OF FATTY LIPIDS.

In earlier studies in this laboratory, it has been shown that the thermally evaporated films of fatty acids/amines can be spontaneously organized via selective ionic interaction of cations/anions by simple immersion of the film in a suitable electrolyte.¹ This leads to an organized lamellar film structure similar to c-axis oriented Y-type LB films, which is termed as self-organized multilayers (SOMs). Recognizing that this principle is general, this approach was extended to the electrostatic binding of surface modified colloidal nanoparticles² and to intercalate proteins/enzymes.³ In this thesis, this principle has been used to intercalate DNA and PNA molecules.⁴ The process has been explained in detail in Scheme 2.2.1



Scheme 2.2.1: Diagram Showing the Various Stages of the DNA-PNA-ODA Composite Film Formation

2.2.1 Deposition of ODA films :

As shown in scheme 2.2.1, 250 Å and 425 Å thick octadecylamine (ODA, Aldrich) films were thermally evaporated onto gold-coated 6 MHz AT-cut quartz crystals, quartz substrates and Si (111) wafers which were kept at a suitable distance above the molybdenum boat for quartz crystal microgravimetry (QCM), contact angle measurements, fluorescence - spectroscopy and Fourier Transform Infrared (FTIR) and X-ray Photoelectron Spectroscopy (XPS) measurements respectively. The molecules when heated evaporate and condense onto these substrates giving more or less same thickness uniform films on each substrate. The films were deposited in an Edwards E306A vacuum coating unit operated at a pressure of better than 1×10^{-7} Torr. The thickness of the deposited films was monitored *in-situ* using an Edwards FTM5 quartz crystal microbalance (QCM). The films deposited were tested by IR for possible decomposition, and were found that the films did not decompose on deposition in vacuum. The thickness of the films was crosschecked using ellipsometry

Basic principles:

The possibility of depositing thin films in a vacuum by Joule heating of platinum wires was discovered in 1887 by Nahrwold and a year later by Kundt for the purpose of measuring refractive indices of metal films. During the last 25 years, evaporated films have found industrial usages for an increasing number of purposes.⁵

Deposition of thin films by vacuum evaporation consists of following steps:

1. Transition of a condensed phase, which may be a solid or a liquid into the gaseous state.
2. Vapour traversing the space between the evaporation source and the substrate at reduced gas pressure.
3. Condensation of the vapor upon arrival of the substrates.

Accordingly, the theory of vacuum evaporation includes the thermodynamics of phase transitions from which the equilibrium vapor pressure of materials can be derived, as well as the kinetic theory of gases, which provides models of the atomistic processes.

The films used for DNA/PNA immobilization in this thesis have been deposited using an Edwards E306 coating unit. The coating unit consists of a rotary pump, which can pump up to 10^{-3} Torr. Below this pressure, an oil diffusion pump is employed and can go up to 10^{-7} Torr.⁵ Both these pumps are used in conjunction for backing and roughing the deposition chamber.

A liquid nitrogen trap was also used. Deposition of organic thin films is done under vacuum due to the following reasons:

- a) The quality of deposition is better due to the increased mean free path of a molecule under vacuum as compared to atmosphere. This results in a linear trajectory of the thermally evaporated molecule.
- b) The melting point is reduced under vacuum enabling low current requirements for thermal evaporation. The amphiphilic molecules required for deposition, were taken in a molybdenum boat and subjected to a low tension DC of about 20 amps less than 10^{-7} Torr vacuum.

2.3. SYNTHESIS OF OLIGONUCLEOTIDES AND PNA OLIGOMERS

2.3.1. Synthesis of oligonucleotides.

Chemical synthesis for all the oligonucleotides used in this thesis was done on a solid phase using the phosphite triester method. Oligonucleotides of different sequences were synthesized by b-cyanoethyl phosphoramidite chemistry on a Pharmacia GA plus DNA synthesizer and purified by FPLC and rechecked by RP HPLC.

Synthesis of oligonucleotides is basically a condensation between the hydroxyl group in position 5 of one nucleotide with the phosphate group of the second nucleotide. The condensation reaction (coupling) takes place under absolutely waterfree conditions in organic solvents like acetonitrile, to avoid competition of the water hydroxyl groups with the sugar hydroxyl group. Oligonucleotides are extremely hydrophilic (short fragments of DNA) and

therefore insoluble in organic solvents. Furthermore there are a number of functional groups in oligonucleotides which may cause ambiguous reactions during coupling. Because of this, hydrophobic groups are used during the synthesis as protecting groups for the reactive sites. This procedure makes the oligonucleotides hydrophobic and hence soluble in organic solvents. Moreover the protection of the synthesis product prevents interaction that may occur in its biologically active form.

Phosphite Triester Synthesis The phosphoramidite procedure⁶ is the modern method of phosphite triester synthesis. Instead of chlorine (which is highly reactive) a secondary amine (preferably diisopropyl amine) is bound to the phosphite group to give a phosphoramidite. This functional group itself not reactive towards hydroxyl groups but is easily activated by a weak acid such as tetrazole which converts the amidite into a tetrazolide. This intermediate reacts with the 5' – hydroxyl group with a yield exceeding 98% within a few minutes. The most common solvent employed in this reaction is acetonitrile.

A great advantage of the phosphoramidite method is the stability of the amidites both as a powder and in solution. In phosphite triester synthesis, advantage is taken of the extreme reactivity of trivalent phosphorous. In this state the phosphorous atom is electron deficient and react readily with any electron donating group, such as the sugar 5' hydroxyl group of a deprotected deoxyribonucleoside. The negative aspect of this reactivity is that the trivalent phosphorous also can accept electrons from any other similar donating group including water. As a consequence, phosphite triester coupling must be carried out under totally anhydrous conditions and reagents must be carefully stored. After the coupling, excess reagents are washed away with acetonitrile.

A solid support for use in solid phase synthesis needs to have the following features.

1. Insoluble, unswellable, and inert towards all solvents and reagents used during the synthesis.
2. Should be macroporous to give rapid access to reagents.
3. Should have a large area.
4. Rigid enough to withstand solvent pressure applied during the synthesis.

Types of solid supports :

Silica

Glass beads

Plastic (polystyrene)

Cellulose paper

A new type of solid support, used by Pharmacia for oligonucleotide synthesis in Gene Assembler Plus was *MonoBeads*. It has a very small particle diameter, and even size distribution, diffusion rates are very high. This allows rapid access of the reagents and

solvents used in the synthesis of oligonucleotides. Removal of excess reagents by washing is also very efficient.

2.3.2. Synthesis of PNA oligomers

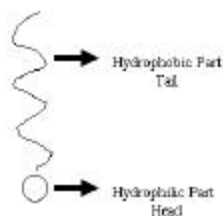
The PNA oligomer H-GTAGATCACT-NH(CH₂)₂-COOH was synthesized manually using a Merrifield resin derivatized with β-alanine (0.013 meq/g) employing the standard Boc-protection strategy. Cleavage from the solid support using the TFA-TFMSA cleavage procedure yielded the PNA oligomer with a free carboxylic acid at its 'C' terminus. The oligomer was purified by RP-FPLC and its purity rechecked by RP-HPLC and confirmed by MALDI-TOF mass spectroscopy. For the work described in this thesis, pre-formed DNA-PNA solutions were obtained by mixing equimolar quantities of DNA solutions and complementary PNA solution under standard hybridization conditions.⁷

2.4. LANGMUIR BLODGETT (LB) TECHNIQUE.

The interaction of DNA with Langmuir monolayers has received considerable attention⁸ with a view to understand templated supramolecular organization⁹ as well as the transfer of DNA across biological bilayer membranes in gene therapy.¹⁰ We have looked at the hybridization of DNA by sequential electrostatic and hydrogen-bonding immobilization of single-stranded complementary oligonucleotides at the air-water interface with cationic Langmuir monolayers.¹¹ The complexation of the single-stranded DNA molecules with octadecylamine (ODA) Langmuir monolayers was followed in time by monitoring the pressure-area isotherms. Langmuir-Blodgett (LB) films of the ODA-DNA complex were formed on different substrates and characterized using quartz-crystal microgravimetry (QCM), Fourier transform infrared spectroscopy (FTIR), polarized-UV-vis and fluorescence spectroscopy as well as thermal melting studies. We have also studied the hybridisation of DNA with PNA (a DNA mimic), with cationic monolayers by the LB technique.¹² The DNA-PNA hybrids formed with Langmuir monolayers have been characterized by monitoring the pressure-area isotherms. LB films of the ODA-DNA-PNA complex were characterized by QCM and UV-melting measurements.

2.4.1 Amphiphilic molecules:

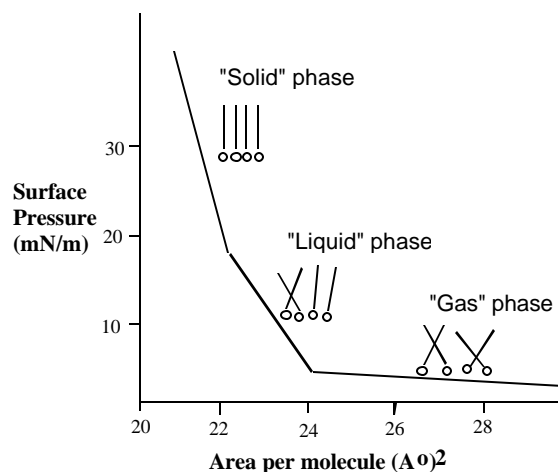
An amphiphilic molecule has a hydrophobic and a hydrophilic part. Amphiphilic molecules or ions in aqueous solution respond to the hydrophobic effect by migration to the surface of the aqueous solution medium to form monolayers in which the polar head group remains in the water while the hydrophobic moieties are expelled from it.



Scheme 2.4.1: A schematic of an amphiphilic molecule showing the hydrophobic (long chain hydrocarbons) and hydrophilic regions (polar groups).

2.4.2. Pressure-Area Isotherms (π -A isotherm)

Monolayers of amphiphilic molecules at an interface can exist in a number of different physical states, analogous to the gaseous, liquid and solid states of matter in bulk. Information regarding the transition between these states can be obtained by measuring the surface pressure of a monolayer as a function of the surface concentration.¹³ *The surface pressure π is the lateral pressure that must be applied to prevent the film from spreading.*



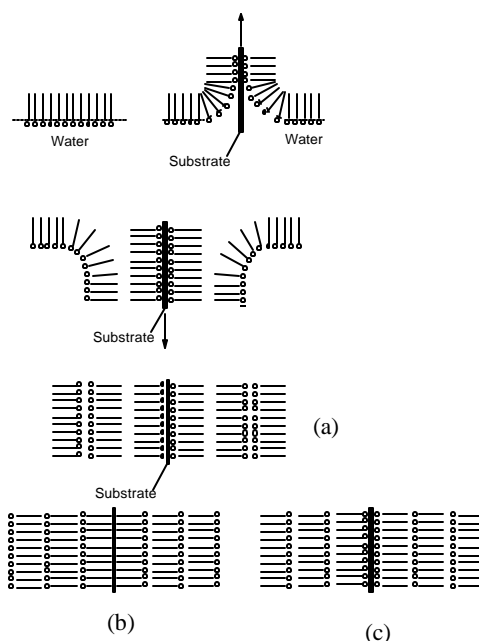
Scheme 2.4.2: A typical pressure-area (π -A) isotherm showing the various phase transitions of the floating monolayer.

π -Isotherms give information about the stability of the molecules in the two-dimensional system, phase transitions and conformational transitions. The pressure-area isotherm also gives some idea of the amount of pressure that has to be applied to the film on the sub phase, to enable deposition of the LB film in the solid-like phase. Thus at appropriate pressure, the film can be transferred to the substrate.

2.4.3. The LB film preparation technique.

In a typical experiment, measured amount of appropriate surfactant is dissolved in a volatile solvent like chloroform (CHCl_3), and is spread on the air-water interface. Due to

their amphiphilicity, the molecules orient themselves on the water surface with their heads in the water and their tails in air. This film is then compressed until the molecules are in a solid-like phase with two-dimensional order. The two different methods used for film formation are: a) Vertical-lifting technique developed by Langmuir and Blodgett and b) the horizontal deposition method known as the Schaefer's method. We have used the vertical deposition Langmuir-Blodgett technique for the deposition of ODA-DNA/PNA LB films. In this method, as shown in scheme 2.3.3, the deposition occurs during both the upward and downward stroke of the substrate. The different types of LB films are also shown in the scheme.



Scheme 2.4.3. Vertical deposition method showing the deposition of monolayer films on a solid substrate during dipping and retraction. (a) Y-type (b) X-type (c) Z-type LB films.

2.5 QUARTZ CRYSTAL MICROGRAVIMETRY

Numerous reports have been devoted to basic principles of quartz resonators including Quartz Crystal Microbalance.¹⁴ Quartz crystals attained significance as an analytical device after the discovery by Sauerby¹⁵ in 1959 that there is a linear relationship between deposited mass and the frequency response. He showed that this proportionality only holds good if the ideal layer of foreign mass is strongly coupled to the resonator. This is the reason for calling such a device a Quartz Crystal Microbalance. Quartz crystal based microgravimetry is a powerful tool to study various adsorption processes^{16a,b} and more recently, the adsorption of proteins at fictionalized surfaces.^{16c,d,e} This technique is well suited for the quality control of multilayers prepared by the langmuir –Blodgett technique^{17a,b,c} or

self-organization processes.^{17d-f} Nowadays, QCM technique is introduced as a powerful tool in detection of nucleic acids. Much work is done in developing a mass sensitive nucleic acid detecting device in immobilizing single stranded oligonucleotide on the resonator surface which hybridizes selectively with the complementary strand from solution.^{18a, b} Most of the methods are based on 1) the electrostatic interactions of the negatively backbone and the positively charged amine monolayers^{18c} and 2) binding of biotinylated oligonucleotides to the surface –confined avidin or streptavidin.^{18d} QCM has been employed recently to monitor kinetic studies of enzymatic DNA cleavage reactions.¹⁹

For the work discussed in this thesis, QCM has been extensively used for estimating the DNA and PNA equilibrium mass loadings and further calculating the DNA/ODA and DNA-PNA-ODA charge ratios.

Basic Principles:

QCM comprises of a thin quartz crystal sandwiched between two metal electrodes that establishes an alternating electric field across the crystal, causing vibrational motion of the crystal at its resonant frequency. This resonant frequency is sensitive to mass changes of the crystal and its electrodes.

Piezoelectric effect: In 1880, Jacques and Pierre Curie discovered that mechanical stress applied to the surfaces of various crystals such as quartz, Rochelle and tourmaline, afforded a corresponding electrical potential across the crystal whose magnitude was proportional to the applied stress.²⁰ This was referred to as the *piezoelectric effect*. Shortly, after their initial discovery, the Curie's experimentally verified the converse piezoelectric effect wherein application of a voltage across these crystals afforded a corresponding mechanical strain. This converse piezoelectric effect is the basis of the quartz crystal microgravimetry (QCM) technique.

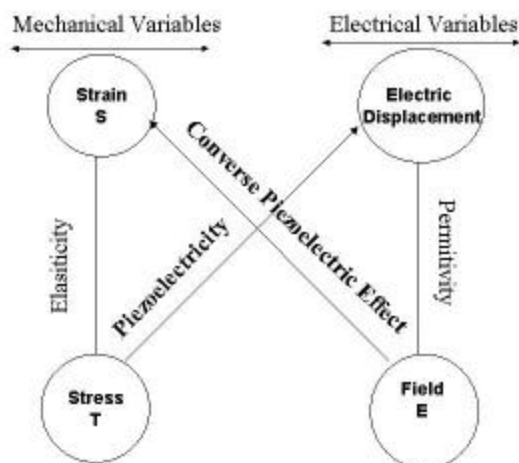


Figure 2.5.1: Shows schematically the general relationships between electrical and mechanical variables.

Pre-requisite for the occurrence of Piezoelectricity:

This property only exists in materials that are acentric, viz. those crystallize in non-Centrosymmetry space groups. A single crystal of an acentric material will possess a polar axis due to dipoles associated with the orientation of atoms in the crystalline lattice. When stress is applied across an appropriate direction, there is a shift of dipoles resulting from the displacement of atoms. This atomic displacement leads to a corresponding change in the net dipole moment. This will produce a net change in electrical charge on the faces of the crystal. Application of electric field across the crystal causes a vibrational motion of the quartz crystal, with amplitude parallel to the surface of the crystal.^{14a} This is depicted in figure 2.5.2.

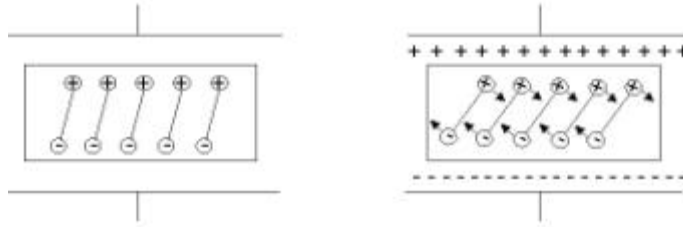


Figure 2.5.2. Schematic representation of the converse piezoelectric effect in shear mode.

The result of the vibrational motion of the quartz crystal is the establishment of a transverse acoustic wave that propagates across the thickness of the crystal, reflecting back into the crystal at the surfaces. When a uniform layer of foreign material is added to the surface of the quartz crystal, the acoustic wave will travel across the interface, and will propagate through the layer. This leads to decrease in the frequency of the crystal.

The Frequency changes on deposition of the film can be converted to mass loading using the Saurbrey formula.¹⁵

Saurbrey formula:

$$\Delta f = -2 f_0^2 \times \frac{\Delta m}{A \times (\mu_q \times \rho_q)^{1/2}}$$

Where Δf - frequency shift, f_0 - frequency of the crystal prior to a mass change, Δm - mass change, A - Piezo electrically active area, ρ_q - density of quartz, μ_q - shear modulus for quartz. ($\mu_q = 2.95 \times 10^{11} \text{ g cm}^{-1} \text{ s}^{-2}$, $\rho_q = 2.65 \text{ g/cm}^3$).

Why AT-cut Quartz Resonators?

Although a large number of crystals show piezoelectricity, only quartz provides the unique combination of mechanical, electrical, chemical and thermal properties that has led to its commercial significance. Crystals cut with the proper angles with respect to the crystalline axes exhibit shear displacements. Depending on the cut angle, a large number of different resonator types such as thickness-shear mode, plate and flexural resonators can be obtained from a mother crystal with eigen frequencies ranging from 5×10^2 – 3×10^8 Hz. Generally AT-cut quartz crystals are used for QCM purposes in which thin quartz wafer is prepared by slicing a quartz rod at an angle of 35.25° with respect to the X-axis of the crystal, resonates in the *thickness shear mode*.

AT cut quartz crystals exhibit a high frequency stability of $\Delta f/f \sim 10^{-8}$, which makes them well suited for many electronic devices. Since AT-cut quartz crystals have a temperature coefficient that is almost zero between 0 – 50°C , this particular cut is the most suitable one for QCM sensors.

In the work described in this thesis we have used a gold coated AT-cut 6 MHz quartz crystal. The frequency counter used was an Edwards FTM5 instrument operating at a frequency stability and resolution of ± 1 Hz. At this resolution and the type of quartz crystal used, the mass resolution would be 12 ng/cm^2 . Different thickness films of lipids were thermally evaporated on the QCM crystals. These crystals were sequentially immersed into single stranded complementary DNA/PNA solutions for different time intervals and the frequency changes were measured *ex situ* after thorough washing (in deionized water) and drying (in flowing nitrogen) of the crystals. The frequency changes were converted to a mass uptake by using the standard Sauerbrey formula.¹⁵ The Sauerbrey equation does not apply for thick films, viscous liquids, elastic solids and viscoelastic bodies. Most reported QCM investigations have assumed ideal rigid behavior and no slip at the resonator-fluid boundary while using the Sauerbrey equation.^{14a} These assumptions are valid when dealing with studies on inorganic thin films, wherein the film deposited is rigid enough to be considered "quartz like". However while dealing with lipid films that are being intercalated with biological molecules such as proteins and DNA, one would need to consider factors such as viscoelastic effects, high mass loadings, surface roughness, surface stress, interfacial slippage and non uniform mass distribution in any piezoelectric measurement.^{14a} The thin films (about 250 \AA), low mass loadings (about $6.12 \mu\text{g}$) as compared to total weight of the crystal, and assuming uniform mass distribution over the film surface supports the validity of the use of Sauerbrey equation in our case.

2.6. UV-VISIBLE SPECTROSCOPY.

The process of hybridization, phase transfer and thermal stability of the surfactant-stabilized DNA double helical molecules has been studied using UV-vis spectroscopy. The

aqueous and organic phases (both before and after the shaking process) were analyzed using UV-vis measurements. The UV-vis measurements were performed on a HP8542A diode array spectrophotometer operated at a resolution of 2 nm. We also performed polarized UV-vis spectroscopy measurements carried out on a Perkin-Elmer Lambda 15 spectrophotometer for hybridized DNA-ODA LB film on quartz. The dichroic ratio at 260 nm was close to 12 indicating a high degree of order in the DNA molecule orientation.^{8d} The double-helical DNA molecules in built-up LB films are oriented parallel to the substrate withdrawal direction.¹¹

Basic principles:

Absorption spectroscopy in the visible region has long been an important tool to the analyst.²¹ Absorption of energy leads to a transition of electron from ground state to excited state. Most of the spectra are very broad, smooth curves and not sharp peaks. This is because any change in the electronic energy is accompanied by a corresponding change in the vibrational and rotational energy levels. A variety of energy absorption is possible depending upon the nature of the bonds within a molecule. For instance, strong σ bonds, in weaker π bonds or non-bonding (n) and when energy is absorbed all of these types of electrons can be elevated to excited antibonding states represented as σ^* , π^* . Most σ to σ^* absorptions for individual bonds take place below 200 nm in the vacuum ultraviolet region and compounds containing just σ bonds are transparent in the near UV/vis region. $\pi \rightarrow \pi^*$ And $n \rightarrow \pi^*$ absorptions occur in the near UV/vis region, and result from the presence in molecules of unsaturated groups known as *chromophores*. The intensity of light passing through a sample is given by the relation:

$$I = I_0 \exp(-\alpha k x)$$

Where I = intensity of transmitted light; I_0 = intensity of incident light; α = molar absorption coefficient; k = constant; x = path length. The combined Beer-Lambert law is used for quantification of exact concentration of "unknown" species in a mixture using UV-vis spectroscopy. This can be done by drawing a graph of intensities of absorption for different concentrations of the sample and comparing with a standard graph.²¹

The Beer-Lambert law is:

$$A = \epsilon c l$$

Where ϵ = proportionality constant known as the absorptivity.

2.7. UV- MELTING (T_M) STUDIES

UV-melting experiments were carried out as a test of hybridization on the ODA-DNA/PNA films formed by using lipid monolayers and bilayers. The T_M measurements were carried out on Perkin Elmer Lambda 15 UV/VIS spectrophotometer fitted with a Julabo water circulator

with programmed heating accessory. The quartz substrates bearing the films were cut so as to fit into the cuvette normally used for liquid samples. The DNA-ODA films were heated at a rate of 0.5°C per minute and the thermal denaturation of the duplex was followed by monitoring changes in the absorbance at 260 nm as a function of temperature.

The non-covalent forces that stabilize the double helix are disrupted by heating or by exposure to low salt concentration. The bases absorb at 260 nm. While heating, the base stacking is disrupted, which is reflected in the absorption at 260nm. The melting is a cooperative phenomenon. The two strands of a double helix separate entirely when all the hydrogen bonds between them are broken. In case of short oligomers, the breaking of the first bond facilitates the breaking of the remaining hydrogen bonds. The process of strands separation is called denaturation or (more colloquially) melting.²² Denaturation of DNA occurs over a narrow range of temperature and results in many of its physical properties. A particularly useful change occurs in the optical density. The heterocyclic rings of nucleotides absorb light strongly in the ultraviolet range with a maximum close to 260nm that is characteristic for each base. But the absorption of DNA itself is some 40% less than would be displayed by a mixture of free nucleotides of the same composition. This is called hypochromic effect; it results from the interactions between the electron systems of the bases, made possible by their stacking in the parallel array of the double helix. Any departure from the duplex state is immediately reflected by a decline in this effect –that is by an increase in the optical density towards the value characteristic of free bases. The denaturation of DNA can be therefore be followed by this hyperchromicity. It is an equilibrium melting process. The midpoint of the temperature range over which the DNA strands separate is called the melting temperature, denoted T_M . An example of melting curve determined by change in optical absorbance is shown in fig 2.7.1. The curve always takes the same form, but its absolute position on the temperature scale is influenced by both the base composition of the DNA and the conditions employed for denaturation.

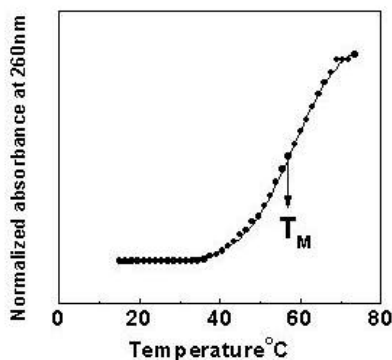


Fig 2.7.1. A typical T_M curve for a duplex DNA.

T_M depends on the proportion of G-C pairs. Because each G-C base pair has three hydrogen bonds, it is more stable than A-T base pairs, which has only two hydrogen bonds. A DNA that is 40% G-C –a value typical of mammalian genomes –a denaturation with a T_M of about 87°C under physiological conditions; a DNA that is 60% under the same conditions has a T_M of 95°C under the same conditions. Thus without the intervention from the cellular systems, duplex DNA is stable at the temperature prevailing in the cell.

2.8. FLUORESCENCE SPECTROSCOPY.

The formation of double helical structures by hybridization of the complementary oligonucleotide sequences was confirmed by introduction of the well-known fluorescent intercalator, ethidium bromide.²³ Enhanced fluorescence from the ethidium bromide molecules occurs on intercalation in the double helical DNA structures²⁴ and may be used to follow the hybridization process. In this thesis, the fluorescence measurements were done on a Perkin Elmer model LS 50-B spectrofluorimeter at 25°C , with slit widths of 5 nm for excitation at 460 nm and 10 nm for the emission monochromators. The LB films were grown on quartz substrates cut to fit precisely in the quartz cuvette normally used for liquid samples. In this thesis fluorescence spectroscopy was also used to establish the hybridization of the complementary single stranded DNA molecules into double helical structures during the course of their phase transfer and retention of the double helical structure is retained after the phase transfer.²⁴

Basic Principles: Electromagnetic radiation (EMR) is a form of energy. EMR possesses properties of both discrete particles termed as photons and of waves. Luminescence occurs when a species in a higher energetic state relaxes to a lower state while simultaneously emitting EMR. Photoluminescence is the type of luminescence that occurs following excitation by absorption of electromagnetic radiation. The most widely used type of photoluminescence in analytical chemistry is fluorescence.²⁵ Fluorescence was first observed as long ago as 1565 and gets its name from the fact that the mineral fluor spar was found to glow under UV radiation.

Fluorescence corresponds to emission of radiation during the electron transition from an excited level to a lower level (ground level) without electron-spin reversal. In case of fluorescence, the lifetime of electron in excited state is 10^{-8} s. If the wavelength of the emitted radiation is identical to the wavelength of the exciting radiation, the fluorescence is resonant fluorescence. In solution, the fluorescent radiation occurs at a longer wavelength compared to that of the absorbed radiation. This type of fluorescence is termed as normal fluorescence.

2.9. FOURIER TRANSFORM INFRARED SPECTROSCOPY (FTIR).

Infrared spectroscopy has been successfully used in studying nucleic acids, since the early work of Fraser and Fraser.²⁶ Talking of more recent work, FTIR technique is used to determine DNA secondary structure and structural variations in DNA–Chlorophyll complexes in aqueous solutions²⁷ and in characterization of cationic lipid-DNA complex and its components.²⁸

Nucleic acid vibrations arise from different parts of the macromolecule,²⁹ and the corresponding IR absorptions are detected in several regions of the spectrum. The main vibrations are observed in the spectral region between 1800cm^{-1} and 700cm^{-1} . Absorption bands due to the stretching vibrations of double bonds in the base planes (between 1800cm^{-1} and 1500cm^{-1}); bands due to the base-sugar entities (between 1500cm^{-1} to 1200cm^{-1}); strong absorption of the phosphate groups and of the sugar between 1250cm^{-1} to 1000cm^{-1} ; and below 1000cm^{-1} , bands due to the vibrations of the phosphodiester chain coupled to the vibrations to the sugar.

Some of the advantages of infrared spectroscopy in the study of nucleic acids are:

- 1) Data from samples can be obtained under an extremely wide variety of physical states.
- 2) No limitation introduced by the size of the investigated molecule, that is, one can work with short oligonucleotides as well as with long polynucleotides.
- 3) Infrared spectroscopy is a nondestructive technique.
- 4) A good FTIR spectrum can be obtained with 2 OD units of material.
- 5) It gives vibrational conformation of nucleic acids.

We have used FTIR technique as an additional evidence for observing DNA hybridization within lipid bilayers^{4a} as well as at the air-water interface with langmuir monolayers¹¹ and the process of hybridization of the surfactant-stabilized DNA double helical molecules.²⁴

For DNA incorporation discussed in this thesis, a 250Å and 500Å thick lipid was deposited onto a Si (111) wafer. FTIR measurements were made on a Shimadzu PC-8201 PC instrument in the diffuse reflectance mode at a resolution of 4cm^{-1} . A total of 250 scans yielded a good signal to noise ratio of the IR spectra

Basic Principles:

The principles of IR can be explained by classical as well as quantum theories.³⁰ The classical model considers a simple ball and spring model wherein diatomic molecule with two masses m_1 and m_2 are connected by a spring.



Fig. 2.9.1 Schematic representation for classical model

Hooke's law: $F = -k \cdot \Delta r$ (k : force constant).

Vibrational frequency can be calculated:

$$\nu = \frac{1}{2\pi} \cdot \sqrt{\frac{k}{\mu}}$$

Where μ is the reduced mass.

Using simple laws of mechanics, a system of masses joined by springs has a number of fundamental modes of vibration each of which has a particular natural frequency. Consider an oscillator such as the electric vector of electromagnetic radiation coupled to a system of masses such as a polyatomic molecule. By scanning through a range of frequencies some may be 'tuned' to the various fundamental modes of vibration by virtue of a change in dipole moment associated with that vibration. So, a series of absorption take place for a polyatomic molecule as we scan through a range of frequencies, radiation is absorbed each time we 'tune-in' or 'come into resonance' with the natural frequency of a fundamental mode which is capable of dipolar interaction.³⁰

Many facts cannot be explained classically (one such fact is the CO_2 splitting) and requires quantum mechanical treatment. This treatment considers the electronic change accompanied by vibration and rotation with discrete energy levels. The energy of quantised energy levels is derived by using Schrodinger wave equation. For polyatomic molecules, the position of each atoms can be described using coordinate geometry, and the degree of freedom are stated for linear molecules ($3N-5$) and for non-linear molecules ($3N-6$). N represents number of atoms.³⁰

Most published work in this area has been for films deposited on silicon substrates, for variety of reasons: a) It is chemically very stable and generally not very reactive even at high temperatures. b) It is excellent for optical studies of deposited films in the visible region using reflection techniques. c) It has no very strong lattice absorption bands in the useful regions of the infrared and thus can be used for transmission studies in this region. To correct for the lattice absorption bands in silicon, a reference silicon sample is used as a reference. All FTIR data presented in the thesis been presented as obtained except for baseline correction.

Peak assignments for Fatty lipids:***C-H Stretching region:***

The two bands at 2920 and 2850 cm^{-1} have been assigned to the antisymmetric and symmetric methylene (CH_2) stretching vibrations respectively and two weak bands at about 2960 and 2875 cm^{-1} to the asymmetric/degenerate and symmetric methyl (CH_3) stretching vibrations respectively. The position of the peaks and the increase in intensity of the methylene stretching vibrations relative to methyl stretching vibration with chain length indicates structural integrity of the molecule. For example, an interesting feature in the hydrophobized and hybridized DNA-ODA film was the drastic reduction in intensity of the methylene antisymmetric and symmetric vibrational modes relative to that of the methyl vibrational modes. This indicates considerable orientational disorder in the DNA-ODA films, which is likely to be a consequence of electrostatic complexation with the cylindrical DNA double helical structures. The fact that the methylene symmetric and antisymmetric vibrational mode frequencies occur at 2850 and 2920 cm^{-1} indicates that the hydrocarbon chains in the ODA sheath are close-packed.³¹

N-H vibrations:

A sharp resonance at 3330 cm^{-1} is seen in the case of the bare ODA film and is due to the N-H stretch vibrations.³² In the case of surfactant stabilized DNA at the liquid-liquid interface, this feature vanishes on complexation of the ODA molecules with DNA.

Peak assignments For DNA:

Three strong resonance's at 1230 cm^{-1} , 1065 cm^{-1} and 964 cm^{-1} are clearly observed from the DNA-ODA composite films which are missing in the as-deposited ODA film. The 1230 and 964 cm^{-1} bands are due to the backbone PO_2 antisymmetric stretching and deoxyribose C-C stretching vibrations respectively and agree well with literature values of hybridized DNA molecules.²⁹ The feature at 1065 cm^{-1} is assigned to the deoxyribose band as well, the presence of which is indicative of Z-DNA double-helical conformation.²⁹ Such a conformation is known to occur for double-helical DNA molecules in an environment of high ionic strength as would be the case during entrapment in the lipid matrix consisting of densely-packed ODA molecules. In the range 1050 – 1750 cm^{-1} yields an increase in intensity of two prominent features at 1109 cm^{-1} and 1719 cm^{-1} in the hybridized DNA LB film and these features are not present in the bare ODA LB film, are clearly signatures from the entrapped DNA molecules in the LB films. The increase in intensity at 1719 cm^{-1} , which is due to resonance in the mainly G-band, has been observed in the case of intercalation of chlorophyllin molecules in hybridized calf-thymus DNA.²⁷ The increase in intensity of the resonance at 1109 cm^{-1} is due to the deoxyribose band and is also an indicator of the hybridization of the DNA molecules in the LB film.²⁷

Table 2.9.1.
Peak assignment for lipid films and that for biocomposite films

BAND	VIBRATION	PEAK POSITION (cm ⁻¹)
Methylene asymmetric stretch	n _a (CH ₂)	2920
Methylene symmetric stretch	n _s (CH ₂)	2850
Amine stretch	N-H	3330
PO ₂ antisymmetric stretching vibration	-PO ₂	1230
Deoxyribose C-C stretching vibrations		964 cm ⁻¹ and 1065 cm ⁻¹ (Z confirmation)

2.10. X-RAY PHOTOELECTRON SPECTROSCOPY (XPS).

Photoelectron spectroscopy is a surface science technique used in understanding atoms, molecules & solids on the surface.³³ Electron spectroscopy characterizes the electrons emitted from a sample. If the incident radiation is x-rays, the spectroscopic technique is either x-ray photoelectron spectroscopy (XPS) or electron spectroscopy for chemical analysis (ESCA). For the work described in this thesis, the XPS C 1s, P 2p and N 1s core levels were recorded from a 250 Å thick double-stranded DNA-ODA composite film grown on Si (111) substrate. XPS measurements were carried out on a VG Microtech ESCA 3000 instrument at a base pressure better than 1 x 10⁻⁹ Torr with un-monochromatized Mg K_α radiation (1253.6 eV energy). The measurements were made in the constant analyzer energy (CAE) mode at a pass energy of 50 eV. This leads to an overall resolution of ~ 1 eV in the measurements. The chemically distinct components in the core level spectra were resolved by a non-linear least squares fitting algorithm after background removal by the Shirley method.³²⁴

Working Principle :

XPS is based on the well-known photoelectric effect first explained by Einstein in 1905. If photons of energy $h\nu$ shined on a solid having the work function ϕ , then the maximum kinetic energy E_k of photoemitted electron is given by the equation:

$$E_k = h\nu - E_b - \phi$$

where E_b is the binding energy of electron in solid. Employing photons with fixed energy $h\nu$, it is obvious that if kinetic energy E_k and work function ϕ of the sample are measured, it is

possible to measure binding energy of electron in solid. Binding energies being characteristic of atoms, different elements present in the sample under investigation are identified. Electrons traveling through a material have a relatively high probability of experiencing inelastic collisions with locally bound electrons as a result of which they suffer energy loss. Due to inelastic scattering process, the flux of photoelectrons emerging from the sample is much attenuated. While the exciting photons penetrate deep into the solid sample, the photoelectrons can escape from only a very short distance beneath the surface ($< 100 \text{ \AA}$). Therefore photoelectron spectroscopy is a *surface sensitive technique*.

Chemical Shifts

Electron spectroscopy for chemical analysis provides qualitative and quantitative information about the elemental composition of matter, particularly of solid surfaces. It also provides useful structural information as well.³³ When one of the peaks of a survey spectrum is examined under conditions of higher energy resolution, the position of the maximum is found to depend to a small degree upon the chemical environment of the atom responsible for the peak. That is, variations in the number of valence electrons and the types of bonds they form influence the binding energies of core electrons. The binding energies increase as the oxidation state becomes more positive. This *chemical shift* can be explained by assuming that the attraction of the nucleus for a core electron is diminished by the presence of outer electrons. When one of these electrons is removed, the effective charge sensed for the core electron is increased; thus an increase in binding energy results.

One of the most important applications of ESCA has been the identification of oxidation states of elements contained in various kinds of compounds.

2.11. Circular Dichroism Spectroscopy (CD)

Circular Dichroism (CD) measurements have been in use for over 20 years to study the conformations of nucleic acids in solution.³³ CD spectroscopy is probably one of the most sensitive techniques available for monitoring structural changes of DNAs in solution or for determining whether a new or unusual structure is formed by a particular polynucleotide sequence.

In the present thesis work, CD spectroscopy has been mainly used to follow the structural and conformational changes in the pre-formed duplexes of varying chain lengths encapsulated within thermally evaporated lipid films. In the present work, CD technique has been used to verify the conformational transition from the native B form to the Z form, as observed in the FTIR analysis of hybridized DNA in lipid films. Such a conformation is known to occur for double-helical DNA molecules in an environment of high ionic strength as

would be the case during entrapment in the lipid matrix consisting of densely packed ODA molecules.

The advantages of CD spectroscopy to study DNA conformations are:

- 1) The sensitivity and ease of CD measurements.
- 2) Non-destructive nature of measurements.
- 3) Relatively small amounts of material.

Although detailed structural information, such as X-ray crystallography or NMR spectroscopy, is not obtainable from CD spectra, the CD spectrum of DNA in solution can provide a reliable determination of its overall conformational state when compared with the CD spectra of reference samples. The information obtained from CD spectra is complementary to that from absorption spectra.

In general, the types of information available from CD spectra of DNA in solution may be divided into three classes.

- 1) The secondary conformations of DNAs containing Watson –Crick base pairs may be studied. These include the secondary A, B and Z conformations, the triple stranded H-form (which has both Watson-Crick and Hoogsteen base pairs) and parallel stranded structures. The value of CD spectra in characterizing the A and B forms of DNA was apparent in the work of Tunis-Schneider and Maestre³⁴ and CD was the technique by which Z conformation of DNA was identified.³⁵
- 2) The nearest –neighbor composition of a B-form DNA can be obtained from a CD spectral analysis.
- 3) The conditions under which unusual base pairs form can be investigated by CD spectroscopy.

The chief practical application of CD spectroscopy to the study of DNA structures has been making empirical comparisons with the CD spectra of known structures.

Basic Principles:

Circular dichroism (CD) spectroscopy is a type of absorption spectroscopy that can provide information on the structures of many types of biological macromolecules.

Circular Dichroism is the difference between the absorption of left and right-handed circularly polarised light and is measured as a function of wavelength. CD is measured as a quantity called **mean residue ellipticity**, whose units are degrees-cm²/dmol. Chiral or asymmetric molecules produce a CD spectrum because they absorb left and right handed polarized light to different extents and thus are considered to be "optically active". Biological macromolecules such as proteins and DNA are composed of optically active elements and

because they can adopt different types of three-dimensional structures, each type of molecule produces a distinct CD spectrum.

The wavelengths of light that are most useful for examining the structure of DNA are in the ultraviolet (UV) or vacuum ultraviolet (VUV) ranges (from 160 to 300 nm) because these are the regions of the electronic transitions of the purine and pyrimidine bases in DNA. Typically the range of data collected on a commercially available CD instrument will be between 190 and 300 nm.

2.12. ELLIPSOMETRY.

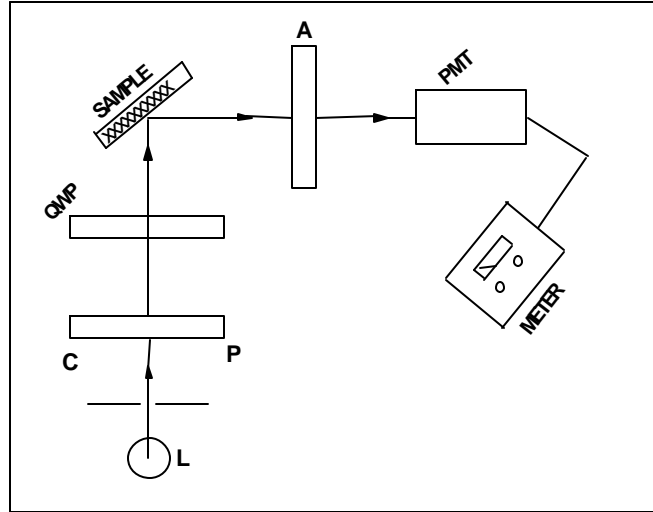
Ellipsometry is one of the most versatile techniques for the study of optical properties of thin films on either solid or liquid surfaces. We have used ellipsometry for the determination of thickness of lipid films before and after DNA intercalation.

Working principle: The technique is based on the principle that the state of polarization of light changes on reflection from an interface. This technique is also known as reflection polarimetry or polarimetric spectroscopy. In its broadest sense, ellipsometry is the measurement of the state of polarization of light. *Paul Drude* was the first to develop fundamental equations of ellipsometry, which demonstrated potential monolayer sensitivity for the detection and characterization of thin films on specular surfaces.^{38a}

When a polarized light beam reflects from any specular surface, changes occur in both the amplitude and phase of the oscillating parallel and perpendicular vector components of the electric field associated with the beam. The main objective of an ellipsometry experiment is to measure these amplitude and phase changes, which provide us information about the reflecting surface through the Fresnel reflection coefficients.^{38b} We have used a Gaertner L 118 manually operated null ellipsometer in the polarizer-compensator-sample-analyser (PCSA) mode to measure the ellipsometric angles of lipid films deposited on Si (111) substrate.

2.12.1 Measurement of ellipsometric angles Ψ and Δ - Calculation of thickness of film:

The basic experimental setup of the null ellipsometer used in the study of the optical properties of the lipid and the biocomposite films is shown in scheme 2.11.1.



Scheme 2.12.1: Schematic of the various optical elements and their configuration in the null-ellipsometry measurements.

The light source (L) is a monochromatic He-Ne laser ($\lambda = 6328 \text{ \AA}$) with a collimator (scheme 2.12.1). The azimuths of the polarizer (P) in conjunction with a compensator (QWP, a quarter wave plate made of mica) determine the state of polarization of the light incident on the sample surfaces (S). The azimuth of the compensator was kept fixed at 45° with respect to the plane of incidence for all measurements reported in this thesis. In null ellipsometry, the state of polarization of the incident light is adjusted by changing the azimuth of the polarizer (P) such that the light reflected from the sample surface is linearly polarized. This can be checked using another polarizer, the analyzer (A) that would give extinction of light under crossed conditions. To obtain improved sensitivity a photo multiplier tube (PMT) is used to detect the null position. Under these null conditions, the ellipsometric angles Ψ and Δ are related to the Fresnel coefficients of their reflecting surface and the azimuths of the analyzer and polarizer (A_0 and P_0 respectively) through equation (2.1).

$$\rho := \frac{r_p}{r_s} = \tan \psi \exp(i\Delta) \quad (2 - 1)$$

where r_p and r_s are Fresnel reflection coefficients³⁹

In case where a uniform thin film of refractive index n and thickness d rests on a infinitely thick substrate of refractive index $n_2 - i.k_2$ (the substrate may be absorbing at the wavelength used for the measurement, hence the imaginary component to the refractive index), the whole system being in an ambient of refractive index n_0 , the Fresnel reflection coefficients are

related to the system material properties through the equation (2-12). For the sample with multiple interfaces, r_p and r_s are given as follows³⁹

$$r_{pj} := \frac{n_j \cdot \cos(\phi_{j-1}) - n_{j-1} \cdot \cos(\phi_j)}{n_j \cdot \cos(\phi_{j-1}) + n_{j-1} \cdot \cos(\phi_j)} \quad j := 1, 2, \dots (2 - 12a)$$

$$r_{sj} := \frac{n_{j-1} \cdot \cos(\phi_{j-1}) - n_j \cdot \cos(\phi_j)}{n_{j-1} \cdot \cos(\phi_{j-1}) + n_j \cdot \cos(\phi_j)} \quad j := 1, 2, \dots (2 - 12b)$$

In the case of the study under consideration in the thesis, there are only two interfaces and hence the range variable runs only up to 2. Reflection from the two interfaces (ambient-film and film-substrate) introduces a phase shift

$$\delta = 2\pi / \lambda n_1 d \cos(\phi_1) \quad (2 - 13)$$

With incorporation of Equation 2-12 in 2-10, the exact equation of ellipsometry now becomes

$$\tan(\Psi) \cdot \exp(i\Delta) = \frac{(r_{p1} + r_{p2} \cdot e^{-2 \cdot i \cdot \delta}) \cdot (1 + r_{s1} \cdot r_{s2} \cdot e^{-2 \cdot i \cdot \delta})}{(1 + r_{p1} \cdot r_{p2} \cdot e^{-2 \cdot i \cdot \delta}) \cdot (r_{s1} + r_{s2} \cdot e^{-2 \cdot i \cdot \delta})} \quad (2 - 14)$$

Equation (2-14) involves complex quantities and yields two equations on separating the real and imaginary parts: thus one set of measurements of Ψ and Δ under certain experimental conditions can be used to determine two unknowns such as the thickness and refractive index of the film. Equation (2-14) cannot be inverted analytically and must therefore be solved numerically. A small application written in MathCAD, written by Dr. Murali Sastry⁴⁰ was used to numerically solve these equations and calculate the thickness of the films.

We have assumed the refractive index of all films (before and after DNA uptake) to be 1.5 and calculated the thickness of the lipid films before and after DNA intercalation by using the exact equation of ellipsometry.

2.13. CONTACT ANGLE MEASUREMENTS.

Contact angle measurements are sensitive to changes in the surface and one can probe any changes in surface hydrophobicity by this technique. We have performed contact angle measurements of our lipid films before and after DNA intercalation using a Rame Hart 100 Goniometer. There is clearly substantial incorporation of the DNA molecules in the lipid matrix in all the DNA molecules studied herein. There are two possible modes by which the DNA may be immobilized in the ODA films, viz., purely surface binding and entrapment within the lipid bilayers. In order to resolve this issue, contact angle measurements were done on a 250 Å thick ODA film on a quartz substrate before and after immersion of the film in 10^{-6} M double-stranded DNA solution for 4 hours and the values obtained were 90° and 89° . These values represent averages over 10 measurements carried out over the whole film surface. These values indicate a hydrophobic surface in both cases. Thus, the DNA molecules are intercalated into the lipid matrix by electrostatic immobilization within the hydrophilic regions of the ODA bilayers.

2.14. REFERENCES:

- (1) a) Damle, C.; Kumar, A.; Sasrty, M. *J. Phys. Chem.* **2002**, *106*, 297; b) Gole, A.; Sastry, M. *Inorg. Chem. Commun.*, **2001**, *4*, 568; c) Pal, S. Ph.D. Thesis, University of Poona, **1996**; d) Ganguly, P.; Pal, S.; Sastry, M.; Shashikala, M.N. *Langmuir* **1995**, *11*, 1078.
- (2) a) Sastry, M. *Curr.Sci.* **2000**, *72*, 1089; b) Patil, V.; Sastry, M. *Langmuir* **2000**, *16*, 2207; c) Patil, V.; Malvankar, R.B.; Sastry, M. *Langmuir* **1999**, *15*, 8197; d) Patil, V.; Mayya, K.S.; Sastry, M. *Langmuir* **1998**, *14*, 2707; e) Sastry, M.; Patil, V.; Sainkar, S.R. *J.Phys.Chem.B.* **1998**, *102*, 1404; f) Sastry, M.; Patil, V.; Mayya, K.S. *Langmuir* **1997**, *13*, 4490; g) Patil, V.; Sastry, M. *Langmuir* **1997**, *13*, 5511; h) Patil, V.; Sastry, M. *J. Chem. Soc., Faraday Trans.* **1997**, *93*, 4347.
- (3) a) Gole, A.; Sastry, M. *Biotech. Bioeng.* **2001**, *74*, 172; b) Gole, A.; Chaudhari, P.; Kaur, J.; Sastry, M. *Langmuir* **2001**, *17*, 5646; c) Gole, A.; Vyas, S.; Sainkar, S.R.; Lachke, A. L.; Sastry, M. *Langmuir* **2001**, *17*, 5964; d) Gole, A.; Dash, C.; Rao, M.; Sastry, M. *J.Chem.Soc.Chem.Comm.* **2000**, 297; e) Gole, A.; Dash, C.; Mandale, A. B.; Rao, M.; Sastry, M. *Anal.Chem.* **2000**, *72*, 4301.
- (4) a) Sastry, M.; Ramakrishnan, V.; Pattarkine, M.; Ganesh, K.N. *J.Phys.Chem.B* **2001**, *105*, 4409; b) Ramakrishnan, V.; Sable, M.; D'Costa, M.; Ganesh, K.N.; Sastry, M. *J.Chem. Soc. Chem.Comm.* **2001**, 2622.
- (5) Handbook of Thin Film Technology by Leon. I. Maissel and Reinhard Glang.
- (6) Beaucage, S.L.; Caruthers, M.H. *Tetrahedron Lett.* **1981**, *22*, 1859.

- (7) Cantor, C.R.; Schimmel, P.R. *Biophysical Chemistry, Part III*, W.H. Freeman, New York (1980).
- (8)a) Ebara, Y.; Mizutani, K.; Okahata, Y. *Langmuir* **2000**, *16*, 2416; b) Kago, K.; Matsuoka, H.; Yoshitome, R.; Yamaoka, H.; Ijio, K.; Shimomura, M. *Langmuir* **1999**, *15*, 5193; c) Shimomura, M.; Nakamura, F.; Ijio, K.; Taketsuna, H.; Tanaka, M.; Nakamura, H.; Hasebe, K. *J.Am.Chem.Soc.* **1997**, *119*, 2341; d) Okahata, O.; Kobayashi, T.; Tanaka, K. *Langmuir* **1996**, *12*, 1326; e) Ijio, K.; Shimomura, M.; Tanaka, M.; Nakamura, H.; Hasebe, K. *Thin Solid Films* **1996**, *284*, 780.
- (9) Ahlers, M.; Muller, W.; Reichert, A.; Ringsdorf, H.; Venzmer, J. *Angew.Chem.Int.Ed.Engl.* **1990**, *29*, 1269.
- (10) Radler, J.O.; Koltover, I.; Salditt, T.; Safinya, C.R. *Science* **1997**, *275*, 810.
- (11) Sastry, M.; Ramakrishnan, V.; Pattarkine, M.; Gole, A.; Ganesh, K.N. *Langmuir* **2000**, *16*, 9142.
- (12) Ramakrishnan, V.; D'Costa, M.; Ganesh, K.N.; Sastry, M. *Langmuir* (in press).
- (13) a) Langmuir, I. *J.Am.Chem.Soc.* **1917**, *39*, 1848; b) Ulman, A. *An introduction to Ultrathin Organic Films: from Langmuir-Blodgett to Self-Assembly*, Academic Press, San Diego, CA, **1991**.
- (14) a) Janshoff, A.; Galla, H.J.; Steinem, C. *Angew.Chem.Int.Ed.* **2000**, *39*, 4004; b) Buttry, D. A.; Ward, M.D. *Chem. Rev.* **1992**, *92*, 1356.
- (15) Sauerbrey, G. *Z.Phys. (Munich)* **1959**, *155*, 206.
- (16) a) Hook, F.; Rodahl M.; Kasemo, B.; Brzezinski, P. *Proc.Natl.Acad.Sci.USA* . **1998**, *95*, 122271; b) Hook, F.; Rodahl, M.; Brzezinski, P.; Kasemo, B. *Langmuir*. **1998**, *14*, 729; c) Muratsugu, M.; Ohta, F.; Miya, Y.; Hosokawa, T.; Kuroswa, S.; Kamo, N.; Ikeda, H. *Anal.Chem.* **1993**, *65*, 2933; d) Cheek, G.T.; O' Grady, W.E. *J.Electroanal. Chem.*, **1990**, *277*, 341; e) Burrell, M. C.; Armstrong, N.R. *Langmuir* **1986**, *2*, 37.
- (17) a) Bright, R.M.; Musick, M.D.; Natan, M.J. *Langmuir* **1998**, *14*, 5695; b) Anzai, J.; Takeshita, H.; Kobayashi, Y.; Osa, T.; Hoshi, T. *Anal.Chem.* **1998**, *70*, 811; c) Patil, V.; Mayya, K. S.; Pradhan, S. D.; Sastry, M. *J. Am. Chem. Soc.*, **1997**, *119*, 9281; d) Caruso, F.; Niikura, K.; Furlong, N.; Okahata, Y. *Langmuir*. **1997**, *13*, 3427; e) Brust, M.; Etchonique, R.; Calvo, E.J.; Gordillo, G.J. *J.C.S. Chem. Commun.*, **1996**, 1949.
- (18) a) Okahata, Y.; Kawase, M.; Niikura, K.; Ohtake, F.; Furusawa, H.; Ebara, Y. *Anal.Chem.* **1998**, *70*, 1288; b) Bardea, A.; Dagan, A.; Ben-Dov, I.; Amit, B.; Willner, I. *J.Chem. Soc. Chem. Commun.* **1998**, 839; c) Caruso, F.; Rodda, E.; Furlong, D.N.; Haring, V. *Sens.Actuators B*. **1997**, *41*, 189; d) Caruso, F.; Rodda, E.; Furlong, D.N.; Niikura, K.; Okahata, Y. *Anal.Chem.* **1997**, *69*, 2043.
- (19) Matsuno, H.; Furusawa, H.; Okahata, Y. *Chem.Commun.* **2002**, 470.

- (20) Curie, P.; Curie, J. C. R. *Acad. Sci.* **1880**, *91*, 294.
- (21) Denney, R.C.; Sinclair, R. *Visible and Ultraviolet Spectroscopy. Analytical Chemistry by open learning series*, John Wiley and Sons, USA.
- (22) Cantor, C.R.; Schimmel, P.R. *Biophysical chemistry, Part II* : W.H. Freeman, New York **(1980)**.
- (23) LePecq, J.B.; Paoletti, C. *J.Mol.Biol.* **1967**, *27*, 87.
- (24) Sastry, M.; Kumar,A.; Pattarkine, M.; Ramakrishnan, V.; Ganesh, K.N. *J.Chem.Soc.Chem. Commun.* **2001**, 1434.
- (25) Rendell, D.; Mowthorpe, D. *Fluorescence and Phosphorescence Spectroscopy: Analytical Chemistry by open learning*. John Wiley & Sons, USA, **1987**.
- (26) Fraser, M.J.; Fraser, D.B. *Nature*.**1951**, *167*, 759.
- (27) Neault, J.F.; Tajmir -Riahi, H.A. *J.Phys.Chem.B.* **1998**, *102*, 1610.
- (28) Pohle, W.; Selle, C.; Gauge r, D.R.;Zantal, R.; Artzner, F.; Radler, J.O. *Phys.Chem.Chem.Phys.* **2000**, *2*,4642.
- (29) Taillandier, E.; Liquier, J. *Methods in Enzymology* **1992**, *211*, 307.
- (30)George, W.O.; McIntyre, P.S. *Infrared Spectroscopy: Analytical Chemistry by open learning*, John Wiley and Sons, USA, **1987**.
- (31) Hostetler, M.J.; Stokes, J.J.; Murray,R.W. *Langmuir*, **1996**, *12*, 3605.
- (32) a) Patil,V.; Malvankar, R.B.; Sastry,M. *Langmuir*, **1999**, *15*, 8197; b) Leff, D.V.; Brandt, L.; Heath,J.R. *Langmuir*, **1996**, *12*, 4723.
- (33) Fundamentals of Photoelectron spectroscopy by Seah and Briggs.
- (34) Shirley, D.A. *Phys.Rev.B.* **1972**, *5*, 4709. An application written by Dr. Murali Sastry(MS) in Mathcad (a commercial mathematical software package), SHIRL.MCD was used for the analysis. This application is available from the Mathsoft public domain site.
- (35) Gray, D.M.; Ratliff, R.L.; Vaughan, M.R. *Methods in Enzymology*, **1992**, *211*, 389.
- (36) Tunis, M.J.B.; Maestre, M.F. *J.Mol.Biol.* **1970**, *52*, 521.
- (37) Pohl, F.M.; Jovin, T.M. *J. Mol.Biol.* **1980**, *142*, 315.
- (38) a) Hall, A.C. *Surf. Sci.*, **1969**, *16*, 1; b) Azzam, R.M.A.; Bashara, N.M.; *Ellipsometry and Polarized Light.*; **1977**, North-Holland: Amsterdam.

- (39) Fresnel reflection coefficients are complex quantities describing the ratio of the reflected electric field component to the incident field component for the p and s directions, respectively. Thus, they are a measure of the amplitude ratio and phase difference upon reflection for the subscripted component. The Fresnel reflection coefficients, r_p and r_s are defined as ratios of the reflected and incident electric fields (including both the amplitude and complex phase factors) for the p and s components.
- (40) Granqvist, C.G.; Hunderi, O.; *Phys. Rev. B*, **1977**, *16*, 3513.
- (41) Sastry, M. *Phys.Edu.* **1996**, 262.

CHAPTER III

IMMOBILIZATION AND HYBRIDIZATION OF DNA AT THE AIR - WATER INTERFACE

The hybridization of DNA by sequential electrostatic and hydrogen-bonding immobilization of single-stranded complementary oligonucleotides at the air-water interface with cationic Langmuir monolayers is demonstrated in this chapter. The complexation of the single-stranded DNA molecules with octadecylamine (ODA) Langmuir monolayers was followed in time by monitoring the pressure-area isotherms. Langmuir-Blodgett (LB) films of the ODA-DNA complex were formed on different substrates and characterized using quartz-crystal microgravimetry (QCM), Fourier transform infrared spectroscopy (FTIR), polarized-UV-vis and fluorescence spectroscopy as well as thermal melting studies. These measurements clearly showed that hybridization of the complementary single-stranded DNA molecules had occurred at the air-water interface leading to the characteristic double-helical structure. Furthermore, it was observed that the DNA molecules in the LB films were oriented parallel to the substrate withdrawal direction.

Part of the work presented in this chapter has been published in: -1) Sastry, M.; **Ramakrishnan, V.**; Pattarkine, M.; Gole, A.; Ganesh, K.N. *Langmuir* **2000**, *16*, 9142; 2) Ramakrishnan, V.; D'Costa, M.; Ganesh, K.N.; Sastry, M. (communicated to Langmuir).

3.1 INTRODUCTION

Molecular recognition is an essential phenomenon in living systems. One of the most important molecular recognition event in nature is the base pairing of nucleic acids, which guarantees the storage, transfer and expression of genetic information in living systems. With the advent of the discovery of the double helix structure of DNA, there has been no looking back in the progress of biomedical research and particularly, in the field of gene therapy.¹ As entrapment of DNA in cationic liposomes has important applications in gene therapy, the immobilization of DNA in different matrixes and on planar supports has become a prime topic of current research. Various routes have been employed for the immobilization of DNA on planar supports such as assembly at the air-water interface with Langmuir monolayers,² which is discussed in detail in the following section. Steel et al³ have compared electrostatic binding of small redox molecules to DNA in solution with DNA immobilized on alkanethiol modified gold surfaces^{3a} and have also reported electrochemical quantification on DNA immobilized on thiolated DNA on gold surfaces.^{3b} Wang et al have immobilized thiol-derivatized PNA (peptide nucleic acids) on gold surfaces.^{3c} Immobilization of oligonucleotides by self assembly process onto quartz crystal oscillators has been recently demonstrated.⁴ Caruso et al have immobilized two 30-mer oligonucleotides, one biotinylated (biotin-DNA) and the other having a mercaptohexyl group at the 5' phosphate end onto modified gold surfaces to study hybridization of nucleic acids for sensor development using a QCM.^{4c} Okahata et al have extensively used QCM technique for immobilization and hybridization of 10-30mer oligonucleotides immobilized on QCM.^{4b,d} Higashi et al have reported the attachment to terminally functionalized self-assembled monolayers (SAMs) via electrostatic^{5a}, and intercalation interactions.^{5b} Recent advances in biosensor technology have contributed significantly to our understanding of the mechanisms of molecular recognition process. In this regard, Yang et al have carried out surface plasmon resonance studies of DNA Polymerases binding to Template/ Primer DNA duplexes immobilized on supported lipid monolayers.⁶ Yet, some other methods include single molecule analysis of DNA immobilized on polystyrene micro spheres described by Balasubramanian et al.⁷

In this chapter, we have demonstrated the hybridization of DNA by sequential and pre-formed electrostatic and hydrogen-bonding immobilization of single-stranded complementary oligonucleotides at the air-water interface with cationic Langmuir monolayers.⁸ The complexation of the single-stranded DNA molecules with octadecylamine (ODA) Langmuir monolayers was followed in time by monitoring the pressure-area isotherms. A large (and slow) expansion of the ODA monolayer was observed during each stage of complexation in the following sequence : primary single-stranded DNA followed by

complementary single-stranded DNA followed by the intercalator, ethidium bromide. Langmuir-Blodgett (LB) films of the ODA-DNA complex were formed on different substrates and characterized using quartz-crystal microgravimetry (QCM), Fourier transform infrared spectroscopy (FTIR), polarized-UV-vis and fluorescence spectroscopy as well as thermal melting studies. These measurements clearly showed that hybridization of the complementary single-stranded DNA molecules had occurred at the air-water interface leading to the characteristic double-helical structure. Furthermore, it was observed that the DNA molecules in the LB films were oriented parallel to the substrate withdrawal direction.

In this chapter, we have also looked at the effect of salt on the hybridization of single stranded oligonucleotides and pre-formed DNA duplexes at the air-water interface with cationic Langmuir monolayers.⁹ It was observed from the pressure area isotherms that there is a large expansion of the monolayer in the presence of salt with the primary strand compared to the pressure area isotherms with only langmuir monolayers. On addition of the complementary strand, there was no further expansion of the monolayer indicating that equilibrium had reached very quickly. In order to check the role of headgroups/ hydrocarbon chain packing, we looked at the immobilization and hybridization of single stranded oligonucleotides and pre-formed duplexes with the double chain lipid 1,2-Dioleoyloxytrimethyl ammonium propane (DOTAP) at the air-water interface. Pre-formed DNA hybrids with salt in solution on complexation with ODA/DOTAP monolayers also showed a very large expansion in the pressure-area isotherms. Furthermore, melting transition temperatures for pre-formed duplexes and sequentially immobilized DNA molecules with ODA as well DOTAP monolayers in presence of salt indicates stabilization of the hybridized DNA molecules at the air-water interface.

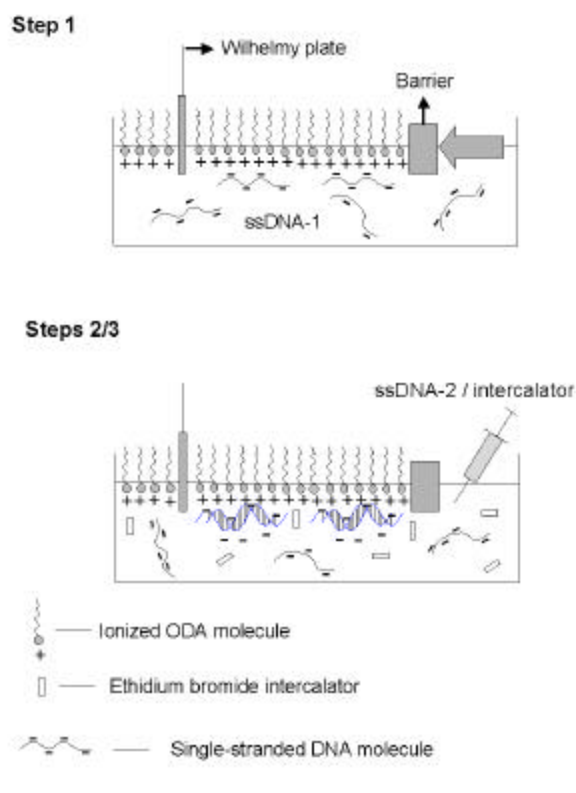
3.2 DNA HYBRIDIZATION AT AIR-WATER INTERFACE

The air-water interface has proven to be excellent media for the organization of large inorganic ions,¹⁰ biomacromolecules such as proteins/enzymes¹¹ and in the growth of oriented crystals.¹² The air-water interface as an organizational medium for nanoscale structures has received considerable attention. In this laboratory, much research effort has been focused on studying the electrostatic immobilization of suitably derivatized colloidal metal particles at the air-water interface using Langmuir monolayers.¹³ Molecular recognition between signal peptides and receptor proteins is a basic feature of many biological processes. Kunitake et al have observed molecular recognition of aqueous Dipeptides at multiple hydrogen bonding sites of mixed monolayers at the air-water interface.¹⁴ Langmuir monolayers of lipid molecules have frequently been used as models to understand the organization and function of biological membranes.¹⁵

Studies on DNA immobilization at the air-water interface have thus far concentrated on electrostatic complexation of preformed double-helical DNA molecules with cationic lipid Langmuir monolayers.² Electrostatic forces have been used as driving force for the complex formation. One such example is the complex of the cationic lipid and the DNA molecule.^{4d} Okahata et al have studied the orientation of DNA strands along the dipping direction of LB film.^{4c} It was confirmed by X-ray diffraction patterns and polarization spectra that the dye-intercalated DNA strands were aligned along the dipping direction in the LB films. Yet, in another study, Kago et al have observed the fine structure of the lipid-DNA complex at the air-water interface by X-ray Reflectometry.^{4a} Also, studies on DNA hybridization at the air-water interface have been carried out involving hydrogen bonding between alkylated monolayer forming nucleobases and complementary water-soluble bases¹⁶ and oligonucleotides.¹⁷ Base pairing between the monolayer forming amphiphilic nucleobases with water soluble bases at the air-water interface might be a driving force of molecular organization termed as molecular recognition directed self-assembly. Shimomura et al have reported the tailoring of two-dimensional DNA-mimetic molecular organization at the air-water interface.¹⁶ They have used fluorescence microscopic imaging for how nucleobase amphiphilicities are organized to two-dimensional (2-D) molecular assemblies at the air-water interface. The lipid monolayer at the air-water interface has been widely used as model surface of biological membranes. Kunitake¹⁷ and other workers¹⁶ have stated that molecular recognition of small molecules based on hydrogen bond formation could be observed at the lipid surface but could not be observed in bulk solution. Through elegant QCM measurements, Okahata and co-workers have recently shown that alkylated monolayer forming nucleobases recognize linear oligonucleotides introduced into the subphase.¹⁸ Hydrogen bonding between complementary bases (alkylated-A and linear oligonucleotide-T molecules) leads to the recognition at the air-water interface while such a hydrogen-bonding is not possible in the bulk of the subphase.¹⁸

The immobilized DNA on monolayers contributes to better understanding of DNA drug interactions and also studying molecular recognition procedures.^{5b} The DNA-lipid LB films would serve as molecular devices for one-dimensional electron transfer and conduction along stacked base pairs.¹⁶

We show herein that complementary ssDNA strands sequentially immobilized at the air-water interface by electrostatic interaction with cationic octadecylamine (ODA) Langmuir monolayers do indeed hybridize to yield double-helical DNA molecules. The procedure is illustrated in Schematic 3.2.1 and will be discussed subsequently.



Scheme 3.2.1 : Diagram showing the various stages of immobilization/hybridization of DNA molecules at the air-water interface with cationic ODA Langmuir monolayers. **Step 1** : spreading of ODA on the ssDNA-1 subphase followed by immobilization of ssDNA-1 at the air-water interface; **steps 2/3** : introduction into the trough and complexation of the complementary ssDNA-2/ethidium bromide intercalator molecules with ssDNA-1 molecules immobilized at the air-water interface. The various components in the diagram are explained at the bottom of the scheme.

3.2.1 Synthesis of DNA sequences :

Oligonucleotides of the sequence GGAAAAACTTCGTGC (ssDNA-1), GCACGAAGTTTTTACC (ssDNA-2) and AGAAGAAGAAAAGAA (ssDNA-3) were synthesized by β -cyanoethyl phosphoramidite chemistry (described in detail in chapter 1) on a Pharmacia GA plus DNA synthesizer and purified by FPLC and rechecked by RP HPLC. ssDNA-1 and ssDNA-2 are complementary oligonucleotides while ssDNA-1 and ssDNA-3 are non-complementary.

3.2.2 Surface complexation of DNA and formation of LB films:

A known quantity of 1 mg/ml concentrated solution of octadecylamine (ODA, used as-received from Aldrich) in chloroform was spread on the surface of 10^{-8} M concentrated solution of ssDNA-1 in deionized water (pH = 5.8) in a Nima 611 Langmuir-Blodgett trough equipped with a Wilhelmy plate for surface pressure sensing (Scheme 3.2.1, step 1). After

evaporation of the solvent (typically 20 minutes after spreading the monolayer), pressure–area (π -A) isotherms were recorded at room temperature as a function of time at a compression/expansion rate of 50 cm²/minute.

After equilibration of the ssDNA density at the air-water interface, the ODA-ssDNA-1/dsDNA monolayer was transferred by the Langmuir-Blodgett technique¹⁹ onto gold-coated quartz substrates for quartz crystal microgravimetry (QCM) measurements. QCM's are known to be very sensitive mass measuring devices in which resonance frequency decreases with increase of mass on the electrode at the nM level.²⁰ After the QCM measurements mentioned above, 4 ml of ssDNA-2/3 in water was injected into the non-monolayer side of the trough to yield an overall oligonucleotide concentration in the aqueous subphase of 10⁻⁸M (Scheme 3.2.1, step 2). Care was taken to remove an equal quantity of water prior to ssDNA insertion and maintain the water level in the trough constant. The π -A isotherms were recorded as a function of time.

In order to test whether the expansion observed in the π -A isotherms on insertion of the complementary ssDNA-2 is due to hybridization and formation of duplex structures at the air-water interface, ethidium bromide was introduced into the trough as illustrated in Scheme 3.2.1, step 3. The concentration of ethidium bromide was adjusted to be 10⁻⁸ M in the subphase. Ethidium bromide is known to intercalate into the base pairs of DNA double helical structures and this process is readily detected by the enhanced fluorescence exhibited by this molecule on intercalation in DNA.²¹ LB films of the ODA-ssDNA-1/ssDNA-2 monolayers after introduction of the intercalator were transferred onto the QCM crystal and the mass uptake recorded as a function of number of immersion cycles.

3.3 PRESSURE-AREA ISOTHERMS AND QCM MEASUREMENTS

Curves 1 and 2 in Fig.3.3.1.A represent the π -A isotherm compression/expansion cycles of the ODA Langmuir monolayer at time = 1 and 12 h respectively after spreading the monolayer on the ssDNA-1 subphase. A large, albeit slow, expansion of the monolayer to an area/molecule value of 35 Å² is observed which remained constant thereafter. This is to be compared with the ~21 Å²/molecule takeoff area for the ODA Langmuir monolayer on 10⁻⁸M ethidium bromide solution as the subphase measured 4 h after spreading the monolayer (dotted line, Fig.3.3.1A).

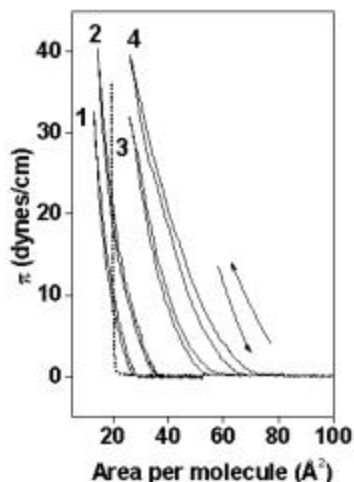


Figure 3.3.1. : π -A isotherms recorded from an ODA monolayer on water at various times after introduction of DNA/intercalator molecules into the subphase (as per Scheme 3.2.1).

Curves 1 and 2 : π -A isotherms recorded 1 h and 12 h after spreading ODA on the ssDNA-1 subphase respectively; curve 3 : π -A isotherm recorded 12 h after introduction of ssDNA-2 into the subphase and curve 4 : π -A isotherm recorded 12 h after introduction of ethidium bromide intercalator into the subphase. The dotted line corresponds to the π -A isotherm recorded from an ODA monolayer on 10^{-8} M solution of ethidium bromide in deionized water as the subphase.

In this situation, both the ODA monolayer and the ethidium bromide molecules are cationic and therefore, the DNA intercalator does not complex with the ODA monolayer and no expansion of the Langmuir monolayer is observed. This slow expansion of the monolayer is clearly due to complexation of ssDNA-1 molecules with the ODA monolayer by attractive electrostatic interaction (Scheme 3.2.1, step 1) and indicates that the diffusion of the DNA molecules to the air-water interface is extremely slow. Sastry et al²² have observed a similar time-dependence in the complexation of surface-modified colloidal silver particles with ODA monolayers at the air-water interface. At pH = 5.8, the ODA molecules ($pK_B = 10.8$) would be completely ionized leading to maximum attractive coulombic interaction with the anionic DNA molecules in solution. We would like to point out that little hysteresis was observed in the compression/expansion cycles of this and other air-water interface complexation experiments to be discussed below. The above result indicates that the ODA-DNA conjugate monolayers at the air-water interface are stable. After equilibration of the ssDNA density at the air-water interface, the ODA-ssDNA-1 monolayer was transferred by the Langmuir-Blodgett technique onto gold-coated quartz substrates for quartz crystal microgravimetry (QCM) measurements. A plot of the QCM mass uptake recorded as a function of number of immersion cycles in the ODA-ssDNA-1 monolayer is shown in Fig.3.3.2, curve 1, circles.

The transfer ratio (Table 3.3.1) was close to unity both during the downward and upward strokes of the QCM substrate.

TABLE 3.3.1

Transfer ratios for sequentially immobilized ssDNA-1+ssDNA-2-ODA monolayer.

No. of Dips	In (%)	Out (%)
1	84	84.3
2	47.2	40.2
3	35.9	35.3
4	29.6	31.4
5	33.8	32.5
6	31.9	32.5
7	20.4	24.0
8	23.3	30.6
9	24.2	19.9
10	20.6	33.3

Uniform, lamellar growth of the ODA-DNA monolayer is thus clearly seen from QCM and transfer ratio data. The slope of the curve was determined from a linear fit to the QCM data to be 1450 ng/cm² per dip. The molecular weight of ODA is 269.5. The number of ODA molecules in the bilayer is $2 / (21 \times 10^{-16})$ and is ca. 9.52×10^{14} /cm². This then represents the number of charges due to ODA in the bilayer, assuming complete ionization of the ODA monolayer. (The mass of the bilayer of ODA/cm² is thus $(9.52 \times 10^{14} \times 269.5) / 6.024 \times 10^{24} \sim 421$ ng/cm²). The molecular weight of ssDNA-1 is 5280. The contribution to the QCM mass uptake from the DNA molecules is $1450 - 426 \sim 1024$ ng/cm². As shown above, the number of DNA molecules/cm² of the film can be shown to be $\sim 1.17 \times 10^{14}$ /cm². Accounting for the charges on the individual DNA molecules (16 per molecule) the charge ratio of DNA: ODA in the bilayers can be calculated to be $1.87 \times 10^{15} : 9.52 \times 10^{14}$ indicating that there is overcompensation of the positive charge due to ODA by the negatively charged DNA molecules by roughly a factor of 2. Such a charge overcompensation is known to occur during complexation of large inorganic ions such as Keggin anions at the air-water interface²³ as well as in electrostatically formed multilayers of cationic and anionic polyelectrolyte films, in multilayer films of polyelectrolytes and DNA,²⁴ as well as in multilayers of positively and negatively charged nanoparticles.²⁵

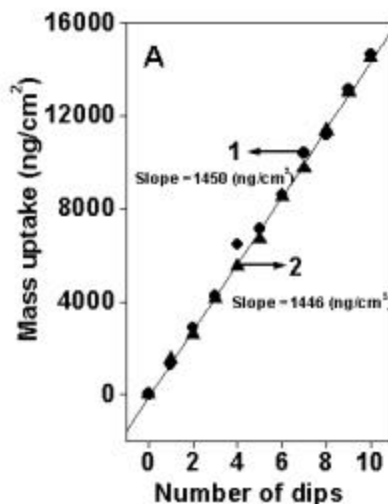


Fig 3.3.2. : QCM mass uptake recorded as a function of number of immersion cycles in ODA monolayers complexed with ssDNA-1 (curve 1) and ODA complexed with ssDNA-1 and further hybridization with ssDNA-2 (curve 2).

After the QCM measurements mentioned above, 4 ml of ssDNA-2 in water was injected into the non-monolayer side of the trough to yield an overall oligonucleotide concentration in the aqueous subphase of 10^{-8} M (Scheme 3.2.1, step 2). Care was taken to remove an equal quantity of water prior to ssDNA insertion and maintain the water level in the trough constant. The π -A isotherms were recorded as a function of time and the isotherm recorded 12 h after introduction of ssDNA-2 is shown as curve 3 in Fig.3.3.1. A further increase in ODA monolayer area is clearly seen, the takeoff area shifting to a stable $53 \text{ \AA}^2/\text{molecule}$. Two possible hypotheses may be advanced to explain this result. The expansion may be either due to direct complexation of the ssDNA-2 molecules with uncoordinated ODA monolayer regions at the air-water interface or an elongation due to uncoiling of the ssDNA molecules already immobilized at the air-water interface during step 1 due to hybridization with the complementary DNA molecules, ssDNA-2. The former is not likely given that charge overcompensation of the ODA monolayer by ssDNA-1 molecules was indicated by QCM measurements. Entropic considerations would lead to some replacement of ssDNA-1 by ssDNA-2 molecules at the air-water interface but since they are of the same length and charged to a similar extent, an expansion of the monolayer would not occur under these circumstances. An uncoiling of the immobilized ssDNA-1 molecules by hybridization of ssDNA-2 molecules is thus indicated.

In order to test whether the expansion observed in the π -A isotherms on insertion of the complementary ssDNA-2 is due to hybridization and formation of duplex structures at the air-water interface (curve 3, Fig.3.3.1), ethidium bromide was introduced into the trough as illustrated in Scheme 3.2.1, step 3. The concentration of ethidium bromide was adjusted to be 10^{-8} M in the subphase. Ethidium bromide is known to intercalate into the base pairs of DNA double helical structures and this process is readily detected by the enhanced fluorescence exhibited by this molecule on intercalation in DNA.²⁶ The π -A isotherm recorded 12 h after introduction of ethidium bromide shows a further expansion in the monolayer with the takeoff area shifting to $70 \text{ \AA}^2/\text{molecule}$ (curve 4, Fig.3.3.1). This result indicates intercalation in the DNA double helix formed by sequential adsorption of ssDNA-1 and ssDNA-2 at the air-water interface thereby leading to a further extension of the double helical DNA molecules adsorbed at the interface. This observation is consistent with atomic force microscopy studies of interaction of probe molecules with DNA where it was demonstrated that among the various binding modes of drug molecules with DNA, intercalation leads to elongation of the DNA double helical structures.²⁷ The ethidium bromide molecules intercalate into alternate base-pair sites in the helical structure and this process is accompanied by a 3.4 \AA expansion in the length of the double helix per intercalator molecule insertion.^{26,27} The expansion in the area per ODA molecule on intercalation of the DNA double helical structures with ethidium bromide (step 3, Scheme 3.2.1) from 53 \AA^2 to 70 \AA^2 (expansion by $\sim 32 \%$) may be accounted for if one assumes that roughly 5 out of the 8 sites per DNA molecule are intercalated by ethidium bromide molecules. This would lead to an increase in length of the DNA molecules by 17 \AA and works out to a $\sim 31 \%$ increase in the length of the DNA molecule (normal length $\sim 55 \text{ \AA}$). This result is consistent with further uptake of ethidium bromide indicated in the fluorescence measurements shown below in Fig.3.4.1.

LB films of the ODA-ssDNA-1/ssDNA-2 monolayers after introduction of the intercalator were transferred onto the QCM crystal and the mass uptake recorded as a function of number of immersion cycles (Fig.3.3.2, curve 2, up triangles). A lamellar growth mode is clearly seen for the hybridized DNA-ODA LB films and interestingly, the mass uptake per dip (slope of curve 2, Fig.3.3.2) is almost identical to that obtained for the ODA-ssDNA-1 LB film. An explanation for this result is postponed until hybridization of the complementary single-stranded DNA molecules at the air-water interface is established.

3.4 FLUORESCENCE STUDIES

19 monolayer (ML, 10 dips) LB films of the ODA molecules complexed with ssDNA-1 followed by ssDNA-2 molecules and ethidium bromide were grown on quartz

substrates and the fluorescence spectrum recorded. Fig.3.4.1. shows the spectrum recorded from the above film (curve 2).

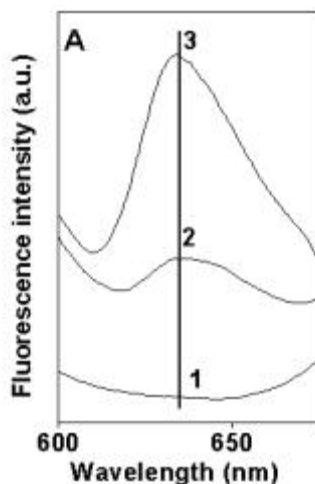


Fig 3.4.1: Fluorescence spectra of : Curve 1 – 19 ML LB film of ODA-ssDNA-1 complexed with ssDNA-3 and ethidium bromide intercalator; curve 2 – 19 ML LB film of ODA-ssDNA-1 hybridized with ssDNA-2 with ethidium bromide as intercalator and curve 3 – spectrum from the 19 ML LB film shown as curve 2 after further immersion in ethidium bromide solution for 12 h.

A clear fluorescence signal at 635 nm can be seen and thus indicates the hybridization of the complementary oligonucleotides ssDNA-1 and ssDNA-2 at the air water interface to form double helical structures. The emission wavelength is red-shifted relative to the solution DNA-intercalant value of 580 nm. This shift may be due to differences in the polarity of the fluorescent probe and is consistent with literature observation on ethidium bromide complexes with DNA.²⁵ Immersion of this film in 10^{-7} M ethidium bromide solution for a further period of 12 h leads to an enhancement of the fluorescence signal (Fig.3.4.1, curve 3). The concentration of ethidium bromide in the DNA subphase is thus clearly not sufficient for complete intercalation in the DNA helical structures formed at the Langmuir monolayer interface and this result is in agreement with estimates of degree of intercalation from expansion of the ODA Langmuir monolayer in step 3 of the protocol (Scheme 3.2.1 and reference 26). In a control experiment, the sequential immobilization procedure was repeated with a non-complementary oligonucleotide, ssDNA-3 in Scheme 3.2.1, step 2 in place of the complementary ssDNA-2 molecules. The protocol is completed by addition of ethidium bromide into the subphase as discussed for the ssDNA-2 hybridization case discussed earlier. The fluorescence spectrum measured from a 19 ML LB film formed in this experiment is shown in Fig.3.4.1, curve 1. It is clear that the ethidium bromide molecules do not bind to the DNA molecules immobilized at the air-water interface. This emphatically shows that

hybridization to yield the double helical structure does not occur in the ssDNA-1/ssDNA-3 sequential assembly experiment and together with the fluorescence results shown in curves 2 and 3, demonstrates the molecular recognition process occurring at the Langmuir monolayer interface.

3.5 FTIR STUDIES

Additional evidence of the hybridization of DNA and intercalation of ethidium bromide is provided by Fourier transform infrared spectroscopy (FTIR) analysis of 19 ML LB films of the ODA-ssDNA-1, ODA-hybridized DNA (with ethidium bromide intercalator) and bare ODA films transferred onto Si (111) wafers by the LB method (Fig.3.5.1).

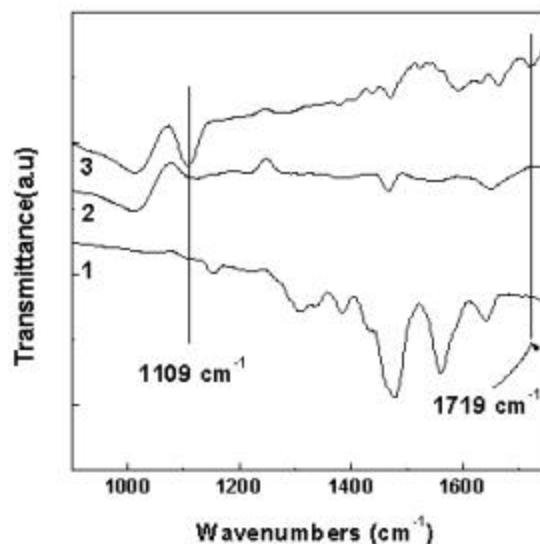


Fig. 3.5.1: FTIR spectra recorded from 19 ML films of ODA deposited onto Si (111) substrates from : curve 1 – aqueous subphase of ethidium bromide; curve 2 – ssDNA-1 solution as the subphase and curve 3 – ssDNA-1 + ssDNA-2 subphase. Two peaks are shown in the figure and indicate hybridization of the DNA strands in sample 3 (curve 3).

A comparison of the FTIR spectra of LB films of ODA-ssDNA-1 (Fig.3.5.1, curve 2) and ODA-hybridized DNA (Fig.3.5.1, curve 3) in the range $1050 - 1750 \text{ cm}^{-1}$ yields an increase in intensity of two prominent features at 1109 cm^{-1} and 1719 cm^{-1} in the hybridized DNA LB film. It is to be noted that these features are not present in the bare ODA LB film (Fig.3.5.1, curve 1) and thus, are clearly signatures from the entrapped DNA molecules in the LB films. The increase in intensity at 1719 cm^{-1} , which is due to resonance in the mainly G-band, has been observed in the case of intercalation of chlorophyllin molecules in hybridized calf-thymus DNA.²⁸ The increase in intensity of the resonance at 1109 cm^{-1} is due to the deoxyribose band and is also an indicator of the hybridization of the DNA molecules in the LB film.²⁸

3.6. UV-MELTING STUDIES

UV –melting studies of a 19 ML thick ODA- DNA film, further confirmed hybridization of the sequentially immobilized oligonucleotides at the air-water interface. . The quartz substrates bearing the films were cut so as to fit into the cuvette normally used for liquid samples. The DNA-ODA films were heated at a rate of 0.5 °C per minute and the thermal denaturation of the duplex was followed by monitoring changes in the absorbance at 260 nm as a function of temperature. A 250 Å thick ODA film on quartz was taken as the reference. The UV-vis transition of a 19 ML thick ODA-hybridized DNA film was measured and yielded a sigmoidal curve characteristic of duplex melting with a transition temperature of 55 °C (Fig.3.6.1). This is to be compared with the solution melting transition temperature of 41 °C for duplexes of ssDNA-1 and ssDNA-2³⁴ and indicates stabilization of the double-helix structure in the ODA lipid matrix.

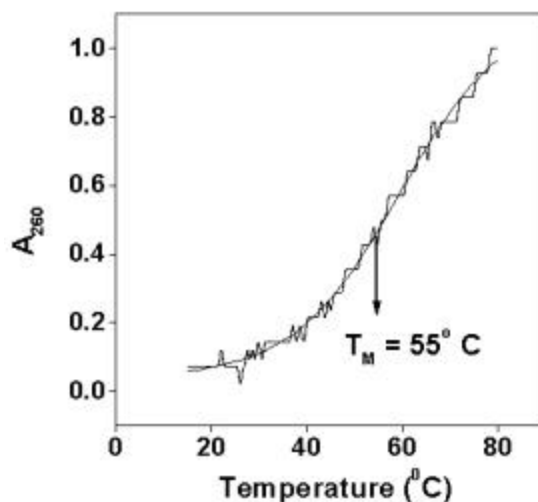


Fig. 3.6.1. UV-temperature plot of a 19 ML ODA film complexed with ssDNA-1 + ssDNA2 double strands on quartz. The melting transition temperature (T_M) is indicated in the figure.

3.7. POLARIZED UV-VIS SPECTROSCOPY.

Polarized UV-vis spectroscopy measurements (carried out on a Perkin-Elmer Lambda 15 spectrophotometer) of a 19 ML hybridized DNA-ODA LB film on quartz indicated clearly orientation of the DNA molecules parallel to the substrate withdrawal direction. The dichroic ratio at 260 nm was close to 12 indicating a high degree of order in the DNA molecule orientation.^{2c}

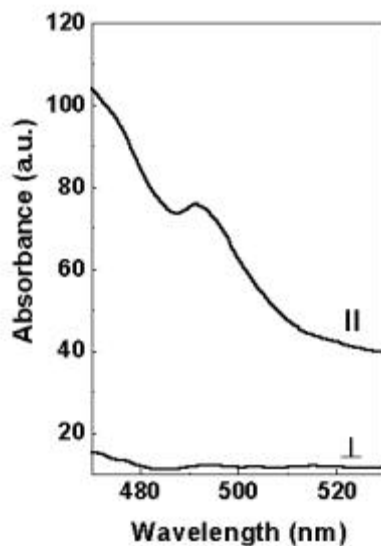


Fig. 3.7.1 : Polarized absorption spectra of a 19 ML hybridized DNA-ODA LB film on quartz.

Through elegant QCM measurements, Okahata and co-workers have recently shown that alkylated monolayer forming nucleobases recognize linear oligonucleotides introduced into the subphase.¹⁷ Hydrogen bonding between complementary bases (alkylated-A and linear oligonucleotide-T molecules) leads to the recognition at the air-water interface while such a hydrogen-bonding is not possible in the bulk of the subphase.¹⁷ As the authors themselves point out, this procedure has the inherent disadvantage that a double helical structure is not possible due to the restricted mobility of the bases bound to the alkyl chains. In that sense, to term the molecular recognition process as “DNA hybridization” may not be appropriate. In this study, there are no such constraints on the freedom of the individual ssDNA molecules. Even though electrostatically immobilized at the air-water interface, the fluorescence results clearly suggest sufficient mobility of the surface-bound ssDNA molecules to permit formation of double helical structures upon approach of the complementary DNA molecules. *The hybridization of the complementary DNA single-stranded molecules at the air-water interface demonstrated herein is thus the two-dimensional analogue of hybridization in solution, the term hybridization used in the strictest sense to mean formation of double helices.* Another interesting observation is that the hybridization of ssDNA-1 and ssDNA-2 is unlikely to occur in the bulk of the solution in the absence of any salt as in this study (deionized water). In order to overcome the repulsion between the negatively charged phosphate backbone, screening of the repulsive interaction with salt (NaCl) is required to promote the hybridization in the bulk solution.²⁹ The hybridization observed in this study occurs only at the air-water interface, with the cationic ODA Langmuir monolayer screening the repulsion between the surface-bound ssDNA-1 and solution phase ssDNA-2 molecules.

An important experimental result is that the QCM mass uptake per immersion cycle of the substrate for the ODA-hybridized DNA monolayer (Fig.3.3.2.A, curve 2) is similar to that obtained for the single-stranded DNA monolayer (Fig.3.3.2.A, curve 1). Since both ssDNA-1 and ssDNA-2 molecules are almost identical in terms of charge, it is to be expected that interactions with a charged surface (such as that provided by the ODA Langmuir monolayer) would also be similar. In order to maintain the DNA : ODA charge ratio at the air-water interface, hybridization of the DNA molecules by hydrogen bonding of ssDNA-2 to surface-bound ssDNA-1 would necessitate detachment of a certain number of surface-bound ssDNA-1 molecules *equal to the number of ssDNA-2 molecules participating in the hybridization events*. Thus, hybridization would not lead to an increase in the effective DNA concentration at the interface (measured in terms of the ssDNA concentration at the air-water interface). However, the monolayer expansion after the hybridization of ssDNA-1 and ssDNA-2 and intercalation of ethidium bromide molecules into the double helical structures (curve 4, Fig.3.4.1, effective ODA area at 30 dynes/cm $\sim 33 \text{ \AA}^2/\text{molecule}$) leads to an effective decrease in the concentration of ODA molecules in the bilayers of the LB films transferred for QCM measurements relative to the LB films formed after complexation of ssDNA-1 alone (curve 2, Fig.3.4.1, effective ODA area at 30 dynes/cm $\sim 20 \text{ \AA}^2/\text{molecule}$) and should consequently lead to a smaller mass uptake in the case of the hybridized DNA LB films. We believe the contribution to the mass uptake per immersion cycle by the intercalated ethidium bromide molecules in the ODA-hybridized DNA LB films offsets this reduction in density of the ODA molecules and results in the similar mass transfers observed in Fig.3.4.1.

3.8. CONCLUSIONS

In conclusion, the hybridization of DNA to yield double helical structures by sequential electrostatic and hydrogen-bonding immobilization of complementary single-stranded DNA molecules at the air-water interface with cationic Langmuir monolayers has been demonstrated. The double-helical DNA molecules in built-up LB films are oriented parallel to the substrate withdrawal direction. This approach is expected to lead to a better understanding of DNA-lipid and DNA-drug interactions, especially in confined spaces. Application in gene-sequencing protocols may also be envisaged.

3.9 SALT INDUCED HYBRIDIZATION OF DNA BY SEQUENTIAL AND PRE-FORMED IMMOBILIZATION OF OLIGONUCLEOTIDES IN THE PRESENCE OF ODA MONOLAYERS AT THE AIR-WATER INTERFACE.

The role of low ionic strength on the binding of preformed DNA duplexes and the hybridization of single stranded oligonucleotides at the air-water interface in the presence of cationic Langmuir monolayers of octadecylamine (ODA) is investigated. The complexation

of the single-stranded DNA molecules and pre-formed duplexes with NaCl in solution with ODA Langmuir monolayers was followed in time by monitoring the pressure-area isotherms wherein a very large and rapid expansion of the ODA monolayer was observed. In the case of sequential immobilization of complementary oligonucleotides, after addition of the complementary strand and intercalator, there was not much expansion, indicative of the fact that equilibrium had been rapidly achieved. Langmuir-Blodgett (LB) films of the ODA-DNA complex were formed on different substrates and characterized using quartz-crystal microgravimetry (QCM), fluorescence spectroscopy, and thermal melting studies. These measurements clearly showed that the pre-formed duplex retained their native form as a double helix and further, hybridization of the complementary single-stranded DNA molecules had occurred at the air-water interface leading to the characteristic double-helical structure.

3.9.1. SYNTHESIS OF DNA SEQUENCES

Oligonucleotides of the sequence GGAAAAACTTCGTGC (ssDNA-1) and GCACGAAGTTTTTCC (ssDNA-2) were synthesized β -cyanoethyl phosphoramidite chemistry on a pharmacia GA plus DNA synthesizer and purified by FPLC and rechecked RPHPLC. Pre-formed DNA duplexes (dsDNA) were obtained by mixing equimolar quantities of ssDNA-1 and ssDNA-2 with NaCl under standard hybridization conditions.³⁰ All the chemicals used were of the highest purity available. ODA was sourced from Aldrich and used as received.

3.9.2. Surface complexation of DNA with ODA monolayers and formation of LB films :

Measurements of pressure area isotherms and the transfer of monolayers on a substrate to prepare LB films were carried on the same instrument mentioned in section 3.2.2. A known quantity of 1mg/ml concentrated solution of ODA in chloroform was spread on the surface of 10^{-8} M concentrated solution of ssDNA-1 containing either 10^{-7} M NaCl for ODA monolayers in the trough. Also, a known quantity of 1mg/ml concentrated solution of ODA in chloroform was spread on the surface of 10^{-8} M concentrated solution of dsDNA containing ethidium bromide intercalator with / without NaCl (10^{-7} M). After evaporation of the solvent (typically 15 min after spreading the monolayer), the pressure area isotherms were monitored at room temperature as a function of time at a compression / expansion rate of $100\text{cm}^2/\text{min}$. After stabilization of the pressure-area isotherms for the ssDNA-1 or dsDNA with salt in solution with ODA monolayers, the ODA-DNA monolayer was transferred by the Langmuir-Blodgett technique onto gold-coated quartz substrates for quartz crystal microgravimetry (QCM) measurements. The monolayer transfer onto different substrates was effected at a surface pressure of 30 dynes/cm for all experiments in this study. After the QCM measurements, 4ml of ssDNA-2 and ethidium bromide as intercalator in water was injected into the non-monolayer of the trough to yield an overall oligonucleotide concentration in the

aqueous subphase of 10^{-8} M. Care was taken to remove an equal quantity of water prior to ssDNA-2 and intercalator insertion and maintain the water level in the trough constant and pressure-area isotherms were monitored till no further expansion of the ssDNA-2 density at the air-water interface was observed. In a similar manner mentioned above, after stabilization of the pressure-area isotherms for the ssDNA-1 and ssDNA-2 with salt and intercalator in solution with ODA monolayers, the ODA-ssDNA-1+2 monolayer was transferred by the Langmuir-Blodgett technique onto gold-coated quartz substrates for QCM measurements. 19 monolayers (ML, 10 dips) LB films each of the ODA monolayers complexed either with ssDNA-1 (with salt) followed by ssDNA-2 molecules and ethidium bromide or pre-formed duplexes (dsDNA) with / without salt and ethidium bromide were grown on quartz substrates and the fluorescence spectrum was recorded. The films grown on quartz substrates were cut to fit precisely in the quartz cuvette normally used for liquid samples. For all the set of UV-melting experiments, the film was heated at a rate of 0.5°C per minute and the thermal denaturation of the duplex was followed by monitoring changes in the absorbance at 260 nm as a function of temperature.

In the previous sections (till 3.8), the hybridization of DNA by sequential immobilization of single-stranded complementary oligonucleotides occurred only at the air-water interface with cationic ODA Langmuir monolayers. The ODA monolayer served as counter ions by effectively screening the repulsion between the surface-bound oligonucleotide sequence and solution phase complementary oligonucleotide molecule, unlike in the bulk of the solution, wherein a little amount of salt is required to promote the hybridization of ssDNA molecules. In the following section, we have looked at the salt induced effect on the pre-formed duplexes as well as sequential immobilization of DNA strands at the air-water interface with ODA monolayers in order to understand the rate of hybridization of DNA molecules and stability of the hybrids formed at the air-water interface.

Curves 4 and 5 in Fig.3.9.1.A represent the π -A isotherm compression / expansion cycles of the ODA Langmuir monolayer at time = 1/2 and 12 h respectively after spreading the monolayer on the ssDNA-1 (10^{-8}M) and salt (10^{-7}M) subphase. A very large and rapid expansion of the monolayer to an area / molecule value of 66\AA^2 is observed which remained almost constant thereafter. This is to be compared with the $\sim 21\text{\AA}^2$ /molecule takeoff area for the ODA Langmuir monolayer on 10^{-8} M ethidium bromide solution as the subphase measured 4 h after spreading the monolayer (dotted line, Fig.3.9.1.A) suggesting of complexation of ssDNA-1 molecules with salt in solution with ODA monolayers at the air-water interface.

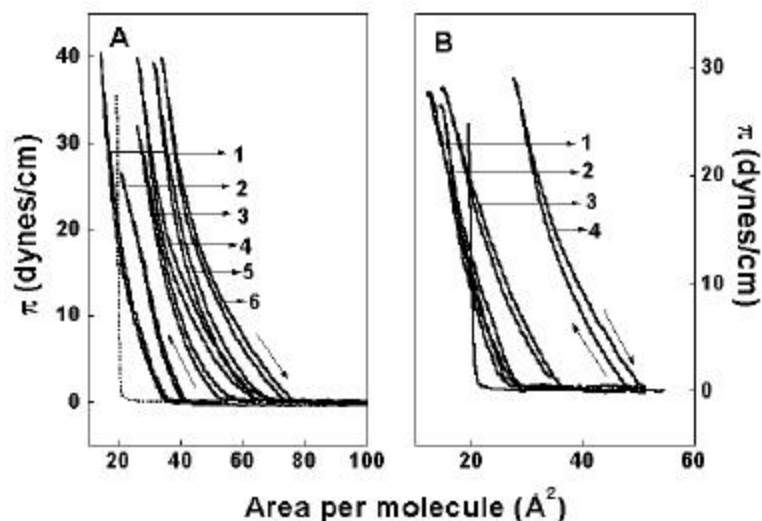


Figure 3.9.1: A) π -A isotherms recorded from an ODA monolayer on water at various times after introduction of DNA/intercalator/salt molecules into the subphase. Curves 1 and 3: π -A isotherms recorded 12 h after spreading ODA on the ssDNA-1 and ssDNA-2 subphase respectively; curves 4 and 5: π -A isotherms recorded 30 min and 12 h after introduction of ssDNA-1 and salt (10^7M) into the subphase and curve 6: π -A isotherm recorded 12 h after introduction of ssDNA-2 and ethidium bromide intercalator into the subphase containing ssDNA-1 and salt (10^7M). Curve 2: π -A isotherm recorded 12 h after spreading ODA on the NaCl (10^7M) subphase. The dotted line corresponds to the π -A isotherm recorded from an ODA monolayer on 10^{-8}M solution of ethidium bromide in deionized water as the subphase. B) π -A isotherms recorded from an ODA monolayer on water at various times after introduction of dsDNA and ethidium bromide into the subphase. Curve 1: π -A isotherm recorded 15 minutes after spreading ODA on the dsDNA (10^{-8}M) and ethidium bromide (10^7M) subphase. Curve 2: π -A isotherm recorded 15 minutes after spreading ODA on the dsDNA (10^{-8}M) containing NaCl (10^7M) and ethidium bromide (10^7M) subphase. Curve 3: π -A isotherm recorded 1 hr after spreading ODA on the dsDNA (10^{-8}M) and ethidium bromide (10^7M) subphase. Curve 4: π -A isotherm recorded 24 h after spreading ODA on a) the dsDNA (10^{-8}M) and ethidium bromide (10^7M) subphase and also b) on the dsDNA (10^{-8}M) containing NaCl (10^7M) and ethidium bromide (10^7M) subphase.

The complexation of ssDNA-1 with salt at the ODA monolayer is interestingly surprising and is different from our previous study regarding the complexation of ssDNA-1 molecules with ODA monolayers at the air-water interface wherein no salt was added. In the study mentioned above, there was a large but slow expansion to an area of 35Å^2 (curve 1, Fig. 3.9.1.A) which remained constant thereafter. In this work, a small amount of salt had a dramatic effect on the complexation of DNA with ODA molecules. The large expansion of the monolayer to an area/molecule value of 66Å^2 suggests that the added amount of salt somehow decreases the screening on the single stranded oligonucleotides by ODA monolayer at the air-water interface, leading to the huge expansion of the monolayer on addition of the primary DNA strand with salt. We also performed a control experiment, in which ODA was complexed with NaCl (10^{-7}M) as indicated in curve 2, Fig. 3.9.1.A. A very small and slow

expansion of the monolayer to an area/molecule value of 38\AA^2 is observed thereby clearly suggesting that the observed expansion of the monolayer after spreading the single stranded DNA containing 10^{-7}M NaCl is due to the complexation of the single strand DNA with salt in solution with the ODA monolayers at the air-water interface. At $\text{pH} = 5.8$, the ODA molecules ($\text{pK}_B = 10.8$) would be completely ionized leading to maximum attractive columbic interaction with the anionic DNA molecules in solution. We would like to point out that little hysteresis was observed in the compression / expansion cycles of this and other air-water interface complexation experiments discussed below. The above result indicates that the ODA-DNA conjugate monolayers at the air-water interface are stable and behave like ideal amphiphilic complexes.

After equilibration of the ssDNA-1 density at the air-water interface with ODA monolayers, the ODA-ssDNA-1 with salt monolayer was transferred by the Langmuir-Blodgett technique onto gold-coated quartz substrates for QCM measurements. A plot of the QCM mass uptake was recorded as a function of number of immersion cycles for the ODA-ssDNA-1-NaCl monolayer is shown in figure 3.9.2.A, curve1, up triangles.

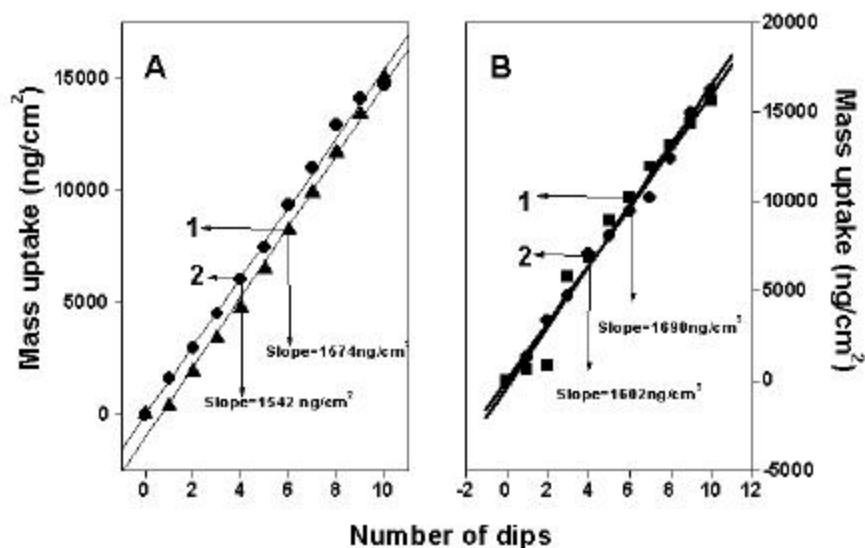


Figure 3.9.2: A) QCM mass uptake recorded as a function of number of immersion cycles in ODA monolayers complexed with ssDNA-1 (10^{-8}M) and NaCl (10^{-7}M) at the air-water interface (curve 1, up triangles) and ODA monolayers complexed with ssDNA-1 (10^{-8}M) and NaCl (10^{-7}M) and further hybridization with ssDNA-2 (10^{-8}M) and ethidium bromide (10^{-7}M) as depicted in curve 2, circles. The solid lines are linear fits to the data. B) QCM mass uptake recorded as a function of number of immersion cycles of ODA monolayers complexed with dsDNA (10^{-8}M) and ethidium bromide (10^{-7}M) subphase (curve 1, squares) and ODA monolayers complexed with dsDNA (10^{-8}M) subphase containing NaCl (10^{-7}M) and ethidium bromide (10^{-7}M) as depicted in curve 2, circles. The solid lines are linear fits to the data.

The transfer ratio was close to unity both during the downward and upward strokes of the QCM substrate. Uniform, lamellar growth of the ODA-DNA monolayer was clearly seen from QCM and transfer ratio data. The slope of the curve was determined from a linear fit to the QCM data to be 1574 ng/cm^2 per dip and is compared with our above mentioned work⁹ on sequential immobilization of ssDNA strands with ODA monolayers in absence of salt (Fig. 3.3.2, curve1) wherein the slope of the QCM curve came out to be 1450 ng/cm^2 per dip which is less than that obtained for ssDNA-1 with salt complexed with ODA monolayer. The molecular weight of ODA is 269.5. The number of ODA molecules in the bilayer is $2 / (21 \times 10^{16})$ and is ca. $9.52 \times 10^{14} / \text{cm}^2$. This then represents the number of charges due to ODA in the bilayer, assuming complete ionization of the ODA monolayer. (The mass of the bilayer of ODA/ cm^2 is thus $(9.52 \times 10^{14} \times 269.5) / 6.024 \times 10^{23} \sim 426 \text{ ng/cm}^2$). The molecular weight of ssDNA-1 is 5280. (The DNA molecular weights are calculated using the formula $330 \times$ number of bases in a sequence $\times 2$ for a DNA duplex). The contribution to the QCM mass uptake from the DNA molecules is $1574 - 426 \sim 1148 \text{ ng/cm}^2$. As shown above, the number of DNA molecules/ cm^2 of the film can be shown to be $\sim 1.31 \times 10^{14} / \text{cm}^2$.

In the case of ssDNA-1 with NaCl (10^{-7} M) complexed with ODA at the air-water interface, accounting for the contribution from the ODA bilayer, the concentration of DNA in the interlamellar regions of the ODA bilayer structure can easily be calculated to be $1.31 \times 10^{14} \text{ cm}^{-2}$. Accounting for the charges on the individual DNA molecules (16 per molecule) the charge ratio of DNA : ODA in the bilayers can be calculated to be $2.096 \times 10^{15} : 9.52 \times 10^{14}$ indicating that there is overcompensation of the positive charge due to ODA by the negatively charged DNA molecules by roughly a factor of 2.

As mentioned in the earlier sections, we had observed a similar charge overcompensation in our earlier studies wherein overcompensation of the ODA charge by the DNA molecules was observed (by nearly a factor of 2).⁹ After completing the QCM measurements, as mentioned in section 3.9.2, 4 ml of ssDNA-2 and ethidium bromide intercalator in water was injected into the non-monolayer side of the trough to yield an overall oligonucleotide concentration in the aqueous subphase of 10^{-8} M . The π -A isotherms were recorded as a function of time and the isotherm recorded 12 h after introduction of ssDNA-2 and intercalator is shown as curve 6 in Fig.3.9.1.A wherein a marginal increase in ODA monolayer area is seen, the takeoff area shifting to a stable $72 \text{ \AA}^2/\text{molecule}$. Interestingly, in the previous case,⁹ the takeoff area shifted to a stable $53 \text{ \AA}^2/\text{molecule}$ after introduction of the ssDNA-2 in the subphase as shown in curve 3, Fig.3.9.1.A. Furthermore, π -A isotherm recorded 12 h after introduction of ethidium bromide in the above study showed a further expansion in the monolayer with the takeoff area shifting to $70 \text{ \AA}^2/\text{molecule}$ ⁹ indicative of intercalation in the DNA double helix formed by sequential adsorption of ssDNA-1 and

ssDNA-2 at the air-water interface thereby leading to a further extension of the double helical DNA molecules adsorbed at the interface. In our present study, the Cl⁻ ions serve as counterions and probably react with the uncomplexed ODA molecules resulting in a marginal expansion in the monolayer after the addition of the secondary strand and intercalator. After equilibration of the ssDNA-2 density at the air-water interface, the ODA-ssDNA-1+2 monolayer was transferred by the Langmuir-Blodgett technique, onto gold-coated quartz substrates for QCM measurements. A plot of the QCM mass uptake recorded as a function of number of immersion cycles in the ODA-ssDNA-1+2 monolayer is shown in (Fig.3.9.2.A, curve 2, circles). The slope of the curve was determined from a linear fit to the QCM data to be 1544 ng/cm² per dip and is compared with our previous work⁹ on sequential immobilization of ssDNA strands with ODA monolayers in absence of salt (Fig. 3.3.2, curve 2, up triangles) wherein the slope of the QCM curve came out to be 1446 ng/cm² per dip which is less than that obtained for ssDNA-1 +ssDNA-2 with salt complexed with ODA monolayer. The reasons for this are not clear because the screening of the charges due to the presence of salt should effectively result in a lower slope, which is not the case. In the case of ssDNA-1+2 with NaCl (10⁻⁷ M) complexed with ODA at the air-water interface, accounting for the contribution from the ODA bilayer in a similar manner mentioned above, the concentration of DNA in the interlamellar regions of the ODA bilayer structure can easily be calculated to be 1.27 X 10¹⁴ cm⁻². Accounting for the charges on the individual DNA molecules (16 per molecule) the charge ratio of DNA: ODA in the bilayers can be calculated to be 2.032 x 10¹⁵: 9.52 x 10¹⁴ suggests overcompensation of the ODA charge by the DNA molecules by nearly a factor of 2.

19 monolayer (ML, 10 dips) LB films of the ODA molecules complexed with ssDNA-1 with NaCl (10⁻⁷ M) followed by ssDNA-2 molecules and ethidium bromide were grown on quartz substrates and the fluorescence spectrum recorded is shown in (Fig.3.9.3.A, curve 2,) and may be compared with the fluorescence spectrum of sequentially immobilized ssDNA-1 + ssDNA-2 with ODA monolayers at the air-water interface shown in (Fig. 3.9.3.A, curve 1).⁹

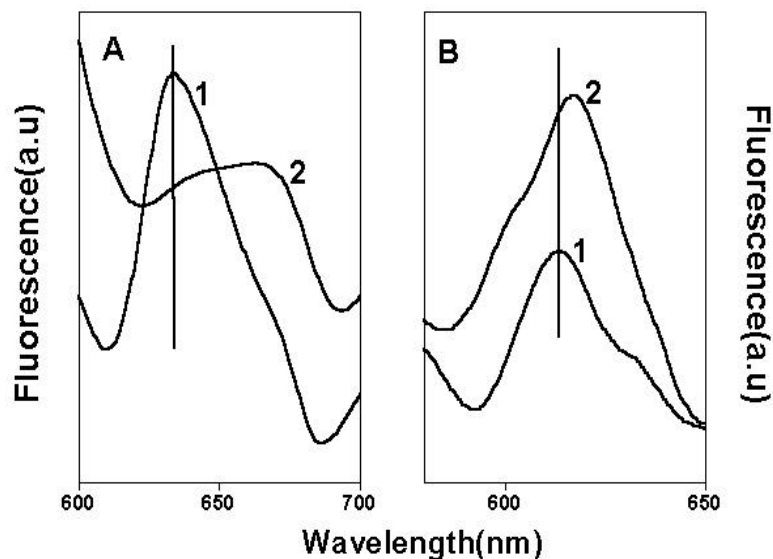


Figure 3.9.3. A) Fluorescence spectra of : -19 ML LB film of ODA-ssDNA-1+ ssDNA-2 in presence of ethidium bromide (10^7 M) intercalator (curve 1) and 19 ML LB film of ODA-ssDNA-1+ ssDNA-2 with NaCl (10^7 M) in presence of ethidium bromide (10^7 M) as shown in (curve 2).

B) Fluorescence spectra of: Curve 1:- 19 ML LB film of ODA - dsDNA (10^{-8} M) - ethidium bromide (10^{-7} M) intercalator. Curve 2:- 19 ML LB film of ODA complexed with pre-formed DNA containing NaCl (10^7 M) and ethidium bromide (10^{-7} M) as intercalator.

A broad fluorescence signal at 663 nm can be seen for the sequentially immobilized ssDNA strands containing salt with ODA monolayers and thus indicates the hybridization of the complementary oligonucleotides ssDNA-1 and ssDNA-2 at the air water interface to form double helical structures. The emission wavelength is red-shifted relative both to the solution DNA-intercalant value of 580 nm and also to the sequentially immobilized ssDNA molecules with ODA monolayers at the air-water interface which showed a clear fluorescence signal at 635 nm (Fig. 3.9.3.A, curve 1).⁹ As discussed earlier, this shift may be due to differences in the polarity of the fluorescent probe and is consistent with literature observation on ethidium bromide complexes with DNA .

UV-melting experiments on the ODA-DNA sequentially hybridized films were carried out as a test of hybridization. The UV-vis transition of a 19 ML thick ODA-in-situ hybridized DNA with salt film was measured and yielded a sigmoidal curve characteristic of duplex melting with a transition temperature of 60° C (Fig.3.9.4 A, curve 3, squares.).

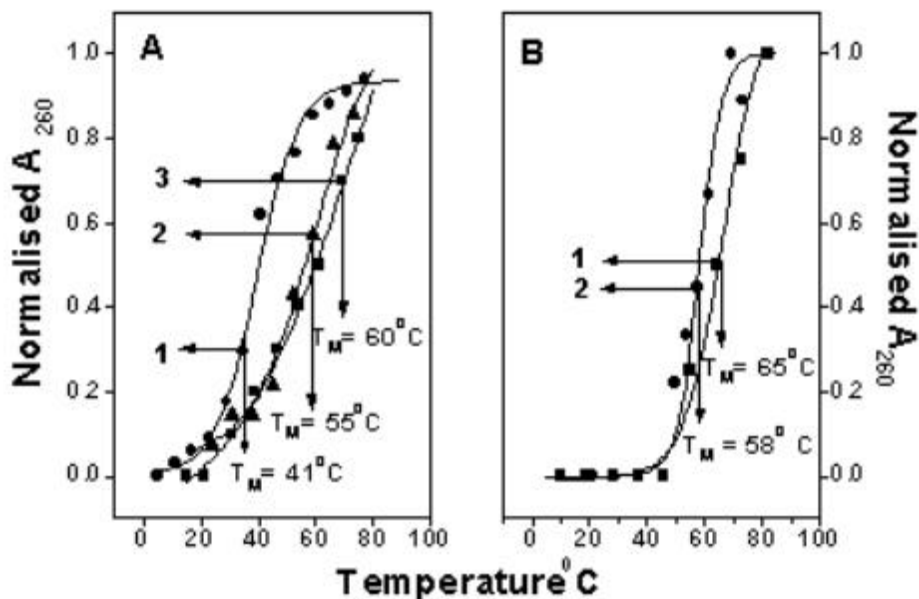


Figure 3.9.4: A) UV-temperature plots of solution melting of ssDNA-1 + ssDNA-2 in presence of 10mM NaCl (curve 1, circles), 19 ML ODA film complexed with ssDNA-1 + ssDNA-2 with intercalator on quartz (curve 2, up triangles) and curve 3 \div 19 ML ODA film complexed with ssDNA-1 + NaCl (10^7M) + ssDNA-2 with intercalator on quartz (curve 3, squares). The solid lines are sigmoidal fits to the data. The melting transition temperature (T_M) is indicated in the figure.

B) UV-temperature plots (T_M) of curve 1 \div 19 ML ODA film complexed with pre-formed DNA (10^{-8}M) and intercalator on quartz (curve 1, squares) and curve 2 \div 19 ML ODA film complexed with dsDNA (10^{-8}M), intercalator and NaCl (10^7M) as depicted in (curve 2, circles). The solid lines are sigmoidal fits to the data. The melting transition temperatures (T_M) are indicated in the figure.

This is to be compared with the solution melting transition temperature of 41°C for duplexes³⁴ of ssDNA-1 and ssDNA-2 as shown in (Fig 3.9.4.A curve1, circles) and the T_m of a 19 ML thick ODA-in-situ hybridized DNA film yielded a sigmoidal curve characteristic of duplex melting with a transition temperature of 55°C (Fig 3.9.4.A, curve 2, up triangles and also in 3.6.1.), thereby indicating much more stabilization of the DNA duplex with NaCl.³⁷

3.10. IMMOBILIZATION OF PRE-FORMED DNA (dsDNA) HYBRIDS (WITH / WITHOUT SALT) COMPLEXED WITH ODA MONOLAYERS AT THE AIR-WATER INTERFACE.

We also looked at the immobilization of pre-formed DNA (dsDNA) hybrids (with / without salt) complexed with ODA monolayers at the air-water interface. Curves 1, 3, and 4 in Fig. 3.9.1.B represent the π -A isotherm compression / expansion cycles of the ODA Langmuir monolayer at time = 15 minutes, 1 and 24 h respectively after spreading the

monolayer on the dsDNA and ethidium bromide subphase. A very large expansion of the monolayer to an area / molecule value of 50\AA^2 is observed which remained almost constant thereafter. This is to be compared with the $\sim 21\text{\AA}^2$ /molecule takeoff area for the ODA Langmuir monolayer on 10^{-8}M ethidium bromide solution as the subphase measured 4 h after spreading the monolayer (dotted line, Fig. 3.9.1.B) suggesting complexation of dsDNA molecules with ODA monolayers at the air-water interface. Curves 2 and 4 in Fig. 3.9.1.B represent the π -A isotherm compression / expansion cycles of the ODA Langmuir monolayer at time = 15 minutes and 24 h respectively after spreading the monolayer on the dsDNA-1 (10^{-8}M) containing NaCl (10^{-7}M) and ethidium bromide (10^{-7}M) solution as the subphase. In this case too, there was a large expansion of the monolayer to an area / molecule value of 50\AA^2 observed which remained constant thereafter. Interestingly, addition of salt in the subphase did not affect the complexation of dsDNA molecules with ODA monolayers. This result is at variance with the sequentially immobilized ssDNA strands with salt at the air-water interface with ODA monolayers (Fig. 3.9.1.A, curves 4 and 5) wherein, we saw a dramatic shift in the area / molecule value of 66\AA^2 compared with that of sequentially immobilized single stranded DNA molecules complexed with ODA monolayers (area / molecule value of 35\AA^2) in absence of salt shown in (Fig. 3.9.1. A, curve 1).

As mentioned above in section 3.9.2, after equilibration of the dsDNA with ethidium bromide density at the air-water interface with ODA monolayers, the ODA-dsDNA - intercalator monolayer was transferred by the Langmuir-Blodgett technique onto gold-coated quartz substrates for QCM measurements. A plot of the QCM mass uptake was recorded as a function of number of immersion cycles for the ODA-dsDNA-ethidium bromide monolayer (Fig. 3.9.2.B, curve 1, squares). The transfer ratio was close to unity both during the downward and upward strokes of the QCM substrate. Uniform, lamellar growth of the ODA-DNA monolayer was clearly seen from QCM and transfer ratio data. The slope of the curve was determined from a linear fit to the QCM data to be 1690 ng/cm^2 per dip and is compared with QCM mass uptake recorded as a function of number of immersion cycles for the ODA - dsDNA - ethidium bromide - NaCl monolayer, wherein the slope was 1602 ng/cm^2 per dip (Fig. 3.9.2.B, curve 2, circles). In the case of dsDNA complexed with ODA at the air-water interface, accounting for the contribution from the ODA bilayer, the concentration of DNA in the interlamellar regions of the ODA bilayer structure can be calculated to be $7.21 \times 10^{13}\text{ cm}^{-2}$. Accounting for the charges on the individual DNA molecules (16 per molecule) the charge ratio of DNA: ODA in the bilayers can be calculated to be 2.307×10^{15} : 9.52×10^{14} indicating that there is overcompensation of the positive charge due to ODA by the negatively charged DNA molecules by roughly a factor of 2. In the case of dsDNA molecules complexed with ODA monolayers in presence of NaCl (10^{-7}M) and ethidium bromide (10^{-7}M), the

charge ratio of DNA: ODA in the bilayers can be calculated to be $2.147 \times 10^{15} : 9.52 \times 10^{14}$ indicating that here too, there is overcompensation of the positive charge due to ODA by the negatively charged DNA molecules by roughly a factor of 2.

19 monolayer (ML, 10 dips) LB films of the ODA molecules complexed with dsDNA (10^{-8} M) and ethidium bromide were grown on quartz substrates and the fluorescence spectrum recorded is shown in (Fig. 3.9.3. B, curve 1) and may be compared with the fluorescence spectrum of pre-formed duplex (dsDNA) with salt (10^{-7} M) immobilized with ODA monolayers at the air-water interface shown in (Fig. 3.9.3.B, curve 2). A clear fluorescence signal at 613 nm for the pre-formed duplex with ODA monolayers and also the fluorescence signal at 618 nm for the pre-formed with NaCl (10^{-7} M) with ODA monolayers indicates that the pre-formed duplex has retained the double helical structure in both the cases. The emission wavelength is red-shifted relative both to the solution DNA-intercalant value of 580 nm. This shift may be due to differences in the polarity of the fluorescent probe and is consistent with literature observation on ethidium bromide complexes with DNA.²⁵

Fig. 3.9.4.B shows plots of the UV-melting data recorded from 19 ML ODA films complexed with dsDNA and intercalator (Fig. 3.9.4.B, curve 1, squares) and 19 ML ODA films complexed with dsDNA and intercalator with salt (Fig.3.9.4.B, curve 2, circles). An interesting result of the investigation is the fact that the melting transition of DNA hybrids complexed with ODA monolayers (65°C , Fig. 3.9.4.B, curve 1, squares) is much higher than the T_m of the ODA film containing DNA duplexes with salt (58°C , Fig. 3.9.4.B, curve 2, circles). The above results suggests that presence of salt effectively plays no role in the complexation and hybridization of pre-formed duplexes with ODA monolayers at the air-water interface which is also reflected in the pressure area isotherms for pre-formed duplexes. This result is surprisingly different to the in-situ hybridized DNA oligonucleotides with salt in solution with ODA monolayers as stated earlier, in which case, there was a large expansion in the monolayer and also a marginal increase in melting transition temperature compared to the sequentially immobilized oligonucleotides without salt at the interface with ODA monolayers. An important point of observation is that melting transition temperatures of pre-formed duplexes and in-situ hybridized DNA molecules with / without salt had a higher melting transition temperature than the solution melting of 41°C for duplexes³⁴ of ssDNA-1 and ssDNA-2 as shown in (Fig 3.9.4.A, curve 1, circles) .

3.11 SALT INDUCED HYBRIDIZATION OF DNA BY SEQUENTIAL AND PRE-FORMED IMMOBILIZATION OF OLIGONUCLEOTIDES IN THE PRESENCE OF DOTAP MONOLAYERS AT THE AIR-WATER INTERFACE.

In order to check the role of headgroups/ hydrocarbon chain packing, we looked at the immobilization and hybridization of single stranded oligonucleotides and pre-formed

duplexes with the double chain lipid 1,2-Dioleoyloxytrimethyl ammonium propane (DOTAP) at the air-water interface.

Curve 1 in Fig 3.11.1A represents the π -A isotherm compression / expansion cycles of the DOTAP Langmuir monolayer in the de-ionized water subphase measured 12 h after spreading the monolayer. There is a very large and rapid expansion of the order of nearly $100 \text{ \AA}^2/\text{molecule}$ takeoff area for the DOTAP Langmuir monolayer. This rapid expansion of the monolayer may be due to the larger head group size of DOTAP. When DNA is complexed with DOTAP molecules at the air-water interface, the number of DOTAP molecules per DNA strand is quite less. So the DNA molecules are not closely packed with DOTAP. This may be the reason that there is no further expansion of the monolayer even after 12 h of addition of the ssDNA-1 and salt ($0.5 \times 10^{-7} \text{ M}$) in the subphase as seen in Curve 2 in Fig.3.11.1A.

In the case of DNA molecules complexed with DOTAP monolayers, after equilibration of the ss-DNA-1 plus salt density at the air-water interface, 4 ml of ssDNA-2 and intercalator ethidium bromide in water was injected into the non-monolayer side of the trough to yield an overall oligonucleotide concentration in the aqueous subphase of 10^{-8} M . The π -A isotherms recorded 12 h after introduction of ssDNA-2 and intercalator in the subphase, did not show any expansion in the DOTAP monolayer apparent from curve 3 in Fig.3.11.1A.

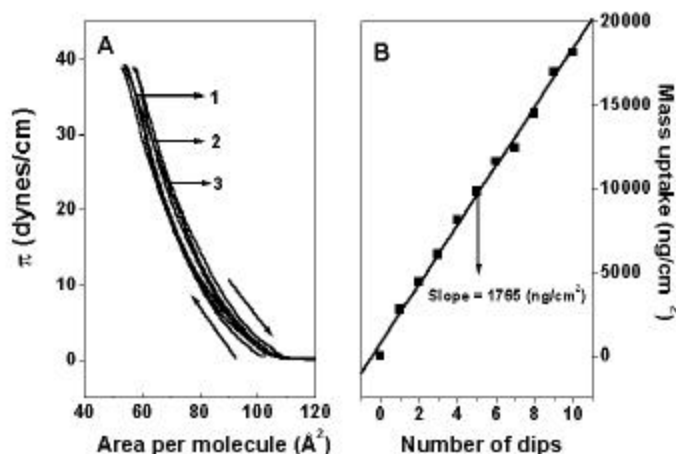


Figure 3.11.1. A) π -A isotherms recorded from an DOTAP monolayer on water at various times after introduction of DNA molecules into the subphase. Curve 1: π -A isotherm recorded 12 h after spreading DOTAP on the water subphase. Curve 2: π -A isotherm recorded 12 h after spreading DOTAP on the ssDNA-1 with salt ($0.5 \times 10^{-7} \text{ M}$) subphase. Curve 3: π -A isotherm recorded 12 h after introduction of ssDNA-2 and intercalator into the subphase.

B) QCM mass uptake recorded as a function of number of immersion cycles of DOTAP monolayers complexed with ss-DNA1 and NaCl ($0.5 \times 10^{-7} \text{ M}$) and further hybridization with ss-DNA-2 and intercalator by sequential immobilization at the air-water interface. The solid lines are linear fits to the data.

The DOTAP-DNA monolayers prepared by sequential insertion of the DNA strands in the trough was transferred by the LB technique on to the gold-coated quartz substrates for QCM measurements. Fig 3.11.1.B (squares) is a plot of QCM mass uptake recorded as a function of number of immersion cycles in the DOTAP-DNA monolayer for the sequential method of immobilization. The slope for the curve was determined from a linear fit to the QCM data to be 1765ng/cm^2 per dip for the sequentially formed DNA. Number of DNA molecules in the interlamellar regions of DOTAP bilayer structure was calculated in a similar manner mentioned above for ODA molecules³⁶ to be $8.2 \times 10^{13}\text{cm}^{-2}$ after accounting for the contribution from DOTAP bilayer alone to be $2 \times 10^{14}\text{cm}^{-2}$ indicating much overcompensation of positively charged DOTAP monolayer (2×10^{14}) by the anionic DNA molecules (2.62×10^{15}) at the air – water interface by a factor of 13.

19 monolayer (ML, 10 dips) LB films of DOTAP molecules complexed with in-situ hybridized DNA molecules and preformed DNA duplexes were grown on quartz substrates and the fluorescence spectrum recorded. Fig 3.11.2.A shows the spectrum recorded for the above films. Interestingly, it is observed that while the emission maximum occurs at ca. 633 nm for the in-situ hybridized DNA – DOTAP film (Fig 3.11.2.A, curve 1), it was shifted to ca.647 nm accompanied by broadening for the preformed DNA – DOTAP film (Fig 3.11.2.A, curve 2).

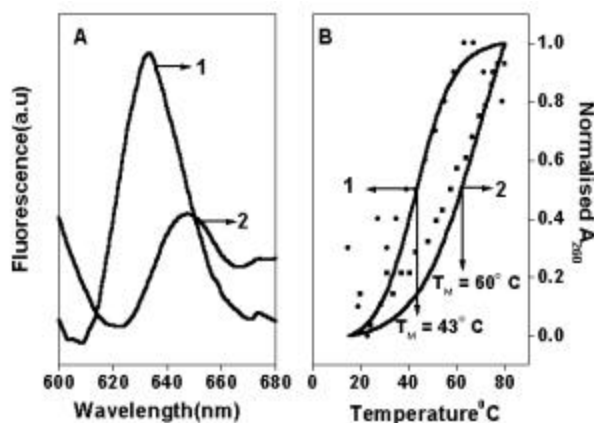


Figure 3.11.2. A) Fluorescence spectra of: Curve 1:- 19 ML LB film of DOTAP-ssDNA-1+2 (in-situ hybridized) with NaCl ($0.5 \times 10^{-7}\text{M}$) and ethidium bromide intercalator. Curve 2:- 19 ML LB film of DOTAP complexed with pre-formed DNA containing NaCl ($0.5 \times 10^{-7}\text{M}$) and ethidium bromide as intercalator.

B) UV –temperature plots (T_M) of curve 1:- 19 ML DOTAP film complexed with pre-formed DNA, NaCl ($0.5 \times 10^{-7}\text{M}$) and intercalator on quartz (curve 1, circles) and curve 2:- T_M plot of a 19 ML DOTAP film complexed with in-situ hybridized DNA, intercalator and NaCl ($0.5 \times 10^{-7}\text{M}$) as depicted in (curve 2, squares). The solid lines are sigmoidal fits to the data. The melting transition temperatures (T_M) are indicated in the figure.

Strong emission signal clearly seen for the sequentially hybridized DNA film is characteristic of intercalation suggesting that the DNA molecules are encapsulated in the bilayer without distortion to the double helix structure permitting the binding of ethidium bromide. A clear fluorescence signal at 633 nm seen for sequentially immobilized DNA with complementary ssDNA strand thus indicates the hybridization of complementary oligonucleotides at the air–water interface to form double helical structure. The emission wavelength is red shifted relative to the solution DNA– intercalant values of 580 nm. This may be due to the different binding modes with DNA duplex in the two situations and is consistent with literature observation on ethidium bromide complexes with DNA.²⁵ In spite of the red shift of the emission wavelengths in both the situations, the hybridization of DNA in the DOTAP bilayer films is indeed responsible for the fluorescent signal.

The UV-vis transition of a 19 ML thick DOTAP-hybridized DNA film containing intercalator and salt was measured and yielded a sigmoidal curve for the preformed DNA ($T_M = 43^{\circ}\text{C}$), (as seen in Fig 3.11.2.B, curve 1, circles) as well as for the in-situ hybridized DNA ($T_M = 60^{\circ}\text{C}$) (as seen in Fig 3.11.2.B, curve 2, squares). The increased T_M value for the in-situ hybridized DNA with DOTAP molecules indicates stabilization of the duplex formed at the air-water interface. Pre-formed DNA-DOTAP films yielded a low T_M value, reasons of which are not clear.

3.12. CONCLUSION

In conclusion, addition of salt at low concentration enhanced the rate of hybridization of DNA by allowing quick immobilization/complexation of pre-formed hybrids and single stranded complementary oligonucleotides at the air-water interface with cationic ODA as well as DOTAP monolayers. This approach of complexing DNA molecules with the lipid monolayer in presence of salt is expected to lead to a better understanding of DNA-lipid and DNA-drug interactions, thereby finding applications as antisense/antigene therapeutic agents.

3.13. SUMMARY

In this chapter, sequential as well as pre-formed immobilization of oligonucleotides with octadecylamine (ODA) Langmuir monolayers at the air-water interface and also the effect of salt on the both the methods of immobilization at the air-water interface is demonstrated. Further, Salt induced Hybridization of DNA by Sequential Immobilization of Oligonucleotides in the presence of DOTAP monolayers at the Air-Water Interface is also discussed.

The complexation of the single-stranded DNA molecules with octadecylamine (ODA) Langmuir monolayers was followed in time by monitoring the pressure-area

isotherms. Quartz-crystal microgravimetry (QCM), Fourier transform infrared spectroscopy (FTIR), polarized-UV-vis and fluorescence spectroscopy as well as thermal melting studies measurements clearly showed that hybridization of the complementary single-stranded DNA molecules had occurred at the air-water interface leading to the characteristic double-helical structure. Furthermore, it was observed that the DNA molecules in the LB films were oriented parallel to the substrate withdrawal direction.

This approach is expected to lead to a better understanding of DNA-lipid and DNA-drug interactions, especially in confined spaces. Application in gene-sequencing protocols may also be envisaged.

In this chapter, we have also looked at the effect of salt on the hybridization of single stranded oligonucleotides and pre-formed DNA duplexes at the air-water interface with cationic Langmuir monolayers. It was observed from the pressure area isotherms that there is a large expansion of the monolayer in the presence of salt with the primary strand. On addition of the complementary strand, there was no further expansion of the monolayer indicating that equilibrium had reached very quickly. Pre-formed DNA hybrids with salt in solution on complexation with ODA/DOTAP monolayers also showed a very large expansion in the pressure-area isotherms. Furthermore, melting transition temperatures for pre-formed duplexes and sequentially immobilized DNA molecules with ODA as well DOTAP monolayers in presence of salt indicates stabilization of the hybridized DNA molecules at the air-water interface.

This approach of complexing DNA molecules with the lipid monolayer in presence of salt is expected to lead to a better understanding of DNA-lipid and DNA-drug interactions, thereby finding applications as antisense/antigene therapeutic agents.

3.14 REFERENCES

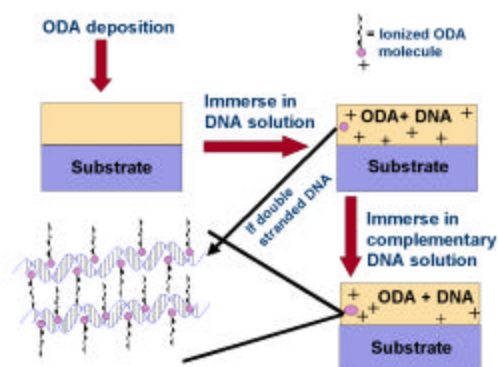
- (1) a) Huang, L.; Li, S. *Annu. Rev. Biophys. Biomol. Struct.* **2000**, *29*, 27; b) Huang, L. *Gene Ther.* **2000**, 731; c) Miller, A. D. *Angew. Chem. Int. Ed. Engl.* **1998**, *37*, 1768.
- (2) a) Kago, K.; Matsuoka, H.; Yoshitome, R.; Yamaoka, H.; Ijro, K.; Shimomura, M. *Langmuir* **1999**, *15*, 5193; b) Vijayalakshmi, R.; Dhathathreya, A.; Kanthimathi, M.; Subramanian, V.; Nair, B.U.; Ramasami, T. *Langmuir* **1999**, *15*, 2898; c) Okahata, O.; Kobayashi, T.; Tanaka, K. *Langmuir* **1996**, *12*, 1326; d) Ijro, K.; Shimomura, M.; Tanaka, M.; Nakamura, H.; Hasebe, K. *Thin Solid Films* **1996**, *284*, 780.
- (3) a) Steel, A. B.; Herne, T. M.; Tarlov, M. J. *Bioconjugate. Chem.* **1999**, *10*, 419; b) Steel, A. B.; Herne, T. M.; Tarlov, M. J. *Anal. Chem.* **1998**, *70*, 4670; c) Wang, J.;

- Nielsen, P.E.; Jiang, M.; Cai, X.; Fernandez, J.R.; Grant, D.H.; Ozsoz, M.; Begleiter, A.; Mowat, M. *Anal.Chem.* **1997**, *69*, 5200.
- (4) a) Zhou, X. C.; Huang, L.Q.; Li, S. F.Y. *Biosens. Bioelectron.* **2001**, *16(1-2)*, 85; b) Okahata, Y.; Kawase, M.; Niikura, K.; Ohtake, F.; Furusawa, H.; Ebara, Y. *Anal. Chem.* **1998**, *70*, 1288; c) Caruso, F.; Rodda, E.; Furlong, D.N. *Anal.Chem.* **1997**, *69*, 2043; d) Matsuura, K.; Ebara, Y.; Okahata, Y. *Langmuir* **1997**, *13*, 814.
- (5) a) Higashi, N.; Takahashi, M.; Niwa, M. *Langmuir* **1999**, *15*, 111; b) Higashi, N.; Inoue, T.; Niwa, M. *J.Chem.Soc., Chem.Commun.* **1997**, 1507.
- (6) Tsoi, P. Y.; Yang, J.; Sun, Y.T.; Sui, S.F.; Yang, M. *Langmuir* **2000**, *16*, 6590.
- (7) Osborne, M.A.; Furey, W.S.; Klenerman, D.; Balasubramanian, S. *Anal.Chem.* **2000**, *72*, 3678.
- (8) Sastry, M.; Ramakrishnan, V.; Pattarkine, M.; Gole, A.; Ganesh, K. N. *Langmuir* **2000**, *16*, 9142.
- (9) Ramakrishnan, V.; D'Costa, M.; Ganesh, K. N.; Sastry, M.; *Langmuir* (communicated)
- (10) a) Clemente-Leon, M.; Agricole, B. M.; Mingotaud, C.; Gomez-Garcia, C. J.; Coronado, E.; Delhaes, P. *Langmuir* **1997**, *13*, 2340; b) Bardosova, M.; Tregold, R. H.; Ali-Adib, Z. *Langmuir* **1995**, *11*, 1273; c) Ganguly, P.; Paranjape, D.V.; Sastry, M. *J. Am. Chem. Soc.* **1993**, *115*, 793.
- (11) a) Riccio, A.; Lanzi, M.; Antolini, F.; De Nitti, C.; Tavani, C.; Nicolini, C. *Langmuir* **1996**, *12*, 1545; b) Reiter, R.; Motschmann, H.; Knoll, W. *Langmuir* **1993**, *9*, 2430; c) Herron, J. N.; Muller, W.; Paudler, M.; Roegler, H.; Ringsdorf, H.; Suci, P. A. *Langmuir* **1992**, *8*, 1413.
- (12) a) Heywood, B.R.; Mann, S. *Chem. Mater.* **1994**, *6*, 311; b) Rajam, S.; Heywood, B. R.; Walker, J. B. A.; Mann, S.; Davey, R. J.; Birchall, J.D. *J. Chem. Soc. Faraday Trans.* **1991**, *87*, 727.
- (13) a) Sastry, M.; Mayya, K. S.; Patil, V. *Langmuir* **1998**, *14*, 5198; b) Mayya, K. S.; Sastry, M. *J. Phys. Chem. B.* **1997**, *101*, 9790; c) Patil, V.; Mayya, K. S.; Pradhan, S. D.; Sastry, M. *J. Am. Chem. Soc.* **1997**, *119*, 9281; d) Sastry, M.; Mayya, K. S.; Patil, V.; Paranjape, D.V.; Hegde, S. G. *J. Phys. Chem. B.* **1997**, *101*, 4954.
- (14) Cha, X.; Ariga, K.; Kunitake, T. *J. Am. Chem. Soc.* **1996**, *118*, 9545.

- (15) Ahlers, M.; Muller, W.; Reichert, A.; Ringsdorf, H.; Venzmer, J. *Angew .Chem .Int . Ed. Engl.* **1990**, *29*, 1269.
- (16) Shimomura, M.; Nakamura, F.; Ijio, K.; Taketsuna, H.; Tanaka, M.; Nakamura, H.; Hasebe, K. *J. Am. Chem. Soc.* **1997**, *119*, 2341.
- (17) Ebara, Y.; Mizutani, K.; Okahata, Y. *Langmuir* **2000**, *16*, 2416.
- (18) Sasaki, D.Y.; Kurihara, K.; Kunitake, T. *J.Am.Chem.Soc.* **1991**, *113*, 9685.
- (19) Ulman, A., *An introduction to ultrathin organic films : from Langmuir-Blodgett to self-assembly* : Academic Press, San Diego (1991). The monolayer transfer onto different substrates was effected at a surface pressure of 30 dynes/cm for all experiments in this study.
- (20) Sauerbrey, G *Z. Phys.* **1959**, *155*, 206.
- (21) LePecq, J.B.; Paoletti, C. *J.Mol.Biol.* **1967**, *27*, 87.
- (22) Mayya, K.S.; Sastry, M. *Langmuir* **1998**, *14*, 74.
- (23) Cuvillier, N.; Rondelez, F. *Thin Solid Films* **1999**, .
- (24) Decher, D. *Science* **1997**, *277*, 1232 and references therein.
- (25) a) Lvov, Y.; Ariga, K.; Onda, M.; Ichinose, I.; Kunitake, T. *Langmuir* **1997**, *13*, 6195;
b) Kumar, A.; Mandale, A.B.; Sastry, M. *Langmuir* **2000**, *16*, 6921.
- (26) Coury, J.E.; Anderson, J.R.; McFail-Isom, L.; Williams, L.D.; Bottomley, L.A. *J.Am.Chem.Soc.* **1997**, *119*, 3792.
- (27) Lerman, L.S. *J.Mol.Biol.* 1961, *3*, 18.
- (28) Neault, J.F.; Tajmir-Riahi, H.A. *J.Phys.Chem.B.* **1998**, *102*, 1610.
- (29) Pattarkine, M.V.; Ganesh, K.N. *Biochem.Biophys.Res.Comm.* **1999**, *263*, 41.
- (30) Cantor, C. R; Schimmel, P.R. *Biophysical Chemistry, Part III*, W.H. Freeman, New York (1980).
- (31) *Methods in Enzymology*, Vol *211*, 208.

CHAPTER IV

STUDIES RELATED TO THE HYBRIDIZATION OF ENCAPSULATED DNA IN CATIONIC LIPID FILMS



The encapsulation of double-stranded DNA of varying chain lengths (dsDNAs) and *in-situ* hybridization of complementary single-stranded DNA (ssDNA) molecules in a thermally evaporated cationic fatty lipid film (ODA) at close to physiological pH is demonstrated in this chapter. The diffusion of the DNA molecules into the cationic lipid film is dominated by attractive electrostatic interaction between the negatively charged phosphate backbone of the DNA molecules and the protonated amine molecules in the thermally evaporated film and has been quantified using quartz crystal microgravimetry (QCM). Fluorescence studies of DNA-ODA films obtained by sequential immersion of the ODA matrix in the complementary single stranded DNA solutions using ethidium bromide intercalator clearly showed that the hybridization of the DNA single strands had occurred within the lipid matrix. Furthermore, fluorescence studies of the preformed dsDNA-ODA biocomposite film indicated DNA encapsulation without distortion to the native double helix structure. The DNA biocomposite films have been further characterized with Fourier Transform Infrared (FTIR) and X-ray Photoelectron Spectroscopy (XPS) measurements.

Part of the work presented in this chapter has been published in: - Sastry, M.; Ramakrishnan, V.; Pattarkine, M.; Ganesh K.N. *J.Phys.Chem.B.* 2001, 105, 4409.

4.1. INTRODUCTION

The development of efficient methods for immobilizing DNA on planar supports is essential for generating DNA chip and DNA array-based instruments.¹ Biochips and biosensors can make use of immobilized nucleic acids to provide for selective binding interactions.²

In this chapter, the encapsulation of double-stranded DNA (dsDNA) and *in-situ* hybridization of complementary single-stranded DNA (ssDNA) molecules in a fatty lipid matrix is demonstrated. The immobilization of DNA is accomplished by simple immersion of a thermally evaporated octadecylamine film (ODA) in the DNA solution at close to physiological pH. The diffusion of the DNA molecules into the cationic lipid film is dominated by attractive electrostatic interaction between the negatively charged phosphate backbone of the DNA molecules and the protonated amine molecules in the thermally evaporated film and has been quantified using quartz crystal microgravimetry (QCM). Fluorescence studies of DNA-ODA films obtained by sequential immersion of the ODA matrix in the complementary single strand DNA solutions using ethidium bromide intercalator clearly showed that the hybridization of the DNA single strands had occurred within the lipid matrix. Furthermore, fluorescence studies of the preformed dsDNA-ODA biocomposite film indicated DNA encapsulation without distortion to the native double helix structure. The DNA biocomposite films have been further characterized with Fourier Transform Infrared (FTIR) and X-ray Photoelectron Spectroscopy (XPS) measurements. The DNA-fatty lipid composite films would serve as model systems for understanding DNA-membrane interactions as well as in the study of DNA-drug/protein interactions. This approach also shows promise for the synthesis of patterned DNA films and consequent application in disease detection and genome sequencing.

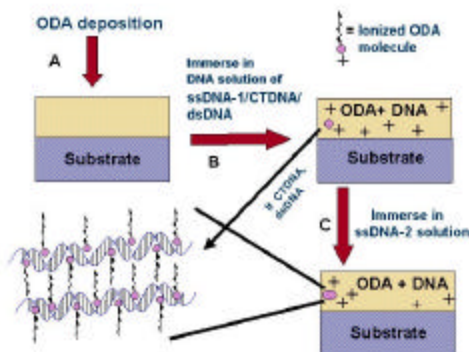
In this chapter, we have also looked at the electrostatic entrapment and thermal stability of pre-formed DNA duplexes of different lengths within thermally evaporated cationic lipid films. In addition, the specificity of base pairing within a sequence was also studied.

4.2. ENTRAPMENT AND *IN-SITU* HYBRIDIZATION OF DNA IN THERMALLY EVAPORATED CATIONIC FATTY LIPID FILMS

The immobilization of DNA on a two-dimensional solid surface is of interest both in studies of DNA itself and in various applications. Different routes have been reported for the immobilization of DNA on planar supports. Watterson et al.³ have immobilized single stranded DNA and used it as a selective reagent to bind complementary nucleic acids for applications including detection of pathogenic organisms and general mutations. Various DNA immobilization methods have been described (*discussed in detail in chapter 1*) including adsorption,⁴ copolymerisation,⁵ complexation,⁶ and covalent attachment.⁷ Some of the more thoroughly studied methods being assembly at the air-water interface with Langmuir monolayers,⁸ and by self assembled monolayers of thiols.^{2b,9-12}

The motivation for the hybridisation studies of the entrapped DNA within thermally evaporated cationic lipid films was from the earlier work developed in this laboratory. Immersion of thermally evaporated fatty acid films when immersed in electrolyte solutions of PbCl_2 / CdCl_2 resulted in the spontaneous organization of the film into c-axis oriented lamellar structure.¹³ This protocol was further successfully extended to the incorporation of negatively charged carboxylic acid derivatized colloidal nanoparticles of silver gold and CdS into thermally evaporated fatty amine films¹⁴ and protein molecules¹⁵ in fatty lipid matrices. The next important question that arose was whether this protocol could be extended to the intercalation of bio macromolecular molecules such as DNA with negligible distortion to their double helical structure. The successful attempt in this direction has been demonstrated in this chapter and in chapter 5.

In this chapter, we have discussed the immobilization of synthetic (both single-stranded and pre-formed helical structures) and calf-thymus DNA in thermally evaporated films of cationic fatty amine molecules by a simple beaker-based immersion technique. The diffusion of DNA molecules from solution into the lipid matrix is driven by electrostatic interaction between the negatively charged DNA and cationic octadecylamine (ODA) molecules. In the case of double helical DNA structures, the extraction from solution and subsequent entrapment within the lipid matrix occurs without distortion to their double helical structure. The procedure is illustrated in Schematic 4.2.1 and will be discussed subsequently.



Schematic 4.2. 1: Diagram showing the various stages of the DNA-ODA composite film formation.

Step A : Deposition of ODA on solid substrates by thermal evaporation; step B : diffusion of single-stranded DNA 1/double-stranded calf-thymus DNA (CTDNA) (4) /double-stranded DNA (dsDNA) (5) into the lipid matrix during immersion in the different DNA solutions and step C : sequential immersion in complementary single-stranded DNA 2 solution after encapsulating the complementary strands 1. In step C, a negative experiment was also carried out by immersion of the ODA composite film in the non-complementary oligonucleotide solution, 3. The magnified section shows the possible microscopic structure of the DNA-ODA complex.

A particularly exciting result of our investigation is the demonstration that sequential immersion of the fatty amine film in solutions of complementary single-stranded oligonucleotide sequences leads to the immobilization of both the DNA molecules and hybridization to yield double helical structures within the lipid matrix. We would like to point out that the single-stranded DNA

solutions are prepared in deionized water and therefore, under conditions where hybridization does not occur spontaneously in the bulk of the solution.

The cationic lipid matrix thus appears to play a double role, that of electrostatic extraction/immobilization as well as in the role of counterions screening the repulsive electrostatic interactions between the single-stranded DNA molecules, thereby facilitating the hybridization. The formation of the lipid-DNA composite films and the *in-situ* hybridization has been followed by quartz crystal microgravimetry (QCM), fluorescence spectroscopy and Fourier transform infrared spectroscopy (FTIR) measurements while a chemical characterization of the films has been carried out by X-ray photoemission spectroscopy (XPS).

4.2.1. Synthesis of oligonucleotides.

Oligonucleotides of the sequence GGAAAAAACTTCGTGC (1), GCACGAAGTTTTTCC (2) and AGAAGAAGAAAAGAA (3) were synthesized by β -cyanoethyl phosphoramidite chemistry on a Pharmacia GA plus DNA synthesizer and purified by FPLC and rechecked by RP HPLC. The oligonucleotides 1 and 2 are complementary while 1 and 3 are non-complementary.

4.2.2. DEPOSITION OF LIPID FILMS.

250 Å and 425 Å thick octadecylamine (ODA, Aldrich) films were thermally evaporated onto gold-coated 6 MHz AT-cut quartz crystals, quartz substrates and Si (111) wafers for quartz crystal microgravimetry (QCM), contact angle measurements, fluorescence spectroscopy and Fourier Transform Infrared (FTIR) and X-ray Photoelectron Spectroscopy (XPS) measurements respectively as illustrated in Schematic 4.2.1, step A. The films were deposited as per the conditions mentioned in chapter 2, section 2.2. The thickness of the films was crosschecked using ellipsometry.

4.3. QUARTZ CRYSTAL MICROGRAVIMETRY

The diffusion of the DNA molecules into the fatty amine films and the hybridization of the single-stranded DNA molecules 1 and 2 were studied as per the protocol illustrated in Schematic 4.2.1; step B of the procedure consists of immersion of 250 Å thick ODA films on QCM crystals/quartz substrates/Si (111) wafers in 10^{-6} M aqueous, deionized DNA solutions (pH = 6.8) of 1 and calf-thymus DNA (CT-DNA) having one thousand base pairs (1000 bp), 4. The diffusion of the DNA molecules into the fatty lipid matrix was followed by measuring the frequency changes in time of the ODA-coated QCM crystal. This was achieved by *ex-situ* measurement of the QCM resonant frequency after thorough washing and drying of the crystals using an Edwards FTM5 frequency counter. This frequency counter had a resolution and stability of 1 Hz. The frequency change (Δf) was converted to mass loading (Δm) using the relationship $\Delta m = 12.1 \Delta f$ (ng/cm^2). Pre-formed DNA duplexes (dsDNA, 5) obtained by mixing equimolar quantities of 1 and 2 under standard

hybridization conditions¹⁶ were also incorporated in the ODA films by similar immersion in the dsDNA solution (10^{-6} M concentration) and the QCM mass uptake kinetics studied.

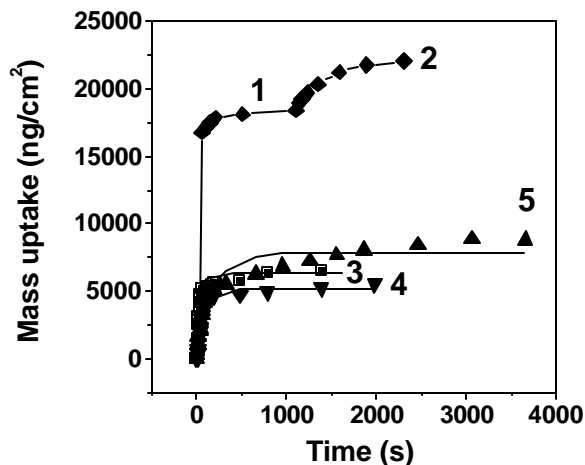


Fig. 4.3.1: QCM mass uptake as a function of time of immersion of a 250 Å thick ODA film in 1 μ M solutions of: 1 (curve 1, diamonds); the ssDNA1-ODA film shown as curve 1 during immersion in 2 (curve 2, diamonds); 5 (curve 3, squares) and 4 (curve 4, down triangles). The figure also shows the QCM mass uptake recorded during immersion of a 425 Å thick ODA film in 1 μ M solution of 5 (curve 5, up triangles). The solid lines in all the curves are fits to the data based on a one-dimensional diffusion analysis.

Fig.4.3.1 depicts the QCM mass uptake kinetics during immersion of 250 Å thick ODA films in aqueous solutions of the DNA molecules 1, 5 and 4 (curves 1, 3 and 4 respectively). The figure also shows the sequential mass uptake recorded from the ODA film first encapsulated with single-stranded DNA 1 (curve 1, Fig.4.3.1; step B, Schematic 4.2.1) during immersion in the complementary single-stranded DNA 2 (curve 2, diamonds; step C, Schematic 4.2.1) as well as the mass uptake recorded during diffusion of DNA 5 into a 425 Å thick ODA film (curve 5).

In order to study the role of the film thickness on the diffusion process, the mass uptake in a 425 Å thick ODA film on a QCM crystal during immersion in the pre-formed DNA duplex solution 5 (10^{-6} M concentration) was also studied. As will be seen subsequently, this important experiment enables one to ascertain whether the DNA molecules are entrapped within the lipid matrix or simply immobilized on the fatty amine film surface. It is observed that the mass uptake is highest for the single-stranded DNA 1. Furthermore, the mass uptake of the complementary DNA strand 2 into the composite film of ODA-1 is ca. 20 % of the mass uptake recorded during diffusion of DNA 1 in the first immersion cycle. This indicates blockage of the diffusion pathways into the ODA-1 composite film available to DNA-2 and therefore, incomplete hybridization of the DNA molecules into double helical structures. The number of DNA molecules entrapped within the lipid

matrix and thereby the charge ratio of the DNA molecules to the ionized ODA molecules in the lipid matrix may be easily estimated by simple calculations. The equilibrium mass uptake after entrapment of DNA 1 and 2 in the fatty lipid film is 21920 ng/cm² as depicted in table 4.3.1. The number of DNA molecules corresponding to this mass is: $(21920 \times 10^{-9} \times 6.024 \times 10^{23})/5280 \sim 2.5 \times 10^{15} \text{ cm}^{-2}$. The number of ODA molecules corresponding to a deposition of 2420 ng/cm² can be similarly shown to be $5.41 \times 10^{15} \text{ cm}^{-2}$ (the molecular weight of ODA = 269.5). Assuming complete ionization of all the ODA molecules in the lipid matrix, the DNA/ODA charge ratio is $(2.5 \times 10^{15} \times 16)/5.41 \times 10^{15} \sim 7.4$. The multiplication by 16 in the numerator is to account for the charges in the 16-mer oligonucleotides used in this study. The DNA/ODA charge ratio for other diffusion experiments was calculated in a similar manner as shown above. The equilibrium DNA mass loadings and the DNA/ODA charge ratios are listed in Table 4.3.1 along with the relevant parameters used in the calculations for the QCM data shown in Fig.4.3.1.

Table.4.3.1

DNA-to-ODA charge ratios in the different DNA-ODA composite films estimated from an analysis of the QCM mass uptake data shown in Fig.4.2.3.1.

Diffusion experiment	ODA matrix mass (ng/cm ²)	DNA equilibrium mass loading	Single stranded DNA/duplex DNA	DNA /ODA charge
Single-stranded	2420 ²	21920	5280	7.2
Double-stranded	2420 ²	6290	10560	2.1
Double-stranded	4115 ³	8760	10560	1.75
Double - stranded calf-thymus DNA	2420 ²	5190	660000	1.8

¹ The DNA molecular weights are calculated using the formula 330 x number of bases in sequence x 1 or 2 (depending on whether the DNA is single-stranded or duplex).

² This data corresponds to the 250 Å thick ODA film.

³ This data corresponds to the 425 Å thick ODA film.

It is interesting to note from Table 4.3.1; that in all cases, there is overcompensation of the ODA lipid matrix charge by the DNA molecules. While the degree of overcompensation is largest in the case of the single-stranded DNA-ODA composite films, the DNA/ODA charge ratio settles at

close to 2 for both the synthetic (DNA 5) and natural DNA duplex structures (calf-thymus DNA 4). Such a charge overcompensation is known to occur during complexation of large inorganic ions such as Keggin anions at the air-water interface¹⁷ as well as in electrostatically formed multilayers of cationic and anionic polyelectrolyte films, in multilayer films of polyelectrolytes and DNA,¹⁸ as well as in multilayers of positively and negatively charged nanoparticles.¹⁹ This important result indicates that the DNA molecules can be entrapped in a highly condensed lipid matrix at concentrations higher than that previously reported.²⁰ A maximum DNA: surfactant charge ratio of 0.8 was observed in DNA – cationic lipid micelles by Ganesh et al.²⁰ DNA molecules entrapped in such a highly condensed lipid matrix may serve as model systems for understanding densely packed DNA in supramolecular organizes such as chromatin.²¹ Degree of overcompensation is much larger in the case of the single-stranded DNA molecules 1 and 2 vis-à-vis the double-stranded DNA molecules 4 and 5. A possible reason for this could be the lower diffusivities of the bulkier DNA double strands as discussed below and in section 4.10 containing the electrostatic entrapment of dsDNAs of different chain lengths.

The QCM mass uptake data shown in Fig.4.3.1 was fit to a one-dimensional diffusion model, which has been used with success in studying the diffusion of surface-derivatized colloidal gold, and silver particles in thermally evaporated lipid films.¹⁴

One – dimensional (1-D) Diffusion Model:

Sastry et al, have extensively used the one-dimensional diffusion model to study diffusion of carboxylic acid derivatized silver colloidal particles in thermally evaporated fatty amine films^{14c} and diffusion of proteins cytochrome-c into acid matrix and haemoglobin in amine matrix.²² In the present situation, the thermally evaporated amine films are disordered (as evidenced by Bragg peaks in the XRD patterns)¹⁴ and therefore, 1-D model may be appropriate. To simplify the calculations, we have omitted the reaction term in the diffusion equation.

The equation for simple 1-D diffusion is written as:

$$\frac{\partial C(x,t)}{\partial t} = D \frac{\partial^2 C(x,t)}{\partial x^2} \quad \dots\dots(1)$$

where $C(x,t)$ is the time and distance dependent DNA concentrations in the film and D is the DNA diffusivity. Scheme 4.3.1 shows the physical situation in this DNA incorporation study and leads naturally to the following boundary conditions:

$$C(L,t) = \begin{cases} 0 & t < 0 \\ C_0 & t = 0 \end{cases} \quad \dots(2a)$$

$$\frac{\partial C(0,t)}{\partial x} = 0 \quad \dots(2b)$$

Where C_0 is the DNA concentration at the film / DNA solution interface (Scheme4.3.2, $x=L$) and condition (2b) is a consequence of the fact that the quartz crystal substrate is impervious to DNA diffusion (at $x = 0$, the film/quartz substrate interface, scheme 4.3.1). The solution of Eq.1 subject to the above boundary conditions (Eq.2) is given by²³

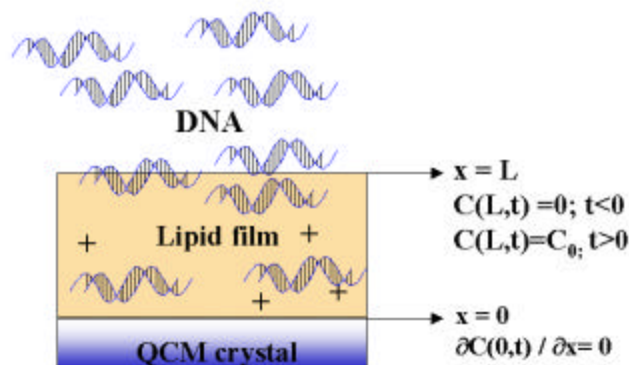
$$C(x,t) = C_0 \left[1 + 4 \cdot \sum_{n=0}^{\infty} e^{-D \cdot \left[(2 \cdot n + 1)^2 \cdot \frac{\pi^2}{4L^2} \right] \cdot t} \cdot \cos \left[\frac{(2 \cdot n + 1) \cdot \pi \cdot x}{2 \cdot L} \right] \cdot \frac{(-1)^{n+1}}{(2 \cdot n + 1) \cdot \pi} \right] \quad \dots\dots\dots (3)$$

In QCM studies, one observes a mass uptake over the whole length of the film covering the sensing electrode. The total mass uptake recorded as a function of time, $M(t)$, is therefore :

$$M(t) = m_0 \cdot \int_0^L C(x,t) dx \quad \dots\dots\dots (4)$$

where m_0 is the mass per DNA molecule. Ellipsometry was used to determine the film thickness before and after DNA incorporation. The final thickness values thus determined (L) were used in

Eq.3 and the QCM kinetics results fitted to Eq.4 using a non-linear least squares procedure using an application written in MathCAD by Dr. Murali Sastry. MathCAD is a commercial mathematical software package for the PC available from Math soft Inc.; Cambridge, Ma 02142, USA.



Scheme 4.3.1. Scheme (not to scale) showing DNA incorporation in a thermally evaporated lipid film during immersion in the DNA solution wherein the boundary conditions are shown.

Analysis of the QCM data using one -dimensional (1-D) Diffusion Model:

The parameters obtained from the fits to the QCM data of Fig.4.2.1 are listed in Table 4.3.2.

Table 4.3.2

Parameters obtained from a one-dimensional diffusion analysis of the QCM mass uptake kinetics data for entrapment of DNA in fatty amine films shown in Fig.4.2.3.1

Diffusion experiment	Film thickness (Å)	D (Å ² /s)	C _o (molecules/cm ³)
Single-stranded DNA 1	250 (500) ¹	1680	4.26 x 10 ¹²
Double-stranded DNA 5	250 (500) ¹	2180	1.43 x 10 ¹²
Double-stranded DNA 5	425 (800) ¹	1880	4.46 x 10 ¹¹
Double-stranded calf-thymus DNA 4	250 (500) ¹	938	2.89 x 10 ¹⁰

¹ The numbers in the parenthesis refer to the film thickness measured (ellipsometrically) after DNA incorporation. This value is used to model the QCM mass uptake data.

The two main parameters obtained from the fits to the QCM mass uptake data are the DNA diffusion coefficient (D , $\text{\AA}^2/\text{s}$) and the concentration of the DNA molecules at the film-solution interface (C_0 , molecules/ cm^3).

In the fits, the mass per single-stranded DNA/duplex DNA molecules has been calculated from the corresponding molecular weights given in Table 4.3.1. The equilibrium mass uptake for dsDNA (curve 3) and CT-DNA (curve 4) in the ODA film is nearly the same and lower by a factor of roughly three compared to the mass loading for the ssDNA (curve 1). It can be seen from Table 4.3.2, that the diffusion coefficients for both the single-stranded DNA 1 and duplex DNA 5 molecules into the lipid matrix is nearly the same (ca. $2000 \text{\AA}^2/\text{s}$). The diffusion coefficient of the calf-thymus DNA 4 molecules is significantly lower and is likely to be a consequence of the much larger mass of these DNA molecules in comparison with the smaller 16-mer synthetic DNA molecules 1 and 2. The concentration of DNA molecules at the film-solution interface does not appear to show a similar trend.

4.4. CONTACT ANGLE MEASUREMENTS

There is clearly substantial incorporation of the DNA molecules in the lipid matrix in all the DNA molecules studied herein. There are two possible modes by which the DNA may be immobilized in the ODA films, viz., purely surface binding and entrapment within the lipid bilayers as shown in the magnified section of Schematic 4.2.1. In order to resolve this issue, contact angle measurements were done on a 250\AA thick ODA film on a quartz substrate by the sessile water drop method ($1 \mu\text{L}$ water droplet) using a Rame-Hart 100 goniometer before and after immersion of the film in 10^{-6} M double-stranded DNA 5 solution for 4 hours and the values obtained were 90° and 89° . These values represent averages over 10 measurements carried out over the whole film surface. These values indicate a hydrophobic surface in both cases. Thus, the DNA molecules are intercalated into the lipid matrix by electrostatic immobilization within the hydrophilic regions of the ODA bilayers as shown in Schematic 4.2.1 (magnified section).

A simple calculation serves to add further weight age to this conclusion. The equilibrium mass loading for the DNA 5/ODA composite film (250\AA thickness) is $6290 \text{ ng}/\text{cm}^2$ (Table 4.3.1). Assuming purely surface binding of the DNA molecules, this works out to ca. 3.6×10^{14} molecules/ cm^2 . The overall projected area of this density of DNA molecules is thus 55\AA (length of 16-mer DNA molecule) $\times 20 \text{\AA}$ (diameter of double helix) $\times 3.6 \times 10^{14} \sim 40 \text{ cm}^2$. In other words, the mass loading of DNA measured would lead to nearly 40 monolayers of DNA molecules in a close-packed state on the surface of the ODA film if only surface binding is considered. This should lead to a significant reduction in the contact angle, which is not the case. Thus, the DNA molecules are entrapped within the lipid matrix.

4.5. TEST OF HYBRIDISATION: FLUORESCENCE STUDIES

The formation of double helical structures by hybridization of the complementary oligonucleotide sequences 1 and 2 may be conveniently studied by introduction of the well-known fluorescent intercalator, ethidium bromide. Enhanced fluorescence from the ethidium bromide molecules occurs on intercalation (described in detail in chapter 2) in the double helical DNA structures²⁴ and may be used to follow the hybridization process. 250 Å thick ODA films on quartz substrates were immersed for 4 hours in aqueous solutions of the following: I) 1.26 μM ethidium bromide intercalator; II) 1 (10⁻⁶ M concentration) with 1.26 μM of intercalator (Schematic 4.2.1, step B); III) 1 followed by immersion in the complementary DNA 2 (10⁻⁶ M concentration) with intercalator; IV) 5 (10⁻⁶ M concentration) with the intercalator and V) in 1 followed by immersion in non-complementary DNA 3 with the intercalator. The excitation wavelength was chosen to match the resonance from the ethidium bromide intercalator. The films grown on quartz substrates were cut to fit precisely in the quartz cuvette normally used for liquid samples. It is to be noted that in the above fluorescence measurements, films I, II and V are controls.

Fig.4.5.1 shows the fluorescence emission spectra recorded from 250 Å thick ODA films on quartz after immersion for 4 hours in aqueous solutions of: ethidium bromide intercalator (curve 1); single-stranded DNA 1 with 1.26 μM of intercalator (curve 2), single-stranded DNA 1 followed by immersion in the non-complementary single-stranded DNA 3 with intercalator (curve 3), double-stranded DNA 4 with the intercalator (curve 4) and single-stranded DNA 1 followed by immersion in complementary single-stranded DNA 2 with the intercalator (curve 5). Fig.4.5.1 also shows the emission spectrum from the sequentially hybridized DNA – ODA film (as in curve 5) after heating at 40° C for 20 minutes (curve 6). It is seen that there is no emission from the intercalator in the bare ODA film (curve 1) as well as from films of single-stranded DNA 1 (curve 2) and single-stranded DNA 1 complexed with non-complementary DNA single strands 3 (curve 3), even after heating.

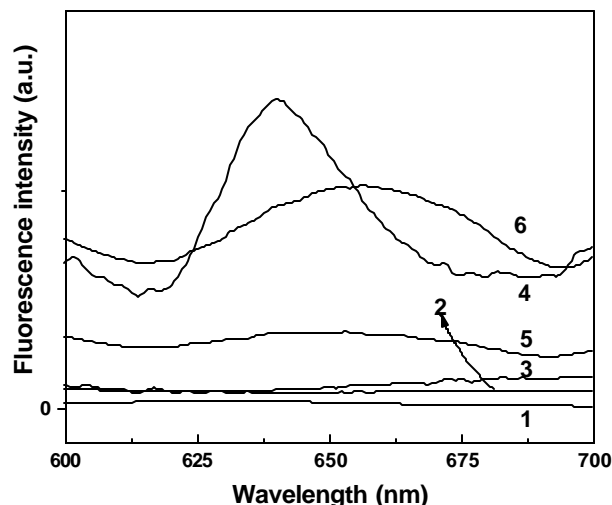


Figure 4.5.1: Fluorescence emission spectra for 250 Å thick ODA films on quartz after immersion in the following solutions for 4 h in aqueous solutions of : ethidium bromide (curve 1); mixture of the single-stranded DNA 1 and intercalator (curve 2); single-stranded DNA 1 followed by non-complementary single-stranded DNA 3 and intercalator (curve 3); hybridized DNA 5 and intercalator (curve 4); single-stranded DNA 1 followed by complementary single-stranded DNA 2 and intercalator (curve 5) and film shown as curve 5 after heating at 40 ° C for 20 minutes (curve 6).

A strong emission signal is clearly seen for the double-stranded DNA 5-ODA composite film (curve 4). This result clearly indicates that the DNA molecules are encapsulated in the ODA matrix without distortion to the double helical structure thereby permitting the binding of ethidium bromide.²⁴ The fluorescence emission spectrum which was weak for the film formed by sequential immersion in solutions of complementary oligonucleotides 1 and 2 (curve 5) increased significantly after heating (curve 6). This is due to the formation of duplex structures after heating, aided by the thermal diffusion of DNAs 1 and 2. Thus hybridization of the DNA strands is possible within the lipid matrix. The observed increase in the fluorescence intensity after heating is not due to the entrapment of the fluoroprobe alone in the hydrophobic matrix, since such an effect was not seen in samples without DNA or composed of non complementary DNA strands. This strongly supports the conclusion that hybridization of DNA 1 and its complementary DNA 2 in the ODA biocomposite film is indeed responsible for the enhanced fluorescence signal. The hybridization of DNA 1 and 2 occurs only within the ODA matrix since the entrapment is accomplished under DNA solution conditions (deionized water) where hybridization does not occur spontaneously in solution.¹⁶ The annealing of the single strands in deionized water is not favoured because of the repulsive forces between the two negatively charged phosphate backbone. While annealing, to overcome the repulsive forces, a small amount of salt is added in water. Thus, the ODA molecules in the lipid matrix act like counterions to screen the repulsive electrostatic interactions between the negatively charged DNA single-strands enabling hybridization to occur. Interestingly, it is observed that while the emission maximum occurs at ca. 640 nm for the double-stranded DNA film (curve 4), it was shifted to ca. 660

nm accompanied by broadening for the *in-situ* hybridized DNA-ODA film (curve 6). This may be due to differences in the polarity of the environment experienced by the fluorescent probe, perhaps due to different binding modes with the DNA duplex in the two situations. While the features of curve 4 are typical of intercalation, the broad, red-shifted fluorescence (curve 6) is indicative of binding at a second site, such as on the DNA duplex surface by mere electrostatic interaction. This interpretation, which is also consistent with the literature observation on DNA-ethidium bromide complexes,²⁵ is a definite consequence of DNA duplex formation within lipid matrix.

4.6. DNA STRUCTURAL STUDIES

After determining the optimum immersion times from the QCM measurements mentioned above, 250 Å thick ODA films on Si (111) wafers were immersed in 10^{-6} M solutions of 4 and 5, thoroughly washed and dried and studied by FTIR. The FTIR measurements were carried out in the diffuse reflectance mode on a Shimadzu PC-8201 PC instrument at a resolution of 4 cm^{-1} . Sufficient number of scans (at least 256) were taken to obtain a good signal-to-noise ratio. The FTIR spectra recorded from 250 Å thick ODA films on Si (111) substrates before and after immersion in 10^{-6} M solutions of double-stranded DNA 5 and calf-thymus DNA 4 are shown as curves a, b and c respectively in Fig.4.6.1.

Three strong resonances at 1230 cm^{-1} , 1065 cm^{-1} and 964 cm^{-1} (features 1-3 in Fig.4.6.1) are clearly observed from the DNA-ODA composite films (spectra b and c, Fig.4.6.1) which are missing in the as-deposited ODA film (curve a, Fig.4.6.1). The 1230 and 964 cm^{-1} bands are due to the backbone PO_2 antisymmetric stretching and deoxyribose C-C stretching vibrations respectively and agree well with literature values of hybridized DNA molecules.²⁶

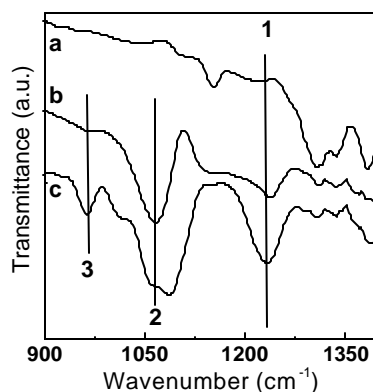


Fig. 4.6.1: FTIR spectra of 250 Å thick ODA films on Si (111) substrates before (curve a) and after immersion for 4 hours in double-stranded DNA 5 (curve b) and calf-thymus DNA 4 (curve c) solutions. Three features 1-3 at 1230 , 1065 and 964 cm^{-1} are labelled in the figure.

The feature at 1065 cm^{-1} is assigned to the deoxyribose band as well, the presence of which is indicative of ZDNA double-helical conformation.²⁷ Such a conformation is known to occur for double-helical DNA molecules in an environment of high ionic strength as would be the case during entrapment in the lipid matrix consisting of densely-packed ODA molecules. This result also supports the large red shift observed in the fluorescence emission signal observed from the double-helical DNA-ODA composite films, which is a consequence of a highly polar environment (Fig.4.5.1, spectrum 4).

4.7. XPS STUDIES

XPS measurements of the C 1s, N 1s, O 1s and P 2p core levels was carried out on a VG Microtech ESCA 3000 instrument at a base pressure better than 1×10^{-9} Torr with un-monochromatized Mg K_{α} radiation (1253.6 eV energy). The measurements were made in the constant analyzer energy (CAE) mode at a pass energy of 50 eV. This leads to an overall resolution of ~ 1 eV in the measurements.

The chemically distinct components in the core level spectra were resolved by a non-linear least squares fitting algorithm after background removal by the Shirley method.²⁸ The alignment of the different core levels was done taking the binding energy of adventitious carbon to be 285eV. The XPS C 1s, P 2p and N 1s core levels were recorded from a 250 \AA thick double-stranded DNA 5-ODA composite film grown on Si (111) substrate and spectra obtained are shown in Figs.4.7.1 (A-C) respectively.

The C 1s spectrum could be decomposed into two components at 285 and 287.5 eV binding energy (curves 1 and 2 respectively, Fig.4.7.1.A). The low binding energy (BE) component is assigned to electron emission from the hydrocarbon chains of ODA, the sugars and bases in the DNA while the higher BE component is from the carbons co-ordinated to the phosphates in the backbone.

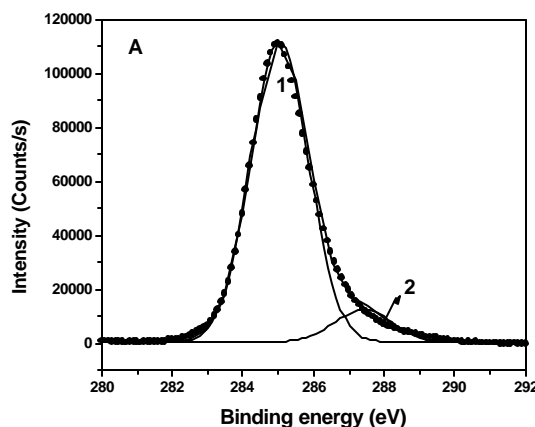


Figure 4.7.1.A. C 1s core level spectrum recorded from a 250 \AA thick 5-ODA composite film on Si (111) substrate. Two chemically distinct components are shown.

The P 2p core level, which clearly arises due to electron emission from the phosphate backbone of the entrapped DNA molecules, could be decomposed into a single spin-orbit pair as shown in Fig.4.7.1.B. The P 2p_{3/2} BE was evaluated to be 132.8 eV (Fig.4B) and agrees fairly well with reported values of DNA films immobilized self-assembled monolayer surfaces by Higashi et al.⁹ and indicates no degradation of the DNA molecules due to coordination with the ODA molecules. Higashi et al reported the BE of 190 and 136 eV for the P 2s and P 2p core level respectively recorded from DNA molecules immobilized on self-assembled monolayer surfaces.⁹ The agreement between this BE value and that observed by us would improve if the P 2p envelope of Higashi et al. were decomposed into the 2 p_{3/2} and 2 p_{1/2} core levels as done by us.

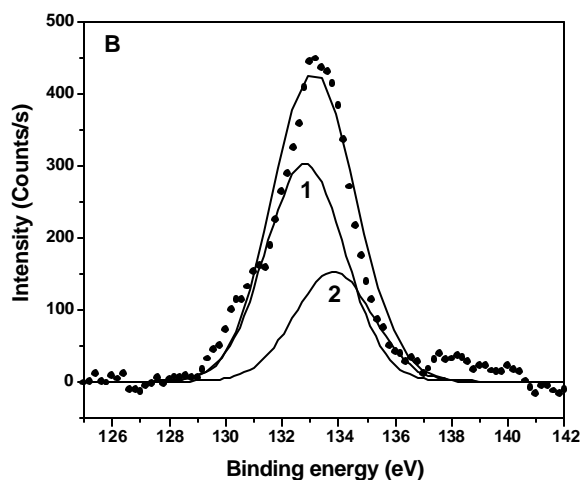


Figure 4.7.1.B: P 2p core level spectrum from a 250 Å thick 5-ODA composite film on Si (111) substrate. The two 2p spin-orbit components are shown.

The N 1s core level showed a single component centred at 399.7 eV (Fig.4.7.1.C) and is due to the electron emission from the nitrogens in the ODA and base molecules of DNA.

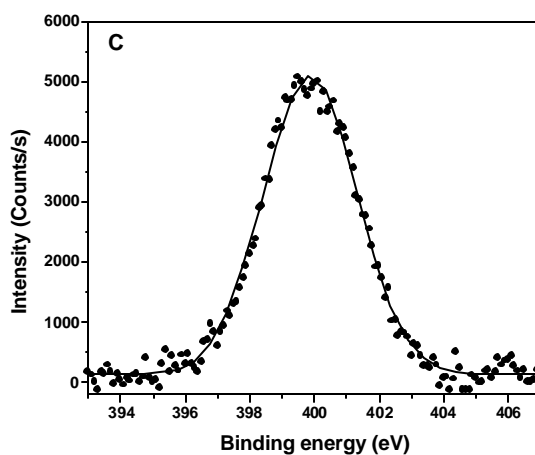


Fig. 4.7.1.C: N 1s core level spectrum from a 250 Å thick 5-ODA composite film on Si (111) substrate. The data is fit to a single Gaussian.

4.8. UV-MELTING MEASUREMENTS

Additional evidence of the retention of the double helical structure of the DNA molecules on entrapment in the ODA matrix was provided by UV melting measurements carried out on a 250 Å thick double-stranded DNA 5-ODA film on quartz.

The UV melting experiments were carried out on Perkin Elmer Lambda 15 UV/VIS spectrophotometer fitted with a Julabo water circulator with programmed heating accessory. The quartz substrates bearing the films were cut so as to fit into the cuvette normally used for liquid samples. The DNA-ODA films were heated at a rate of 0.5 °C per minute and the thermal denaturation of the duplex was followed by monitoring changes in the absorbance at 260 nm as a function of temperature.

The UV melting curve of this film is shown as Fig.4.8.1.

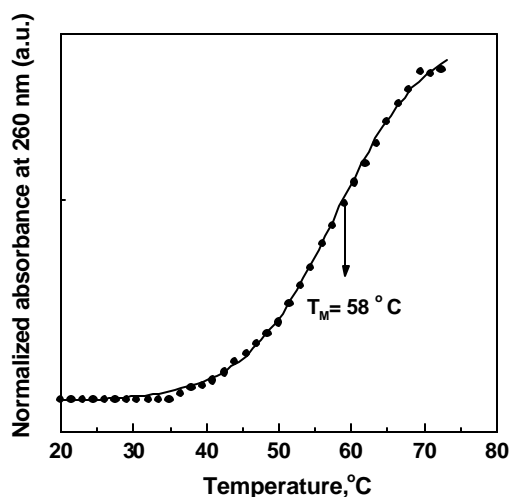


Fig. 4.8.1: UV melting data for the composite film of double-stranded DNA 5 in a 425 Å ODA film on quartz. The melting transition temperature, T_M is indicated in the figure.

A melting transition temperature (T_M) of 58 °C was measured for this film clearly showing the double-helical structure of the DNA molecules in the film. Furthermore, the T_M value is considerably higher than the solution melting temperature value of 41 °C reported for the 16-mer duplexes used in this study.²⁰ This large shift in the T_M value towards higher temperatures indicates considerable stabilization of the double-helical structure by the lipid matrix.

4.9. CONCLUSIONS

In conclusion, it has been demonstrated that DNA molecules may be electrostatically encapsulated in thermally evaporated cationic lipid films by a simple solution immersion procedure without altering the double-helix structure of DNA. Furthermore, sequential immersion in complementary single stranded DNA solutions leads to hybridization of the DNA molecules within the lipid matrix.

4.10. STUDIES RELATED TO THE ELECTROSTATIC ENTRAPMENT AND THERMAL STABILITY OF PRE-FORMED DNA DUPLEXES OF DIFFERENT LENGTHS WITHIN THERMALLY EVAPORATED CATIONIC LIPID FILMS

Developing on the work, described in the above sections, we have looked at the immobilization and thermal stability of pre-formed duplexes of varying lengths within thermally evaporated amine films. The formation of the lipid-DNA composite films of different chain lengths has been followed by quartz crystal microgravimetry (QCM), fluorescence spectroscopy, and UV melting measurements (T_M) while a structural characterization of the films has been carried out by Circular Dichroism (CD) studies.

4.10.1. Synthesis of Pre-formed DNA sequences:

Oligonucleotides of different sequences and their complementary sequence were synthesized by β -cyanoethyl phosphoramidite chemistry on a Pharmacia GA plus DNA synthesizer and purified by FPLC and rechecked by RP HPLC. Pre-formed DNA duplexes (dsDNAs) were obtained by mixing equimolar quantities of ssDNA complementary strands under standard hybridizations conditions.¹⁶

Various dsDNA sequences used were:

10 mer : GCATACATGT and CGTATGTACA

16 mer : GGAAAAAAGTTCGTGC and GCACGAAGTTTTTCC

20 mer : GAGCCAAGGACAGGTAC and CTCGGTTCCTGTCCATG

30 mer: GGAATTTCGAAACATCTTAGATAGATGTAT and

CCTTAGCTTTTGTAGAATCTATCTACATA

All the chemicals used were of the highest purity available. ODA was sourced from Aldrich and used as received.

4.10.2. Quartz Crystal Microgravimetry

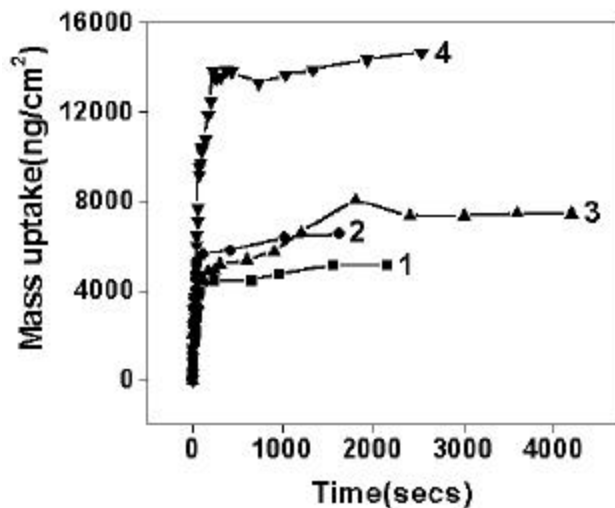


Figure 4.10.2. : QCM mass uptake as a function of time of immersion of a 250 Å thick ODA film in 1 μM pre-formed DNA (dsDNA) solutions of: ds-10 mer (curve 1, squares); ds-16 mer (curve 2, circles); ds-20 mer (curve 3, up triangles) and ds30-mer (curve 4, down triangles).

Fig.4.10.2. depicts the QCM mass uptake kinetics during immersion of 250 Å thick ODA films in aqueous solutions of the dsDNA molecules of varying lengths of 1 (curve 1, squares), 2 (curve 2, circles), 3 (curve 3, up triangles) and 4 (curve 4, down triangles).

It is observed that the mass uptake is highest for 30mer and least for 10 mer DNA. This result suggests that as the length of the DNA sequence increases, the mass uptake also increases. *But interestingly, the diffusivity within the lipid matrix is independent of the chain length.* As observed in the above sections, one would expect that the smallest chain length (10 mer) to diffuse at much faster rate compared to the bulkier 30 mer. However it is observed that the heavier DNA molecule (30 mer) having the largest mass uptake, diffuses at a much faster rate compared to the other sequences, which diffuse almost at the same rate.

4.10.3. Fluorescence studies: Retention of the double helical structure within lipid films.

The retention of the double helical structures may be conveniently studied by introduction of the well-known fluorescent intercalator, ethidium bromide. As mentioned above, enhanced fluorescence from the ethidium bromide molecules occurs on intercalation (described in detail in chapter 2) in the double helical DNA structures²⁴ and may be used to follow the hybridisation process. 250 Å thick ODA films on quartz substrates were immersed for 4 hours in aqueous solutions containing ethidium bromide intercalator of the following: I) 1 μM dsDNA-10mer; II) 1 μM

dsDNA-16mer; III) $1\mu\text{M}$ dsDNA-20mer IV) $1\mu\text{M}$ dsDNA-30mer. The fluorescence measurements on the ODA-DNA composite films were carried out on a Perkin Elmer model LS 50-B spectrofluorimeter at 25°C , with slit widths of 5 nm for excitation at 460 nm and 10 nm for the emission monochromators. The excitation wavelength was chosen to match the resonance from the ethidium bromide intercalator. The films grown on quartz substrates were cut to fit precisely in the quartz cuvette normally used for liquid samples.

Fig.4.10.3 shows the fluorescence emission spectra recorded from 250 \AA thick ODA films on quartz after immersion for 4 hours in aqueous solutions and ethidium bromide intercalator of $1\mu\text{M}$ dsDNA-10mer (curve 1); $1\mu\text{M}$ dsDNA-16mer (curve 3), $1\mu\text{M}$ dsDNA-20mer (curve 2) and $1\mu\text{M}$ dsDNA-30mer (curve 4).

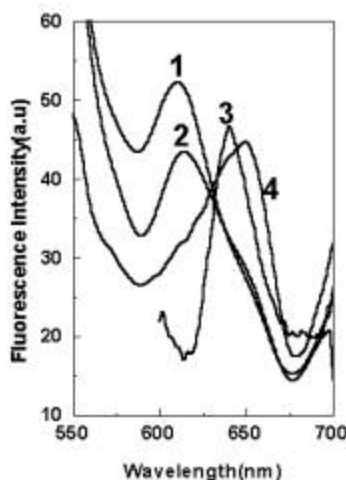


Fig. 4.10.3. : Fluorescence emission spectra for 250 \AA thick ODA films on quartz after immersion in $1\mu\text{M}$ preformed DNA solutions and ethidium bromide : dsDNA -10mer (curve 1), dsDNA-16mer (curve 3), dsDNA-20 mer (curve 2), dsDNA-30mer (curve 4).

A strong emission signal is clearly seen for all the double-stranded DNA - ODA composite films. This result clearly indicates that the DNA molecules are encapsulated in the ODA matrix without distortion to the double helical structure thereby permitting the binding of ethidium bromide.²⁴

Interestingly, it is observed that while the emission maximum occurs at ca. 610 nm for the dsDNA film of 10 mer (curve 1) and dsDNA film of 20 mer (curve 2), it was shifted to ca. 640 nm for dsDNA film of 16 mer (curve 3) and dsDNA film of 30 mer (curve 4). In spite of the shift in the peak position, all the features are typical of intercalation.

4.10.4. Further evidence of the retention of the double helical structure from UV-melting studies.

Additional evidence of the retention of the double helical structure of the DNA molecules of different lengths on entrapment in the ODA matrix was provided by UV melting measurements carried out on a 250 Å thick double-stranded DNA -ODA film on quartz.

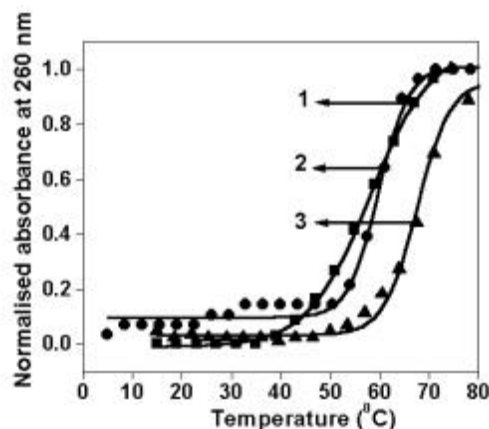


Figure 4.10.4: UV melting data for 250 Å thick ODA films on quartz after immersion in 1 μm pre- formed DNA (dsDNA) solutions of: ds 16 (curve1, squares) ; ds20 (curve 2, circles) ; and ds30-mer (curve 3, up triangles). The solid lines are sigmoidal fits to the data.

A melting transition temperature (T_M) of 58 °C was measured for dsDNA-16 mer film (curve 1, squares, also shown in section 4.8) clearly showing the double-helical structure of the DNA molecules in the film. The T_M of 59 °C for dsDNA-20 mer (curve 2, circles) and T_M of 67 °C for dsDNA-30 mer (curve 3, up triangles) proved further that the retention of the duplex form of DNA within the ODA bilayers had occurred. T_M for dsDNA-10 mer could not be obtained.

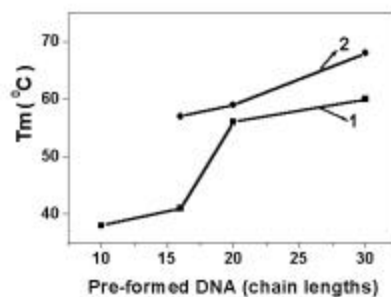


Figure 4.10.5. : A plot of melting transition temperatures (T_M) as a function of different lengths of pre-formed DNA solutions of 1 μm each containing 10mM NaCl as seen in (curve 1, squares) and is compared with the plot of melting transition temperatures vs different lengths of pre-formed DNA solutions intercalated within 250 Å thick ODA film (curve 2, circles).

Furthermore, the T_M values for the dsDNA-ODA film (16,20,30 mer) is considerably higher than the corresponding solution melting temperature values reported for the duplexes used in this study shown in figure 4.10.5. This large shift in the T_M value towards higher temperatures indicates considerable stabilization of the double-helical structure by the lipid matrix.

4.10.6. Conclusions

We have demonstrated the immobilization and thermal stability of pre-formed duplexes of varying lengths within the thermally evaporated amine films. The formation of the lipid-DNA composite films of different chain lengths was followed by QCM, fluorescence spectroscopy, and UV melting measurements (T_M) while a structural characterization of the films has been carried out by Circular Dichroism (CD) studies. From QCM, it is very clear that the diffusivity within the lipid matrix is independent of the length of DNA used. Fluorescence studies show a strong emission signal for all the double-stranded DNA - ODA composite films indicating that the DNA molecules are encapsulated in the ODA matrix without distortion to the double helical structure thereby permitting the binding of ethidium bromide. The T_M values obtained for all the dsDNA-ODA films is considerably higher than the corresponding solution melting temperature values reported for the duplexes used in this study, indicates considerable stabilization of the double-helical structure by the lipid matrix.

4.11. SUMMARY

In this chapter, we have demonstrated the encapsulation of double-stranded DNA and *in-situ* hybridization of complementary single-stranded DNA molecules in a fatty lipid matrix. The immobilization of DNA is accomplished by simple immersion of a thermally evaporated octadecylamine film (ODA) in the DNA solution at close to physiological pH. The diffusion of the DNA molecules into the cationic lipid film is dominated by attractive electrostatic interaction between the negatively charged phosphate backbone of the DNA molecules and the protonated amine molecules in the thermally evaporated film and has been quantified using QCM. Fluorescence studies of DNA-ODA films obtained by sequential immersion of the ODA matrix in the complementary single strand DNA solutions using ethidium bromide intercalator clearly showed that the hybridization of the DNA single strands had occurred within the lipid matrix. Furthermore, fluorescence studies of the preformed dsDNA-ODA biocomposite film indicated DNA encapsulation without distortion to the native double helix structure. The FTIR spectrum of the DNA-ODA composite film showed signatures of DNA, clearly suggesting the entrapment and retention of the double helical structure of DNA in lipid matrices. Additional evidence of the retention of the double helical structure of the DNA molecules on entrapment in the ODA matrix was provided by UV melting measurements. A melting transition temperature (T_M) of 55 °C was measured for DNA-ODA

film clearly showing the double-helical structure of the DNA molecules in the film. Furthermore, the T_M value is considerably higher than the solution melting temperature value indicating considerable stabilization of the double-helical structure by the lipid matrix.

We have also demonstrated the immobilization and thermal stability of pre-formed duplexes of varying lengths within thermally evaporated amine films. Fluorescence studies show a strong emission signal for all the double-stranded DNA - ODA composite films indicating that the DNA molecules are encapsulated in the ODA matrix without distortion to the double helical structure thereby permitting the binding of ethidium bromide. The T_M values obtained for all the dsDNA-ODA films is considerably higher than the corresponding solution melting temperature values reported for the duplexes used in this study, indicates considerable stabilization of the double-helical structure by the lipid matrix.

The ease with which diffusion into the lipid matrix occurs in conjunction with contact angle measurements suggests entrapment of the DNA molecules within the lipid matrix in a DNA-lipid bilayer structure, wherein the DNA molecules are bound to the ionized hydrophilic regions of the matrix. It is interesting to note that though the DNA-lipid interaction is mainly electrostatic, there could be differences in the final templated structures formed in solution and in the rigid matrix. Such DNA-lipid composites are expected to be ideal model systems for studying the permeability of DNA and PNA in cell membranes, important for DNA antisense therapeutics.⁹ Another exciting possibility is the potential formation of patterned, multi-DNA arrays in DNA chip applications.¹⁰

The DNA-fatty lipid composite films would serve as model systems for understanding DNA-membrane interactions as well as in the study of DNA-drug/protein interactions. This approach also shows promise for the synthesis of patterned DNA films and consequent application in disease detection and genome sequencing.

4.12. REFERENCES

- (1)a) Hayward, R.E.; DeRisi, J.L.; Alfadhi, S.; Kaslow, D.C.; Brown, P.O.; Rathod, P.K. *Mol. Microbiol.* 2000, 35, 6; b) Heiskanen, M.A.; Bittner, M.L.; Chen, Y.; Khan, J.; Adler, K.E.; Trent, J.M.; Meltzer, P.S. *Cancer. Res.* 2000, 60, 799.
- (2)a) Peterson, A.W.; Heaton, R.J.; Georgiadis, R. *J.Am.Chem.Soc.* 2000, 122, 7837; b) Higashi, N.; Inoue, T.; Niwa, M. *J.Chem.Soc., Chem.Commun.* 1997, 1507; c) Xu, X.H.; Yang, H.C.; Mallouk, T.E.; Bard, A.J. *J. Am. Chem. Soc.* 1994, 116, 836.
- (3) Watterson, J.H.; Piunno, P.A.E.; Wust, C.C.; Krull, U.J. *Langmuir* 2000, 16, 4984.
- (4) Nikiforow, T.T.; Rogers, Y.H.; *Anal.Biochem.* 1995, 227, 201.

- (5) a) Rehman, F.N.; Audeh, M.; Abrauns, E.S.; Hammond, P.W.; Kenney, M.; Boles, T.C.; *Nucleic Acids Res.* 1999, *27*, 649; b) Proudnikov, D.; Tunofeev, E.; Mirzabekov, A. *Anal. Biochem.* 1998, *259*, 34.
- (6) Niemyer, C.M.; Boldt, L.; Ceyhan, B.; Blohm, D. *Anal. Biochem.* 1999, *268*, 54.
- (7) Tarlov, M.J.; Herne, T.M. *J. Am.Chem.Soc.* 1997, *119*, 8916.
- (8) a) Okahata, O.; Kobayashi, T.; Tanaka, K. *Langmuir* 1996, *12*, 1326; b) Ijiro, k.; Shimomura, M.; Tanaka, M.; Nakamura, H.; Hasebe, K. *Thin Solid Films* 1996, *284-285*, 780; c) Shimomura, M.; Nakamura, F.; Ijiro, K.; Taketsuna, H.; Tanaka, M.; Nakamura, H.; Hasebe, K. *J.Am.Chem.Soc.* 1997, *119*, 2341; d) Kago, K.; Matsuoka, H.; Yoshitome, R.; Yamaoka, H.; Ijiro, K.; Shimomura, M. *Langmuir* 1999, *15*, 5193; e) Ebara, Y.; Mizutani, K.; Okahata, Y. *Langmuir* 2000, *16*, 2416.
- (9) Higashi, N.; Takahashi, M.; Niwa, M. *Langmuir* 1999, *15*, 111.
- (10) a) Steel, A. B.; Herne, T. M.; Tarlov, M. J. *Bioconjugate. Chem.* 1999, *10*, 419; b) Steel, A. B.; Herne, T. M.; Tarlov, M. J. *Anal.Chem.* 1998, *70*, 4670; c) Wang, J.; Nielsen, P.E.; Jiang, M.; Cai, X.; Fernandez, J.R.; Grant, D.H.; Ozsoz, M.; Begleiter, A.; Mowat, M. *Anal.Chem.* 1997, *69*, 5200.
- (11) Tarlov, M.J.; Herne, T.M. *J. Am.Chem.Soc.* 1997, *119*, 8916.
- (12) Huang, E.; Zhou, F.; Deng, L. *Langmuir* 2000, *16*, 3272.
- (13) a) Gole, A.; Sastry, M. *Inorg.Chem.Commun.* 2001, *4*, 568; b) Pal, S.; Ph.D. Thesis, University of Poona, 1996; c) Ganguly, P.; Pal, S.; Sastry, M.; Shashikala, M.N. *Langmuir* 1995, *11*, 1078.
- (14) a) Sastry, M. *Curr.Sci.* 2000, *78*, 1089; b) Patil, V.; Malvankar, R.B.; Sastry, M. *Langmuir* 1999, *15*, 8197; c) Sastry, M.; Patil, V.; Sainkar, S.R. *J.Phys.Chem.B.* 1998, *102*, 1404.
- (15) a) Gole, A.; Dash, C.V.; Rao, M.; Sastry, M. *J. Chem.Soc., Chem.Commun.* 2000, 297; b) Gole, A.; Dash, C.V.; Mandale, A.B.; Rao, M.; Sastry, M. *Anal.Chem.* 2000, *72*, 4301.
- (16) Cantor, C.R; Schimmel, P.R. *Biophysical Chemistry, Part III*, W.H. Freeman, New York (1980).
- (17) Cuvillier, N.; Rondelez, F. *Thin Solid Films* 1998, *327-329*, 19.
- (18) Decher, D. *Science* 1997, *277*, 1232 and references therein.
- (19) a) Lvov, Y.; Ariga, K.; Onda, M.; Ichinose, I.; Kunitake, T. *Langmuir* 1997, *13*, 6195; b) Kumar, A.; Mandale, A.B.; Sastry, M. *Langmuir* 2000, *16*, 6921.
- (20) Pattarkine, M.V.; Garesh, K.N. *Biochem.Biophys.Res.Commun.* 1999, *263*, 41.
- (21) a) Klug, A.; *Philos.Trans.Roy.Soc. London Ser. A.* 1994, *348*, 167; b) Trubetskoy, V.S.; Loomis, A.; Slattum, P.M.; Hagstron, J.E.; Budker, V.G.; Wolff, J.A. *Bioconjugate Chem.* 1999, *10*, 624.
- (22) Gole, A.; Kaur, J.; Pavaskar, N.R.; Sastry, M. *Langmuir*, 2001, *17*, 8249.
- (23) Carslaw, H.S.; Jaeger, J.C. *Conduction of heat in solids*; Clarendon Press: Oxford, 1960, 101.
- (24) LePecq, J.B.; Paoletti, C. *J.Mol.Biol.* 1967, *27*, 87.

- (25) Coury, J.E.; Anderson, J.R.; McFail-Isom, L.; Williams, L.D.; Bottomley, L.A. *J. Am. Chem. Soc.* 1997, *119*, 3792.
- (26) Neault, J.F.; Tajmir-Riahi, H.A. *J.Phys.Chem.B.* 1998, *102*, 1610.
- (27) Taillandier, E.; Liquier, J. *Methods in Enzymology* 1992, *211*, 307.
- (28) Shirley, D.A. *Phys.Rev.B.* 1972, *5*, 4709. An application written by one of us (MS) in Mathcad (a commercial mathematical software package), SHIRL.MCD was used for the analysis. This application is available from the Mathsoft public domain site.
- (29) *Methods in Enzymology* ed. Phillips, M.I. : Vol. 313 (Academic Press, San Diego, 2000).

CHAPTER V

FORMATION OF PNA-DNA HYBRIDS

WITH OCTADECYLAMINE

MOLECULES

In this chapter sequential immobilization and in-situ hybridization of single stranded DNA and complementary PNA molecules in thermally evaporated fatty amine films and at the air-water interface with cationic Langmuir monolayers is demonstrated. The work described in this chapter is based on the use of lipid monolayers and thermally evaporated lipid bilayers. Quartz crystal microgravimetry and UV-melting analysis of the films of ODA-PNA-DNA hybrids formed by both the methods of immobilization; clearly showed that the sequential immobilization process had resulted in hybridization of the complementary single-stranded DNA molecules with PNA at the air-water interface and within lipid bilayer stacks. The specificity of base pairing in the DNA-PNA complexes with the ODA monolayers and within the ODA matrix was also studied by introduction of a single mismatch in the DNA sequence.

"Man is beginning to come up with analogs of things nature made with evolution"

--- Jack Cohen

The work described in this chapter has been published : 1) Ramakrishnan, V.; Sable, M.; D'Costa, M.; Ganesh, K.N.; Sastry, M. *Chem. Soc. Chem.Comm.* **2001**, 2622; 2) Ramakrishnan, V.; D'Costa, M.; Ganesh, K.N.; Sastry, M. *Langmuir* (in press).

5.1 INTRODUCTION

The most important molecular recognition event in nature is the base-pairing of nucleic acids, which guarantees the storage, transfer and expression of genetic information in living systems. So one wouldn't have thought the need of replacing or updating DNA or RNA since these two nucleic acids have carried out faithfully the traditional roles of coding and passing on the genetic information. Yet some very simple and very fundamental questions remain unanswered. *Why has nature chosen or settled on DNA as the central genetic material of life? Is DNA the only possibility or could other chemical structures fulfil the requirements and support another form of life? What makes DNA such a good candidate in terms of structure, stability and molecular recognition?* We will probably never get the final answers to all these questions, but studying DNA and DNA analogues and mimics will bring us closer to these answers. Since the investigation of oligonucleotides as potential therapeutics that target nucleic acids was initiated,¹ the search for nucleic acid mimetics with improved properties such as strengthened binding affinity to complementary nucleic acids, increased biological stability and improved cellular uptake has accelerated rapidly. Furthermore, with the coming of modern biomedicine and its vision of using bits of DNA and RNA to tag or combat harmful genes, the natural compounds did not always fit the bill anymore. In the last few years, attempts to optimise the properties of oligonucleotides have resulted in the synthesis and analyses of a huge variety of new oligonucleotides derivatives with modification to the phosphate group, the ribose or the nucleobase.²

However the most radical change to the natural structure was made by the Danish group of chemists, Michael Egholm, Peter Nielsen, Ole Buchardt and Rolf Berg.

"It was believed that God created the best nucleic acid backbone in the world and nothing else would work"

--- Michael Egholm

In a pioneering report, Nielsen and co-workers demonstrated that the entire sugar-phosphate backbone in DNA could be replaced by an N-(2-aminoethyl) glycine based polyamine structure and that the DNA bases could be attached to the peptide backbone yielding a class of molecules known as peptide nucleic acids (PNA).³ The Danish team did away with the phosphate – sugar backbone and instead attached each base to a peptide group- one of the family of units that link up to form proteins

PNA was originally designed and developed as a mimic of a DNA-recognizing, major-groove-binding, triplex forming oligonucleotide.^{3d-f} Nielsen et al.⁴ reported in 1993, that PNA containing all four natural nucleobases hybridises to complementary oligonucleotides obeying the Watson-Crick base-pairing rules and thus PNA is a true DNA mimic in terms of base-pair recognition. The neutral character of the PNA backbone is an important feature that has many consequences. One of the most impressive is the high binding affinity of PNA to complementary DNA sequences (mentioned in chapter 1, wherein the structure and properties of PNA has been discussed in detail) and obey Watson-Crick base pairing rules, thus making PNA-DNA duplexes thermally more stable than the corresponding DNA-DNA duplexes.⁴ Moreover, the stability of PNA-DNA duplexes is almost

unaffected by the ionic strength of the medium in contrast to the behavior of DNA double helical structures.⁵ In a careful study by Tomac et al.,^{5b} the melting transition temperature (T_m) of DNA-DNA hybrids was shown to increase considerably with increasing salt concentration (0.01 to 0.5M NaCl), whereas the T_m of PNA-DNA duplexes is almost identical at 0.5 M. The contrasting effect of ionic strength on duplex formation can be explained by the association of counter ions in the case of DNA-DNA duplex formation and by the displacement of counterions in the case PNA-DNA hybrid formation. PNAs exhibit high resistance to Dnases and proteinases making them highly biostable.⁶

Consequently, these favourable properties of PNA have attracted wide attention in medicinal chemistry for development of gene therapeutic (antisense and antigene) drugs⁷ and in molecular diagnostics.^{3a} Potential therapeutic applications for PNAs arise from their biological properties described above. The sequence – specific inhibition of replication (antigene agents), transcription and translation (antisense agents) could be potentially exploited for therapeutic applications.



Fig 5.1 Inhibition of replication and transcription of DNA by antigene PNAs and inhibition of translation of mRNA by antisense PNAs.

Although numerous reports have appeared on translation inhibition by antisense oligonucleotides, there are remarkably few studies of PNA oligomers as antisense agents.⁸

The following properties of PNAs can be exploited in the use of PNAs in DNA diagnostics:

- 1) PNAs have better sequence discrimination, and form more stable hybrids than oligonucleotides.
- 2) In contrast to oligonucleotides, PNAs can cause strand invasion in double stranded DNA.
- 3) PNAs alter the electrophoretic mobility of complementary nucleic acids considerably on binding due to their neutral character.

Thus the excellent hybridization properties of PNA has allowed the development of several techniques for isolation and detection of nucleic acids for analysis in genetic diagnostics.⁹

The immobilization of DNA and analogues of DNA (namely PNA) in different matrixes has attracted wide attraction of researchers around the globe. Many different routes are being employed for the immobilization of DNA-PNA hybrids on planar supports. Some of the methods include use of cationic liposomes or lipids as carriers for PNA-DNA hybrids which has important applications in the development of nonviral vectors in gene therapy.^{7a} Recently, the air-water interface has been used to study interaction of biomolecules with Langmuir monolayers as a means of modelling cellular delivery of DNA/PNA across biological membranes in gene therapy.^{3a,10}

The work described in this chapter is based on the use of lipid monolayers and thermally evaporated lipid bilayers. Developing on our earlier work¹¹ discussed in chapter 4, on the sequential immobilization and in-situ hybridisation of single stranded DNA within thermally evaporated ODA lipid films, in this chapter, we have demonstrated the sequential entrapment of single stranded DNA and complementary PNA molecules in thermally evaporated fatty amine films and shown evidence for their *in-situ* hybridisation. The PNA-DNA hybrids have been characterized by QCM and UV-melting measurements. We also looked at the specificity of base pairing in the DNA-PNA complexes within the ODA matrix. Introduction of a single base pair mismatch in the DNA sequence leads to destabilization of DNA-PNA complex and a measurable lowering of the melting transition temperature.

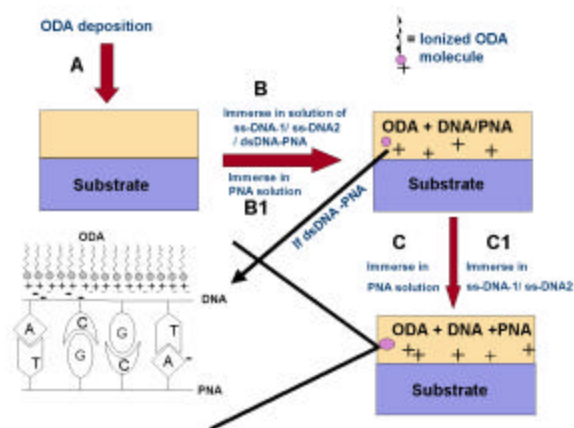
This chapter also deals with the sequential immobilization and hybridization of DNA-PNA molecules at the air-water interface with Langmuir monolayers. In chapter 3, we had demonstrated the hybridization of complementary single stranded oligonucleotides sequentially immobilized at the air-water interface in the presence of the cationic Langmuir monolayer, octadecylamine (ODA).¹² We extend our studies in this direction and show in this chapter, that complementary DNA and PNA sequences may be immobilized at the air-water interface with ODA Langmuir monolayers and furthermore, that facile hybridization of PNA and DNA single strands to yield PNA-DNA hybrids occurs at the interface. The ODA-PNA-DNA hybrid monolayers may be readily transferred onto solid supports by the Langmuir-Blodgett (LB) method, thereby enabling a study of the thermal stability of the PNA-DNA hybrids in the lipid matrix. These results are compared with preformed DNA duplexes bound to the fatty amine monolayer as well as some control experiments involving the sequential binding of PNA to a non-complementary DNA sequence. A measure of the contribution of the lipid matrix to the thermal stability of the intercalated guest molecules was obtained by binding the polyelectrolyte, Xanthan, with ODA monolayers. The specificity of base pairing in the DNA-PNA complexes with the ODA monolayers was also studied. Introduction of a single mismatch in the DNA sequence did not yield any shifts in the UV-melting compared to that of complementary DNA-PNA hybrids.

5.2 SEQUENTIAL ENTRAPMENT OF PNA AND DNA IN LIPID BILAYERS STACKS

PNAs alone are not suitable to be delivered by cationic liposomes, since, being neutral molecules, cannot form electrostatic interactions with the positively charged liposomes. With respect to the biological activity of PNAs, Mischiati, C. et al. have recently reported that DNA-PNA hybrid molecules can be considered for the development of decoy molecules.¹³ Nielsen et al. have pointed out that DNA-PNA hybrids could possibly exhibit aptameric activity on a variety of DNA-binding proteins.⁹ Therefore the next thing which struck the researchers was that whether cationic liposomal formulations can bind to DNA-PNA hybrids by ionic interactions between the positively charged liposomes and the negatively charged DNA strand. In this respect, Nastruzzi, C. et al.^{7a} reported that cationic liposomes are efficient carriers for DNA-PNA hybrids. Their report describes (a) preparation

of positively charged liposomes by the reverse phase evaporation method using different cationic lipids like dioctadecyl-dimethylammonium bromide (DDAB₁₈) and dioleoyltrimethylammonium propane (DOTAP), (b) the differential ability of cationic liposomes to complex PNA-DNA hybrids, (c) the short term toxicity of the cationic liposomes on in vitro cultured human cells, and finally (d) the liposomal mediated delivery of DNA-PNA hybrids to in vitro cultures cells.

Our work is based on the sequential immobilization of single stranded DNA and complementary PNA molecules in thermally evaporated fatty amine films and evidence for their *in-situ* hybridization is demonstrated. Our earlier work on the electrostatic entrapment of charged nanoparticles¹⁴ and protein molecules¹⁵ in fatty lipid matrices and also the present work on the entrapment of DNA in thermally evaporated films of cationic fatty amine molecules¹¹ is explained in detail in chapter 4. In this chapter, we show for the first time that PNA may be immobilized in thermally evaporated lipid films by simple immersion of the lipid film in the PNA solution and furthermore, that this may be extended to a sequential PNA-DNA immobilization strategy for DNA detection. The procedure is illustrated in Schematic 5.2.1 and will be discussed subsequently.



Scheme 5.2.1 Diagram Showing the Various Stages of the DNA-PNA-ODA Composite Film Formation

Step A : Deposition of ODA on solid substrates by thermal evaporation; step B : diffusion of single-stranded DNA -1/ single mismatch sequence of DNA -2 / double-stranded DNA-PNA into the lipid matrix during immersion in the different DNA solutions and step C : sequential immersion in PNA solution after encapsulating the complementary strands 1 or a mismatch sequence 2. In step B1 and C1, another experiment was carried out in which the order of immobilization was reversed i.e. PNA-DNA hybrids formed by first entrapping PNA (step B1) and then ss-DNA1/2 solutions in the ODA matrix (step C1). The magnified section shows the possible microscopic structure of the DNA - PNA - ODA complex.

5.2.1 Synthesis of DNA -PNA sequences :

Oligonucleotides of the sequence AGTGATCTAC (1) and AGTGATCCAC (2) were synthesized by β -cyanoethyl phosphoramidite chemistry on a Pharmacia GA plus DNA synthesizer and purified by FPLC and rechecked by RP HPLC. The PNA oligomer H-GTAGATCACT-NH(CH₂)₂-COOH was synthesized manually using a Merrifield resin derivatized with β -alanine (0.013 meq/g) employing the standard Boc-protection strategy. Cleavage from the solid support using the TFA-TFMSA cleavage

procedure yielded the PNA oligomer with a free carboxylic acid at its 'C' terminus. The oligomer was purified by RP-FPLC and its purity rechecked by RP-HPLC and confirmed by MALDI-TOF mass spectroscopy.

1 is complementary to the PNA sequence while 2 is a mismatch sequence to the PNA sequence. Pre-formed DNA-PNA solutions were obtained by mixing equimolar quantities of 1 and PNA solution under standard hybridization conditions.¹⁶

5.2.2 Deposition of lipid films.

Octadecylamine (ODA, $\text{CH}_3(\text{CH}_2)_{17}\text{NH}_2$, $\text{pKb} \sim 10.5$) which is an amphiphilic molecule was used in this study. As explained in chapter 2, 3 and 4, these lipids were thermally evaporated (using an Edwards E 306A vacuum deposition unit) onto suitable substrates such as gold-coated 6 MHz AT-cut quartz crystals, and quartz substrates for quartz crystal microgravimetry (QCM) and UV-melting measurements respectively. Deposition was done at a slow rate at a pressure of better than 1×10^{-7} Torr and the thickness of the deposited films was monitored *in-situ* using an Edwards quartz crystal microbalance (QCM). The deposited films were checked for degradation using FTIR measurements and found to be intact. The thickness of the films deposited was about 250 Å thick and was cross-checked using ellipsometry.

5.3 QUARTZ CRYSTAL MICROGRAVIMETRY

As explained in chapter 2, 3 and 4, 250 Å thick ODA films deposited on quartz crystals were immersed in 10^{-6} M aqueous, de-ionized solutions of DNA and PNA ($\text{pH} = 6.8$). The diffusion of the DNA and PNA molecules into the fatty lipid matrix was followed by measuring the frequency changes in time of the ODA-coated QCM crystal. This was achieved by *ex-situ* measurement of the QCM resonant frequency after thorough washing and drying of the crystals using an Edwards FTM5 frequency counter. This frequency counter had a resolution and stability of 1 Hz. The frequency change (Δf) was converted to mass loading (Δm) using the standard Sauerbrey relationship¹⁷ [$\Delta m = 12.1 \Delta f (\text{ng}/\text{cm}^2)$] and has been explained in detail in chapter 2. Pre-formed DNA-PNA duplexes were obtained by mixing equimolar quantities of DNA and PNA under standard hybridization conditions¹⁶ were also incorporated in the ODA films by similar immersion in the dsDNA-PNA solution (10^{-6} M concentration) and the QCM mass uptake kinetics studied.

Fig.5.3.1 presents quartz crystal microgravimetry (QCM) data of the diffusion of the DNA and PNA molecules into the fatty amine films during immersion of the ODA-coated QCM crystals in 1 μM aqueous solutions of – ssDNA-1 followed by PNA (up triangles); PNA followed by ssDNA-1 (squares); ssDNA-2 followed by PNA (down triangles) and preformed PNA-DNA complexes (circles).

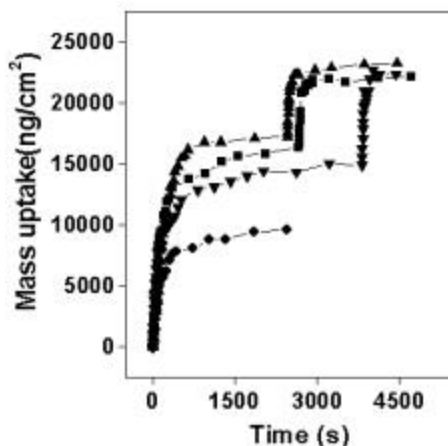


Fig.5.3.1 : QCM mass uptake data recorded during immersion of 250 Å thick ODA films in 1 μm solutions of – preformed PNA-DNA complexes (circles); sequential immersion in ssDNA-2 followed by PNA (down triangles); sequential immersion in PNA followed by ssDNA-1 (squares) and ssDNA-1 followed by PNA (up triangles).

In all cases, it is observed that there is extremely rapid diffusion of the DNA and PNA molecules into the lipid matrix. While the diffusion of DNA molecules (both ssDNA-1 and ssDNA-2) into the ODA film is not surprising and may be explained in terms of attractive electrostatic interaction between the negatively charged DNA phosphate groups and protonated amine groups in the lipid matrix,¹¹ the significant intake of the extremely weakly charged PNA is clearly due to other interactions. The large PNA uptake is all the more interesting since the presence of DNA molecules 1 and 2 in the ODA matrix should effectively block binding sites with the ODA molecules. It is tempting to attribute the PNA diffusion into the ODA matrix to interactions arising from hybridization of the PNA molecules with the already immobilized DNA. However, a comparison of the QCM curves from the sequential immersion of the ODA films in 1 and 2 followed by immersion in PNA solution (up triangles and down triangles respectively, Fig 5.3.1) reveals that the mass uptake due to PNA alone (the mass increase in the second part of the QCM mass uptake curves) is similar in both cases. This clearly shows that hybridization alone cannot account for the diffusion of PNA into the DNA-ODA films and entropic factors/other interactions drive the diffusion of PNA into the lipid matrix. Indeed, immersion of the ODA films first into PNA solution followed by DNA (squares, Fig.5.3.1) resulted in significant PNA entrapment further attesting to the above fact.

Equilibration of the number density of preformed PNA-DNA complexes in the ODA matrix (circles) occurs on time-scales similar to that observed for the single -stranded DNA molecules 1 and 2 as well as PNA. The lower mass uptake in this case (preformed PNA-DNA complexes) may be due to duplex structure preventing complete neutralization of the negative charge on the DNA by the positively charged ODA matrix.

Even though QCM may be used to determine the presence of DNA and PNA molecules in the ODA matrix, it is clearly insufficient in determining whether hybridization had occurred between the entrapped PNA and DNA molecules. Consequently, UV-melting experiments were carried out as a test

for hybridization of DNA-PNA in ODA films which is discussed in the next section. From the QCM measurements presented in Fig.5.3.1, optimum times of immersion of the ODA films in the different DNA and PNA solutions were determined and used in the preparation of ODA-DNA/PNA composite films for UV melting measurements (Fig.5.4.1).

5.4 UV-MELTING (T_m) STUDIES

UV-melting experiments on the ODA-DNA/PNA conjugate films were carried out as a test of hybridization.¹⁸ Unlike in the case of hybridization of complementary DNA strands where fluorescent intercalators such as ethidium bromide are routinely used,^{12,19} reports on the use of intercalators for the detection of PNA-DNA hybrids are relatively scarce.²⁰

Fig.5.4.1 shows plots of the UV-melting data recorded from ODA films in which preformed PNA-DNA duplexes were entrapped (up triangles); an ODA film with sequential immobilization of ssDNA-1 and PNA (squares); an ODA film with ssDNA-2 and PNA intercalated sequentially (circles) and an ODA film first immersed in PNA followed by ssDNA-1 (diamonds).

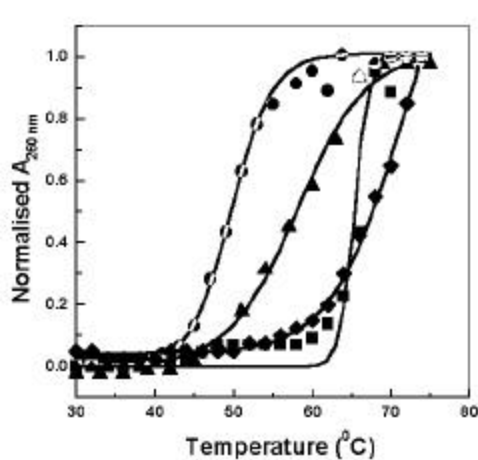


Fig. 5.4.1 UV melting data for 250 Å thick ODA films on quartz after immersion in 1 μm solutions of – ssDNA-2 followed by PNA (circles); preformed PNA-DNA complexes (triangles); ssDNA-1 followed by PNA (squares) and PNA followed by ssDNA-1 (diamonds). The solid lines are sigmoidal fits to the data.

We also looked at the specificity of base-pairing in the DNA-PNA complexes within the ODA matrix. Introduction of a single base pair mismatch in the DNA sequence leads to destabilization of DNA-PNA complex and a measurable lowering of the melting transition temperature. The specificity of base-pairing in the DNA-PNA complexes within the ODA matrix is reflected in the lowering of T_m in the case of single base pair mismatch ssDNA-2 with PNA which is much lower (49° C) than the T_m of complementary ssDNA-1 with PNA (59 °C). Introduction of a single base pair mismatch in the DNA sequence leads to destabilization of DNA-PNA complex and a measurable lowering of the melting transition temperature.

An interesting result of the investigation is the fact that the melting transition of ssDNA-1-PNA hybrids in the lipid matrix (66°C, squares) is much higher than the T_m of the ODA film in which preformed DNA-PNA duplexes were incorporated (59 °C, triangles).

Another important observation is that the order of immobilization of PNA and DNA in the ODA matrix is not of much consequence (T_m of PNA-DNA hybrids formed by first entrapping PNA and then DNA = 68 °C, diamonds) in the extent of hybridization. The increased stability of the PNA-DNA hybrids formed in the ODA bilayers vis-à-vis the duplexes formed in solution and then entrapped within the lipid may be due to the following reason. During sequential immobilisation of DNA followed by PNA (or vice-versa), electrostatic attachment of DNA to the ODA monolayer would leave free and exposed the bases on the DNA molecules. The magnified section in schematic 5.2.1. shows the possible microscopic structure of the DNA- PNA - ODA complex. This mode of organization would then enable facile hydrogen bonding of the complementary PNA molecules with the immobilized DNA a process not so easily done in solution. It is also possible that entrapment of pre-formed PNA-DNA complexes would lead to some orientational disorder within the ODA matrix and therefore reduced binding with the lipid. This would be reflected in terms of a lowering of the melting transition temperature as observed in this study. The UV-melting measurements clearly demonstrate that PNA-DNA immobilization and hybridization occurs within the confines of ODA bilayer stacks and furthermore, that it is sensitive to single base mismatches in the DNA sequence.

5.5 CONCLUSIONS

In the sections above, it has been demonstrated that DNA and PNA molecules may be entrapped in thermally evaporated fatty amine films thus leading to a potentially exciting and novel protocol for the entrapment of oligonucleotides and their analogues. This strategy has been shown to lead to the hybridization of complementary PNA-DNA sequences in the lipid matrix in a sequential immobilization experiment. The specificity of hybridization within the lipid matrix is good and may be easily detected by UV-melting measurements. The possibility of depositing patterned lipid films and entrapping different PNA sequences in the different elements makes this approach promising for gene sequencing applications. A highlight of this approach is that it is both PNA and DNA are friendly – no (fairly complicated) thiolation of these molecules need be done as is required in other gold film-based immobilization strategies.^{3a}

5.6 PNA-DNA HYBRIDIZATION AT THE AIR-WATER INTERFACE WITH LANGMUIR MONOLAYERS

Recently, the air-water interface has been used to study interaction of biomolecules with Langmuir monolayers with a view to observe molecular recognition process at the surface of lipid monolayers²¹ and as a means of modeling cellular delivery of DNA/PNA across biological membranes in gene therapy.^{3a, 10}

In chapter 1 and 3, we have discussed in detail the various routes employed for DNA/PNA immobilization at the air-water interface.²² In chapter 3, we have demonstrated the hybridization of

complementary single stranded oligonucleotides sequentially immobilized at the air-water interface in the presence of the cationic Langmuir monolayer, octadecylamine (ODA).¹² wherein the ODA monolayer served as counterions by effectively screening the repulsion between the surface-bound oligonucleotide sequence and solution phase complementary oligonucleotide molecule, unlike in the bulk of the solution, wherein a small amount of salt is required to promote the hybridization of ssDNA molecules. In this chapter, we have looked at the sequential immobilization of PNA-DNA strands at the air-water interface with ODA monolayers in order to understand the molecular recognition processes such as hybridization of PNA-DNA occurring at the interface and the stability of these hybrids.

The ODA-PNA/DNA hybrid monolayers may be readily transferred onto solid supports by the Langmuir-Blodgett (LB) method, thereby enabling a study of the thermal stability of the PNA-DNA hybrids in the lipid matrix. These results are compared with preformed DNA duplexes bound to the fatty amine monolayer as well as some control experiments involving the sequential binding of PNA to a non-complementary DNA sequence. A measure of the contribution of the lipid matrix to the thermal stability of the intercalated guest molecules was obtained by binding the polyelectrolyte, Xanthan,²³ with ODA monolayers. The specificity of base pairing in the DNA-PNA complexes with the ODA monolayers was also studied. Introduction of a single mismatch in the DNA sequence did not yield any shifts in the UV-melting compared to that of complementary DNA-PNA hybrids.

5.6.1 Synthesis of DNA/PNA sequences :

Oligonucleotide of the sequences AGTGATCTAC (ssDNA-1), AGTGATCCAC (ssDNA-2), GCATACATGT (ssDNA-3), GCATACATGT (ssDNA-4) and ACATGTATGC (ssDNA-5) were synthesized by β -cyanoethyl phosphoramidite chemistry on a Pharmacia GA plus DNA synthesizer, purified by FPLC and rechecked by RP HPLC. The PNA oligomer H-GTAGATCACT-NH(CH₂)₂-COOH was synthesized manually using the same methodology described in section 5.2.1. ssDNA-1 is complementary while ssDNA-3 is non complementary to the PNA sequence. ssDNA-2 is a single mismatch sequence with respect to the PNA strand. Pre-formed DNA duplexes (dsDNA) were obtained by mixing equimolar quantities of ssDNA-4 and ssDNA-5 under standard hybridization conditions.¹⁶

5.6.2 Surface complexation of DNA/PNA and formation of LB films :

The experimental details concerning the surface complexation of DNA and formation of LB films is described at length in chapter 3.

After stabilization of the ssDNA-1/2/3 density at the air-water interface, the ODA-ssDNA-1/2/3 monolayer was transferred by the Langmuir-Blodgett technique²⁴ onto gold-coated quartz substrates for quartz crystal microgravimetry (QCM) measurements. The monolayer transfer onto different substrates was effected at a surface pressure of 30 dynes/cm for all experiments in this study. A 6 MHz AT-cut quartz crystal was used in QCM measurements.

After the QCM measurements of the ODA-ssDNA-1/2/3 LB films, 3 ml of PNA solution in water was injected into the non-monolayer side of the trough to yield an overall PNA concentration in the aqueous subphase of 10^{-8} M. Care was taken to remove an equal quantity of the ssDNA-1/2/3 aqueous solution prior to PNA insertion and thereby, maintain the water level in the trough constant. As in the previous measurement with just ssDNA-1/2/3 in solution, π -A isotherms were recorded as a function of time. LB films of the ODA-ssDNA-1/2/3-PNA monolayers were transferred onto the QCM crystal and the mass uptake recorded as a function of number of immersion cycles. π -A isotherms and QCM measurements for the pre-formed DNA duplexes and the polyelectrolyte Xanthan with ODA monolayers were performed in a manner similar to that detailed above.

5.7 Pressure-Area Isotherms and QCM measurements

Measurement of pressure-area (π -A) isotherms and the transfer of monolayers on different substrates to prepare LB films were carried on a computer controlled NIMA 611 Langmuir Blodgett trough equipped with a Wilhelmy plate for surface pressure sensing. Fig 5.7.1 presents the the π -A isotherm compression/expansion cycles of the ODA Langmuir monolayer after spreading the monolayer on the ssDNA-1 subphase and subsequent addition of PNA in the subphase.

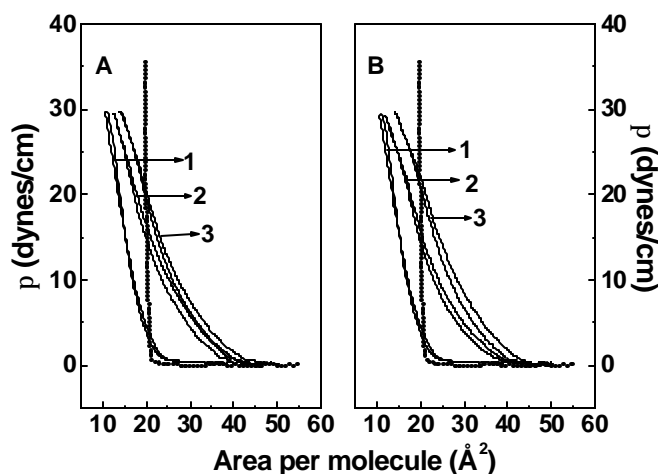


Fig. 5.7.1. A) π -A isotherms recorded from an ODA monolayer on water at various times after introduction of ssDNA-1 and PNA molecules into the subphase. Curves 1 and 2 : π -A isotherms recorded 1 h and 20 h after spreading ODA on the ssDNA-1 subphase respectively; curve 3 : π -A isotherm recorded 20 h after introduction of PNA into the subphase containing ssDNA-1. The dotted line corresponds to the π -A isotherm recorded from an ODA monolayer on plain deionized water as the subphase. ssDNA-1 is a complementary sequence to the PNA.

B) π -A isotherms recorded from an ODA monolayer on water at various times after introduction of ssDNA-2 and PNA molecules into the subphase. Curves 1 and 2 : π -A isotherms recorded 1 h and 20 h after spreading ODA on the ssDNA-2 subphase respectively; curve 3 : π -A isotherm recorded 20 h after introduction of PNA into the subphase containing ssDNA-2. The dotted line corresponds to the π -A isotherm recorded from an ODA monolayer on plain deionized water as the subphase. ssDNA-2 is a single mismatch sequence to the PNA.

Curves 1 and 2 in Fig.5.7.1.A represent the π -A isotherm compression/expansion cycles of the ODA Langmuir monolayer at time = 1 and 20 h respectively after spreading the monolayer on the ssDNA-1 subphase. A large, albeit slow, expansion of the monolayer to a limiting area/molecule

value of 40 \AA^2 is observed which remained constant thereafter. This is to be compared with the $\sim 21 \text{ \AA}^2$ /molecule takeoff area measured for the ODA Langmuir monolayer on deionized water (dotted line, Fig.5.7.1.A).

We have observed a similar slow complexation of single-stranded DNA (16-mer oligonucleotides) with an ODA monolayer at the air-water interface mentioned in chapter 3.¹² This slow expansion of the monolayer is clearly due to complexation of ssDNA-1 molecules with the ODA monolayer by attractive electrostatic interaction between the negatively charged phosphate groups on the DNA and protonated amine groups in the Langmuir monolayer. At the subphase pH of 5.8, the ODA molecules ($pK_B = 10.8$) would be completely ionized leading to maximum attractive coulombic interaction with the anionic DNA molecules in solution. We would like to point out that little hysteresis was observed in the compression/expansion cycles of this and other air-water interface complexation experiments to be discussed below. The above result indicates that the ODA-DNA-PNA hybrid monolayers at the air-water interface are stable and behave like ideal amphiphilic complexes. Assuming complete ionization of the ODA monolayer and a limiting area/molecule of 40 \AA^2 , the surface charge density may be easily calculated to be 2.5×10^{14} charges/cm². Another interesting feature of the π -A isotherms upon complexation of ssDNA-1 with ODA (Fig.5.7.1.A, curves 1 and 2) is that on large compression, the limiting area of ODA molecules reduces to less than 20 \AA^2 /molecule. While microscopic studies would be required to understand this aspect, we speculate that this may be due to the nature of complexes formed between ODA and ssDNA at the air-water interface. It is possible that the ODA molecules form a cylindrical micellar structure around the DNA molecules leading to reduced interaction of the ODA molecules with the water surface and consequently, facile bilayer formation under high compression.

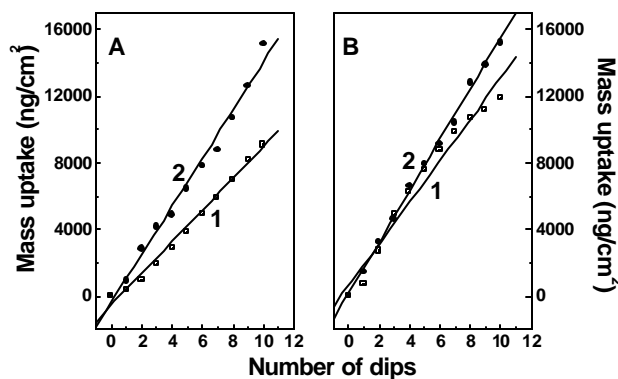


Fig. 5.7.2. A) QCM mass uptake recorded as a function of number of immersion cycles in ODA monolayers complexed ssDNA-1, (curve 1, squares) and ODA complexed with ssDNA-1 and further hybridization with PNA (curve 2, circles). ssDNA-1 is a complementary sequence to the PNA.

B) QCM mass uptake recorded as a function of number of immersion cycles in ODA monolayers complexed with ssDNA-2 (curve 1, squares) and ODA complexed with ssDNA-2 and further hybridization with PNA (curve 2, circles). ssDNA-2 is a single mismatch sequence to the PNA.

After equilibration of the ssDNA-1 density at the air-water interface, the ODA-ssDNA-1 monolayer was transferred onto gold-coated quartz substrates for QCM measurements. A plot of the QCM mass uptake recorded as a function of number of immersion cycles in the ODA-ssDNA-1 monolayer is shown in Fig. 5.7.2.A (curve 1, squares).

The transfer ratio was close to unity both during the downward and upward strokes of the QCM substrate into the subphase. Uniform, lamellar growth of the ODA-ssDNA-1 LB film is thus clearly seen from the QCM and transfer ratio data. The slope of the curve was determined from a linear fit to the QCM data (solid line in the figure) to be 953 ng/cm^2 per dip. Accounting for the contribution from the ODA bilayer, the concentration of DNA in the interlamellar regions of the ODA bilayer structure can easily be calculated to be $9.5 \times 10^{13}/\text{cm}^2$.²⁵ Accounting for the charges on the individual DNA molecules (10 per molecule), the charge ratio of DNA : ODA in the bilayers is calculated to be $9.5 \times 10^{14} : 9.52 \times 10^{14}$, or in other words, there is almost complete neutralization of the charge on the lipid by the DNA molecules. This result is at variance with our earlier studies on 16-mer DNA molecules immobilized at the air-water interface described in chapter 3 wherein overcompensation of the ODA charge by the DNA molecules was observed (by nearly a factor of 2).¹² The reasons for this difference may be due to differences in the length of the DNA used in the different studies.

The π -A isotherms were recorded as a function of time after insertion of PNA into the DNA solution as explained in section 5.6.2. The isotherm recorded 20 h after addition of PNA is represented as curve 3 in Fig.5.7.1.A. It is observed that there is marginal expansion of the monolayer in the presence of PNA. On the electrostatic complexation of 16-mer oligonucleotides at the air-water interface with ODA monolayers discussed in chapter 3, we had observed considerable expansion of the monolayer on injecting the complementary DNA molecules into solution after immobilizing single-stranded DNA at the air-water interface.¹² The monolayer expansion in that case was attributed to an elongation due to uncoiling of the ssDNA molecules already immobilized at the air-water interface leading to hybridization with the complementary DNA molecules. In the present chapter, since a short oligonucleotide is being used (10-mer), the possibility of uncoiling of the immobilized ssDNA-1 molecules is unlikely. It is clear that the π -A isotherms are unable to conclusively show whether the injected PNA molecules are able to complex with the immobilized DNA molecules at the air-water interface and consequently, further QCM and UV-melting analysis of LB films of the ODA-ssDNA-1/PNA monolayers were carried out.

Fig.5.7.2.A shows the QCM mass uptake data recorded as a function of number of immersion cycles in the ODA-ssDNA-1/PNA monolayer-covered subphase (curve 2, circles). The solid line is a linear fit to the data and clearly indicates that as in the case of the ODA monolayer complexed with ssDNA-1 molecules alone (Fig.5.7.2A, curve 1), a lamellar growth mode occurs for this film as well. An important point to note is that the mass uptake per dip (= slope of the line, 1442 ng/cm^2) after

addition of PNA is higher than that recorded for the ODA-ssDNA-1 LB film (curve 1, 953 ng/cm²). The increase in mass uptake per dip is clearly due to PNA molecules now bound to the electrostatically immobilized DNA with the ODA monolayer. From the molecular weight of PNA (2798), the number of PNA molecules per bilayer is calculated to be $1.04 \times 10^{14}/\text{cm}^2$. We recollect that in our earlier studies on the sequential immobilization of complementary DNA molecules at the air-water interface (chapter 3), QCM measurements yielded identical mass uptakes/dip in experiments involving single-stranded DNA complexed with ODA and DNA duplexes complexed with ODA.¹² Unlike in the case of DNA hybridization where both the strands are charged, the fact that PNA is not charged would not require detachment of already bound DNA molecules (for charge neutrality considerations)¹² and consequently, the mass uptake is higher when PNA binds to the ODA-ssDNA-1 complexes.

Since hybridization of PNAs to complementary DNA sequences is characterized by a good mismatch discrimination,⁴ we studied the complexation of a single base mismatch DNA sequence with PNA molecules immobilized at the air-water interface. As in the case of sequential binding of ssDNA-1 and PNA with ODA monolayers, pressure area isotherms, QCM and melting measurements were done for the ssDNA-2-PNA complexes with ODA monolayers as well. Curves 1 and 2 in Fig.5.7.1.B represent the π -A isotherm compression/expansion cycles of the ODA Langmuir monolayer at time = 1 and 20 h respectively after spreading on the ssDNA-2 subphase. As expected, a similar expansion of the monolayer to an area/molecule value of 40 Å² is observed. After equilibration of the ssDNA-2 density at the air-water interface, QCM measurements were done for the ODA-ssDNA-2 monolayer (Fig 5.7.2.B, curve 1, squares) as a function of number of immersion cycles in the ODA-ssDNA-2 monolayer. The slope of the curve was determined from a linear fit to the QCM data to be 1245 ng/cm² per dip. The isotherm-recorded 20 h after introduction of PNA is shown as curve 3 in Fig.5.7.1.B. Here too, there is no further increase in ODA monolayer area, the takeoff remaining to a stable 40 Å²/molecule. LB films of the ODA-ssDNA-2/PNA monolayers were transferred onto the QCM crystal and the mass uptake recorded as a function of number of immersion cycles (Fig.5.7.2.B, curve 2, circles). In the mismatch case as well, the slope of the QCM mass uptake curve (slope = 1530 ng/cm²) is higher than that of the ODA-ssDNA-2 LB films indicating that some degree of binding of the PNA molecules with the ODA-ssDNA-2 Langmuir monolayer at the air-water interface.

5.8 UV-melting studies of LB films of ODA-DNA- PNA :

The QCM results discussed above indicate unequivocally the presence of PNA in the ODA-ssDNA multilayer LB films. However, this is insufficient evidence for the formation of PNA-DNA duplexes within the ODA bilayer structures. As mentioned above in section 5.4, unlike in the case of

hybridization of complementary DNA strands where fluorescent intercalators such as ethidium bromide are routinely used to follow the formation of double helical structures,^{12, 19} reports on the use of fluorescent probes for PNA-DNA hybrids are relatively scarce.²⁰ Consequently, UV-melting measurements are used in the detection of PNA-DNA hybrid formation.⁴ UV-melting measurements were also performed on 19 ML LB films of pre-formed DNA duplexes and Xanthan complexed with ODA Langmuir monolayers.

Fig.5.8.1.A shows the results of UV-melting experiments carried out on the ODA-ssDNA-1/PNA conjugate films ($T_m = 58^\circ\text{C}$, curve 2, up triangles) and are compared with experiments carried out on the ssDNA-3-PNA films (Fig 5.8.1.A, curve 3, squares) and it may be also compared with the melting of ODA-ssDNA-2/PNA conjugates shown in ($T_m = 57^\circ\text{C}$, Fig 5.8.1.A, curve 1, circles).¹⁸

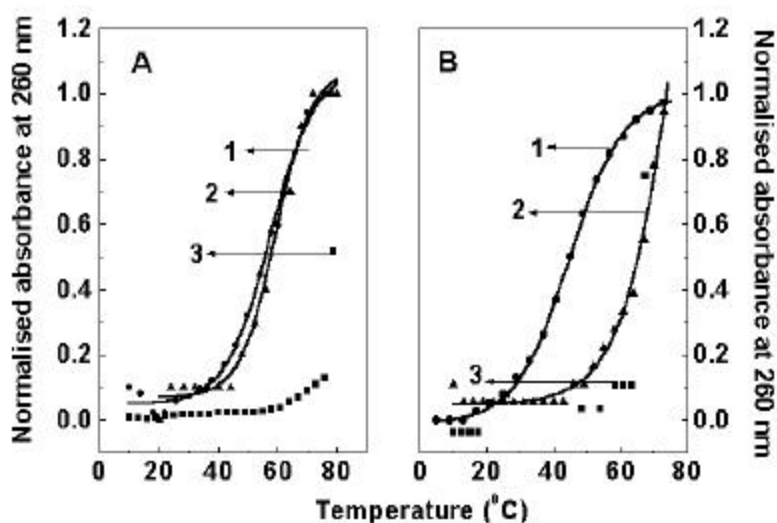


Fig.5.8.1: A) UV-temperature plots of 19 ML LB films on quartz of ssDNA-2 complexed with ODA after further complexation with PNA (curve 1, circles); a 19 ML LB film on quartz of ODA complexed with ssDNA-1 followed by PNA (curve 2, up triangles) and a 19 ML ODA film complexed with ssDNA-3 followed by PNA (curve 3, squares). ssDNA-1 is a complementary sequence to the PNA; ssDNA-2 is a single-mismatch sequence to the PNA while ssDNA-3 is a non-matching, non-complementary sequence to the PNA. The solid lines are sigmoidal fits to the data.

B) UV-temperature plots of ssDNA-1/PNA duplexes in solution (curve 1, circles); a 19 ML dsDNA-ODA LB film on quartz (curve 2, up triangles) and a 19 ML LB film of the polyelectrolyte, Xanthan, complexed with ODA on quartz (curve 3, squares). ssDNA-1 is a complementary sequence to the PNA. The solid lines are sigmoidal fits to the data.

We could not observe the specificity of base-pairing in the DNA-PNA complexes with the ODA monolayers as reflected in the melting transition by introducing a single mismatch in the DNA sequence which is same as that of T_M of in-situ hybridized DNA-PNA complex with ODA.

The UV-melting curves of sequentially immobilized ssDNA-3 with PNA (Fig.5.8.1.A, curve 3, squares) as well as for Xanthan with ODA monolayers (Fig.5.8.1.B, curve 3, squares) at the interface, did not show the characteristic melting transition indicative of the fact that DNA-PNA binding is very specific. An interesting result of the investigation is the fact that there is a large shift in the melting transition of a preformed duplex ($T_m = 65^\circ\text{C}$, Fig. 5.8.1.B, curve 2, up triangles)

compared to the previous work described in chapter 3, of sequentially immobilized ssDNA strands complexed with cationic ODA monolayers ($T_m = 55^\circ\text{C}$) at the interface. This can be explained by the fact that the cationic ODA monolayer acts as a counterion, thus effectively screening the charges thereby further stabilizing the duplex. The increased stability of the in-situ hybridized PNA-DNA hybrids at the ODA surface ($T_m = 58^\circ\text{C}$, Fig 5.8.1.A, curve 2, up triangles) compared to solution melting for DNA-PNA hybrids ($T_m = 45^\circ\text{C}$, Fig 5.8.1.B, curve 1, circles) may be due to the following reason. During sequential immobilization of DNA followed by PNA, electrostatic attachment of DNA to the ODA monolayer would leave free and exposed the bases on the DNA molecules. This would then enable facile hydrogen bonding of the complementary PNA molecules with the immobilized DNA, thereby showing increased melting transition in the ODA-DNA-PNA monolayers at the air-water interface, a process not observed in solution.

5.9 CONCLUSIONS

In conclusion, the hybridization of DNA-PNA by pre-formed and sequential electrostatic and hydrogen-bonding immobilization of complementary single-stranded DNA molecules with PNA at the air-water interface with cationic Langmuir monolayers has been demonstrated. This approach has been shown to lead to the hybridization of PNA-DNA sequences at the air-water interface in a sequential manner.

5.10 SUMMARY OF THE WORK

In this chapter sequential immobilization and in-situ hybridization of single stranded DNA and complementary PNA molecules in thermally evaporated fatty amine films and at the air-water interface with cationic Langmuir monolayers is demonstrated. The work described in this chapter is based on the use of lipid monolayers and thermally evaporated lipid bilayers.

Quartz crystal microgravimetry and UV-melting analysis of the films of ODA-PNA-DNA hybrids formed by both the methods of immobilization; clearly showed that the sequential immobilization process had resulted in hybridization of the complementary single-stranded DNA molecules with PNA at the air-water interface and within lipid bilayer stacks. The specificity of base pairing in the DNA-PNA complexes with the ODA monolayers and within the ODA matrix was also studied by introduction of a single mismatch in the DNA sequence.

Both the methodologies pave the way for use of PNA-DNA conjugates in various diagnostic and therapeutic applications. Furthermore, this approach is expected to lead to a better understanding of PNA-lipid and PNA-drug interactions. The possibility of depositing patterned lipid films and entrapping different PNA sequences in the different elements makes this approach promising for gene sequencing applications.

5.11 REFERENCES

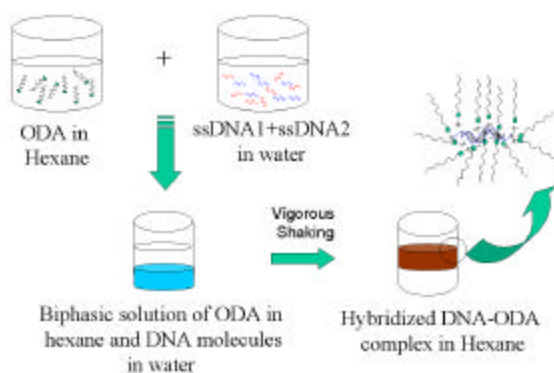
- (1) a) Uhlmann, E.; Peyman, A.; Breipohl, G.; Will, D.W. *Angew. Chem. Int. Ed. Engl.* **1998**, *37*, 2796; b) Croke, S.T.; Bennett, C.F. *Annu. Rev. Pharmacol. Toxicol.* **1996**, *36*, 107; c) Thuong, N.T.; Helene, C. *Angew. Chem. Int. Ed. Engl.* **1993**, *32*, 666.
- (2) Uhlmann, E.; Peyman, A.; Breipohl, G.; Will, D.W. *Encyclopedia of Cancer*, Vol. 1 (Ed: J.R. Bertino), Academic Press, San Diego, CA, **1997**, 64.
- (3) a) Nielsen, P.E. *Curr. Opin. Biol.* **2001**, *12*, 16; b) Nielsen, P.E. *Acc. Chem. Res.* **1999**, *32*, 624; c) Nielsen, P.E.; Haaima, G. *Chem. Soc. Rev.* **1997**, *73*; d) Egholm, M.; Buchardt, O.; Nielsen, P.E.; Berg, R.H. *J. Am. Chem. Soc.* **1992**, *114*, 1895; e) Egholm, M.; Buchardt, O.; Nielsen, P.E.; Berg, R.H. *J. Am. Chem. Soc.* **1992**, *114*, 9677; f) Nielsen, P.E.; Egholm, M.; Berg, R.H.; Buchardt, O. *Science* **1991**, *254*, 1497.
- (4) Egholm, M.; Buchardt, O.; Christensen, L.; Behrens, C.; Freier, S.M.; Driver, D.A.; Berg, R.H.; Kim, S.K.; Norden, B.; *Nature* **1993**, *365*, 566.
- (5) a) Giesen, U.; Kleider, W.; Berding, C.; Geiger, A.; Orum, H.; Nielsen, P.E.; *Nucleic Acids. Res.* **1998**, *26*, 5004; b) Tomac, S.; Sarkar, M.; Ratilainen, T.; Wittung, P.; Nielsen, P.E. *J. Am. Chem. Soc.* **1996**, *118*, 1996.
- (6) Demidov, V.; Potaman, V.N.; Frank-Kamenetskii, M.D.; Buchardt, O.; Egholm, M.; Nielsen, P.E. *Biochem. Pharmacol.* **1994**, *48*, 1309.
- (7) a) Nastruzzi, C.; Cortesi, R.; Esposito, E.; Gambari, R.; Borgatti, M.; Bianchi, N.; Feriotto, G.; Mischiati, C. *J. Controlled Release*, **2000**, *68*, 237; b) Hamilton, S.E.; Simmons, C.G.; Kathiriya, I.S.; Corey, D.R. *Chemistry and Biology* **1999**, *6*, 343; c) Larsen, J.H.; Bentin, T.; Nielsen, P.E. *Biochim. Biophys. Acta.* **1999**, *1489*, 159; d) Hyrup, B.; Nielsen, P.E. *Bioorg. Med. Chem.* **1996**, *4*, 5; e) Nielsen, P.E.; Egholm, M.; Berg, R.H.; Buchardt, O. *Trends Biotech.* **1993**, *11*, 384.
- (8) a) Doyle, D. F.; Braasch, D. A.; Simmons, C.G.; Janowski, B.A.; Corey, D.R. *Biochemistry* **2001**, *40*, 53. b) Hamilton, S.E.; Simmons, C.G.; Kathiriya, I.S.; Corey, D.R. *Chemistry and Biology* **1999**, *6*, 343.
- (9) Nielsen, P.E.; Egholm, M. : Peptide Nucleic Acid (PNA). Protocols and applications. Horizon Scientific Press, Norfolk, **1999**.
- (10) Radler, J.O.; Koltover, I.; Salditt, T.; Safinya, C.R. *Science* **1997**, *275*, 810.
- (11) Sastry, M.; Ramakrishnan, V.; Pattarkine, M.; Ganesh, K.N. *J. Phys. Chem. B* **2001**, *105*, 4409.

- (12) Sastry, M.; Ramakrishnan, V.; Pattarkine, M. ; Gole, A. ; Ganesh, K.N. *Langmuir* **2000**, *16*, 9142.
- (13) Mischiati, C.; Borgatti, M.; Bianchi, N.; Rutigliano, C.; Tomassetti, M.; Feritto, G. *J.Biol.Chem.* **1999**, *274*, 33114.
- (14) a) Sastry, M.; Patil, V.; Sainkar, S.R. *J.Phys.Chem.B.* **1998**, *102*, 1404 ; b) Patil, V.; Malvankar, R.B.; Sastry, M. *Langmuir* **1999**, *15*, 8197; c) Sastry, M. *Curr.Sci.* **2000**, *78*,1089.
- (15) a) Gole, A.; Dash, C.V.; Rao, M.; Sastry, M. *J.Chem.Soc., Chem.Commun.* **2000**, 297; b) Gole, A.; Dash, C.V.; Mandale, A.B.; Rao, M.; Sastry, M. *Anal.Chem.* **2000**, *72*, 1401.
- (16) Cantor, C.R; Schimmel, P.R. *Biophysical Chemistry, Part III*, W.H. Freeman, New York (1980).
- (17) a) Buttry, D. A.; Ward, M.D. *Chem. Rev.* **1992**, *92*, 1356.; b) Janshoff.A.; Galla. H.J.; Steinem. C. *Angew.Chem.Int.Ed* **2000**, *39*, 4004.
- (18) The UV melting experiments were carried out on Perkin Elmer Lambda 15 UV/VIS spectrophotometer fitted with a Julabo water circulator with programmed heating accessory. The quartz substrates bearing the films were cut so as to fit into the cuvette normally used for liquid samples. The DNA-ODA films were heated at a rate of 0.5 °C per minute and the thermal denaturation of the duplex was followed by monitoring changes in the absorbance at 260 nm as a function of temperature. A 250 Å thick ODA film on quartz was taken as the reference.
- (19) LePecq, J.B.; Paoletti, C. *J.Mol.Biol.* **1967**, *27*, 87.
- (20) Wang, J.; Palecek E.; Nielsen, P.E.; Rivas, G.; Cai, X.; Shirashi, H.; Dontha, N.; Luo, D.; Farias, P.A.M. *J.Am.Chem.Soc.* **1996**, *118*, 7667.
- (21) a) Ahlers, M.; Muller, W.; Reichert, A.; Ringsdorf, H.; Venzmer, J. *Angew.Chem.Int.Ed.Engl.* **1990**, *29*, 1269; b) Kurihara, K.; Ohto, K.; Tanaka, K.; Aoyama, Y.; Kunitake, T. *J.Am.Chem.Soc.* **1991**, *113*,444.
- (22) a) Ebara, Y.; Mizutani, K.; Okahata, Y. *Langmuir* **2000**, *16*, 2416; b) Kago, K.; Matsuoka, H.; Yoshitome, R.; Yamaoka, H.; Ijira, K.; Shimomura, M. *Langmuir* **1999**, *15*, 5193; c) Shimomura, M.; Nakamura, F.; Ijira, K.; Taketsuna, H.; Tanaka, M.; Nakamura, H.; Hasebe, K. *J.Am.Chem.Soc.* **1997**, *119*, 2341; d) Okahata, O.; Kobayashi, T.; Tanaka, K. *Langmuir* **1996**, *12*, 1326; e) Ijira, K.; Shimomura, M.; Tanaka, M.; Nakamura, H.; Hasebe, K. *Thin Solid Films* **1996**, *284*,780.

- (23) Xanthan is an extracellular polysaccharide produced by fermentation of the microorganism *Xanthomonas campestris*. Xanthan was obtained from International (now Dowell) Drilling Fluids (IDF) and thoroughly purified using microfiltration at low flow rate through decreasing sizes of micropore filters and ultrafiltration with a molecular cut-off of 20 000 Da. The weight-average molecular weight (Mw) of the sample, as measured by size exclusion chromatography (SEC) coupled with multiangle light scattering, is 1.8×10^6 g/mol.
- (24) Ulman, A.; *An introduction to ultrathin organic films : from Langmuir-Blodgett to self-assembly* : Academic Press, San Diego (1991).
- (25) Assuming an area of 21 \AA^2 /ODA molecule, the weight of the ODA bilayer/cm² of the QCM surface can be easily shown to be $\sim 426 \text{ ng/cm}^2$ (molecular weight of ODA 269.5). The contribution to the QCM mass uptake from the ssDNA molecules is therefore, $954 - 426 = 528 \text{ ng/cm}^2$. From the molecular weight of the 10-mer oligonucleotide used in this study (ssDNA-1) = 3300, the number of DNA molecules/cm² of the bilayer can be shown to be $\sim 9.5 \times 10^{13}$.

CHAPTER VI

PHASE TRANSFER OF DNA BY INTERACTION WITH CATIONIC SURFACTANT MOLECULES AT THE LIQUID / LIQUID INTERFACE



In this chapter, we have looked at the hybridization of complementary single-stranded DNA molecules at the interface between water and hexane containing cationic fatty lipid molecules (octadecylamine, ODA). During vigorous shaking of the biphasic mixture, the individual DNA single strands are bound electrostatically to ODA molecules at the water-hexane interface following which they hybridize into the double helical structure. The binding of the cationic lipid molecules to the DNA double helices renders them hydrophobic and results in the phase transfer of the DNA molecules into the organic phase. Pre-formed DNA double helical structures could also be phase transferred by this method without distortion to the duplex structure. The process of hybridization, phase transfer and thermal stability of the surfactant-stabilized DNA double helical molecules has been studied using UV-vis spectroscopy, fluorescence spectroscopy with ethidium bromide as the intercalator, infrared spectroscopy, UV melting transition and X-ray photoemission spectroscopy measurements.

Part of the work presented in this chapter has been published in: -1) Sastry, M.; Kumar, A.; Pattarkine, M.; Ramakrishnan, V.; Ganesh, K.N. *J. Chem. Soc. Chem. Commun.* **2001**, 1434.

6.1. INTRODUCTION

Following the demonstration of gene therapy in humans by gene transfer,^{1,2} studies into the development of efficient gene carriers has increased many-fold. While most of the clinical trials have been on virus-based gene therapy,³ there is heightened current interest in the development of synthetic, virus-like DNA vectors. In one such approach, Felgner *et al.* have demonstrated that DNA previously complexed with a cationic surfactant lead to enhanced uptake of DNA by eucaryotic cells.⁴ Subsequently, DNA-cationic liposome complexes have been investigated in great detail as non-viral DNA vectors.⁵ Such complexes have a lamellar, spherical structure with DNA entrapped within the hydrophilic regions of the bilayers.^{5b} In such synthetic liposomal vectors, an understanding of DNA-surfactant interactions is extremely important. Understanding DNA-surfactant interactions also assumes importance in transmembrane DNA transport in gene delivery where the DNA molecules experience a highly hydrophobic environment brought about by the membrane bilayer.

An important requirement for the successful transfection of DNA is its immobilization in hydrophobic matrixes. Researchers elsewhere have been trying to accomplish this in a variety of different ways, by complexing DNA with cationic surfactants.

A number of studies have dealt with DNA-surfactant complexes in an aqueous environment as the relative concentrations of DNA/cationic surfactant is varied.⁶ It was observed that in solutions containing equimolar amounts of DNA and the cationic surfactant, the complex formed was water-insoluble but soluble in low-polar organic solvents.^{6a, d} The DNA molecules were rendered hydrophobic by the cationic surfactants to which they were complexed. In a slightly different approach, Reimer *et al.*⁷ have shown that DNA molecules may be hydrophobized by complexation with cationic surfactants in a Bligh and Dyer monophasic system and thereafter partitioning of the monophasic system into a two-phase system lead to the transfer of DNA into the organic phase. The Bligh and Dyer monophasic system is a solution of chloroform/methanol/water in the 1 : 2.1 : 1 ratio. Partitioning of the monophasic system into a two-phase system is accomplished by further addition of water and chloroform.⁷

One of the problems facing researchers trying to pursue gene therapy is the insolubility of DNA in oily environments. We have devised a simple process for rendering DNA soluble. This technique is expected to open the door for gene therapy and other applications in which oil-based formulations are important. In this chapter, the hydrophobization of the DNA molecules is accomplished during vigorous shaking of a biphasic mixture of an aqueous solution of DNA and a hexane solution of the cationic lipid, octadecylamine (ODA). Electrostatic complexation of the DNA molecules with ODA at the liquid-liquid interface renders the DNA hydrophobic and results in their phase transfer into

the organic phase. We have also shown that complementary single-stranded DNA molecules in the bulk aqueous phase hybridize to form double helical structures during electrostatic complexation with ODA at the liquid-liquid interface (and are thereafter transferred to the organic phase) *under conditions where hybridization does not occur spontaneously in the bulk solution*. We would like to point out that previously studied protocols for the hydrophobization of DNA have dealt with *pre-formed* double helical DNA molecules.

6.1.1 Synthesis of DNA sequences

Oligonucleotides corresponding to the sequences GGAAAAAACTTCGTGC(ssDNA-1), GCACGAAGTTTTTCC (ssDNA-2) and AGAAGAAGAAAAGAA (ssDNA-3) were synthesized by β -cyanoethyl phosphoramidite chemistry on a Pharmacia GA plus DNA synthesizer, purified by FPLC and rechecked by RP HPLC. *SsDNA-1 and ssDNA-2 are complementary oligonucleotides while ssDNA-3 is non-complementary to both ssDNA-1 and ssDNA-2.*

6.1.2. Synthesis and characterization of DNA

In a typical experiment, 10 mL of a 10^{-4} M solution of octadecylamine (ODA, Sigma chemicals, used as-received) in hexane was added to 10 mL of 10^{-6} M aqueous solution of ssDNA-1 and ssDNA-2 taken in an equimolar ratio. In order to follow the hybridization of the complementary oligonucleotides ssDNA-1 and ssDNA-2, the intercalator ethidium bromide was added to the aqueous solution at a concentration of 10^{-5} M. Vigorous shaking of the biphasic mixture was carried out for a period of 20 minutes and the mixture allowed to settle and separate. The aqueous and organic phases (both before and after the shaking process) were analyzed using UV-vis and fluorescence spectroscopy measurements. The UV-vis measurements were performed on a HP8542A diode array spectrophotometer operated at a resolution of 2 nm while the fluorescence measurements were carried out on a Perkin Elmer model LS 50-B spectrofluorimeter at 25°C, with slit widths of 5 nm for excitation at 460 nm and 10 nm for the emission monochromators. The excitation wavelength was chosen to match the resonance from the ethidium bromide molecules added to the aqueous phase. As mentioned in all the previous chapters, ethidium bromide is known to intercalate into the base pairs of DNA double helical structures and this process is readily detected by the enhanced fluorescence exhibited by this molecule on intercalation in DNA.⁸ Similar phase transfer experiments were carried with 10^{-6} M equimolar aqueous mixtures of the non-complementary oligonucleotides ssDNA-1 and ssDNA-3 as well as with an aqueous solution of the pre-formed double helical DNA structures of ssDNA-1 and ssDNA-2 (dsDNA12) taken together with the intercalator, ethidium bromide. The pre-hybridization was carried out by heating an equimolar mixture of ssDNA1 and ssDNA2 (10^{-6} M concentration) to 90 °C in an aqueous

solution of 1 mM NaCl followed by slow cooling. In order to test whether hybridization occurs during sequential complexation of ssDNA1 and ssDNA2 with ODA molecules in hexane, a control experiment was performed in the following manner. First, a 10^{-6} M aqueous solution of ssDNA-1 was taken and complexation with ODA and phase transfer into hexane was accomplished as described above. Thereafter, the hexane phase containing the ssDNA-1-ODA complex was separated and added to a 10^{-6} M aqueous solution of ssDNA2 containing the intercalator, ethidium bromide. The complexation of ssDNA-2 with the ssDNA-1-ODA complex in hexane was attempted by shaking the biphasic mixture vigorously for 20 minutes and allowing the individual phases to separate. The hexane phase was analyzed by fluorescence spectroscopy as mentioned above.

Films of the DNA-ODA complex obtained by hybridization of ssDNA-1 and ssDNA-2 during the phase transfer process (DNA(1+2)-ODA complex) as well as the complex obtained from pre-formed DNA double helical structures (dsDNA12-ODA) were deposited on Si (111) wafers and quartz plates by simple solution casting. On evaporation of the solvent (hexane), films of the DNA-ODA complexes were formed on the different surfaces and analyzed by fluorescence and UV-vis spectroscopy, UV melting analysis, Fourier transform infrared spectroscopy (FTIR) and X-ray photoemission spectroscopy (XPS). FTIR measurements of the DNA-ODA complex films on Si (111) substrates were carried out on a Shimadzu FTIR-8201 PC instrument operated in the diffuse reflectance mode at a resolution of 4 cm^{-1} . To obtain good signal to noise ratios, at least 256 scans of the DNA-ODA conjugate films were taken in the range $400 - 4000\text{ cm}^{-1}$. In order to follow the hybridization of the complementary oligonucleotides into double helical structures, the DNA(1+2)-ODA films on quartz substrates together with the dsDNA12-ODA film on quartz were studied by UV melting experiments carried out on Perkin Elmer Lambda 15 UV/VIS spectrophotometer fitted with a Julabo water circulator with programmed heating accessory. The quartz substrates bearing the films were cut so as to fit into the cuvette normally used for liquid samples. The DNA-ODA films were heated at a rate of $0.5\text{ }^{\circ}\text{C}$ per minute and the thermal denaturation of the duplex was followed by monitoring changes in the absorbance at 260 nm as a function of temperature.

XPS studies of the DNA(1+2)-ODA film on a Si (111) substrate were performed on a VG MicroTech ESCA 3000 spectrometer equipped with a multichanneltron hemispherical electron energy analyser at a pressure better than 1×10^{-9} Torr. The electrons were excited with un-monochromatized Mg K_{α} X-rays (energy = 1253.6 eV) and the spectra were collected in the constant analyzer energy mode at a pass energy of 50 eV. This leads to an overall resolution of ca. 1 eV for the measurements. The C 1s, N 1s and P 2p core level spectra were

recorded at an electron takeoff angle (ETOA, angle between the electron emission direction and surface plane) of 55° and aligned with respect to the adventitious carbon binding energy (BE) of 285 eV. Prior to curve resolution by a non-linear least squares procedure, the spectra were background corrected using the Shirley algorithm.⁹

6.2. UV- VISIBLE MEASUREMENTS

The complexation of pre-formed dsDNA12 duplexes of the complementary oligonucleotides ssDNA-1 and ssDNA-2 with ODA molecules at the hexane-water interface and the subsequent phase transfer as described above was studied using UV-vis spectroscopy.

Fig.6.2.1.A shows the UV-vis spectra recorded from the aqueous phase before (curve 1) and after (curve 2) vigorous shaking of the biphasic mixture containing dsDNA12 duplexes in the aqueous phase and ODA molecules in hexane.

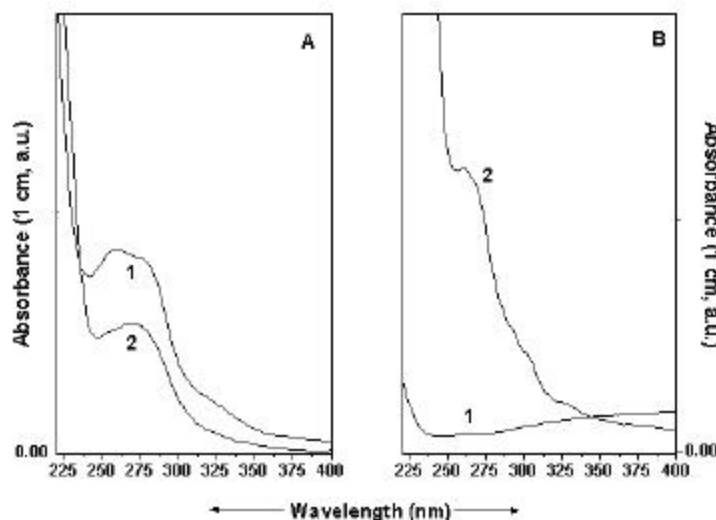


Fig.6.2.1.: A) UV-vis spectra recorded from the aqueous phase before (curve 1) and after (curve 2) shaking a biphasic mixture of dsDNA12 double helical structures (10^6 M concentration with ethidium bromide intercalator) in water and 10^{-4} M solution of ODA in hexane.

B) UV-vis spectra recorded from the hexane phase before (curve 1) and after (curve 2) shaking a biphasic mixture of dsDNA12 double helical structures (10^6 M concentration with ethidium bromide intercalator) in water and 10^{-4} M solution of ODA in hexane.

It is seen that the resonance at ca. 270 nm arising from $n\pi^*$ transitions in the nucleic acid bases¹⁰ is reduced in intensity after the shaking process. This clearly indicates a reduction in the amount of DNA in the aqueous phase and suggests phase transfer of the DNA molecules into hexane.

This was crosschecked by recording the UV-vis spectra of the hexane phase before and after the shaking process and the spectra obtained are shown in Fig.6.2.1.B. There is no indication

of the presence of DNA before the shaking procedure (Fig.6.2.1.B, curve 1) but a strong resonance at 270 nm is induced in the hexane phase (Fig.6.2.1.B, curve 2) by the shaking procedure. The result indicates the phase transfer of the DNA molecules into hexane. During shaking of the biphasic mixture, the DNA molecules come into contact with the ODA molecules at the water/hexane interface. The shaking procedure accelerates this process by formation of a microemulsion-like phase and thereby, increasing the interfacial area between the aqueous and organic phases. At pH = 7, the ODA molecules are protonated and thus become positively charged (pK_B of ODA = 10.8). The negatively charged DNA molecules are thus electrostatically bound to the cationic ODA molecules and when a sufficient number of ODA molecules complex with the DNA double helical structures, the DNA molecules rendered hydrophobic and results in their phase transfer into hexane as observed. We would like to remark here that the relative molar concentrations of DNA: ODA is an important ingredient in achieving a minimum critical hydrophobicity to accomplish the phase transfer. In all the experiments described herein, a nearly 100-fold molar excess of ODA molecules (over DNA) was taken in the hexane phase. We have observed that equimolar ratios of DNA : ODA did not result in a detectable phase transfer of the DNA molecules into hexane.

A similar UV-vis spectroscopy study of the ODA-facilitated phase transfer of an equimolar mixture of ssDNA1 and ssDNA2 in deionized water into hexane was carried out. It is to be noted that in this experiment, double helical structures of ssDNA1 and ssDNA2 do not spontaneously form in the bulk of the aqueous phase. It is well known that in order to achieve hybridization, the repulsive interaction between the negative charges on the DNA single strands must be screened using salt¹¹ and the phase transfer experiments described in this chapter, have been carried out using deionized water. The UV-vis spectra recorded before and after shaking the biphasic mixture of ODA-in-hexane and (ssDNA1+ssDNA2)-in-water is shown in Fig.6.2.2.A as curves 1 and 2 respectively. A comparison of the spectra 1 and 2 in Fig.6.2.2.A shows that in this case as well, a decrease in the intensity of the resonance at 270 nm occurs after the shaking process clearly indicating a loss of the DNA molecules in the aqueous phase.

UV-vis analysis of the hexane phase before and after the shaking process (curves 1 and 2 respectively, Fig.6.2.2.B) shows that while there is no evidence for DNA in the organic phase before the shaking process (spectrum 1, Fig.6.2.2.B), a significant amount of DNA molecules are transferred into hexane after the shaking process (spectrum 2, Fig.6.2.2.B).

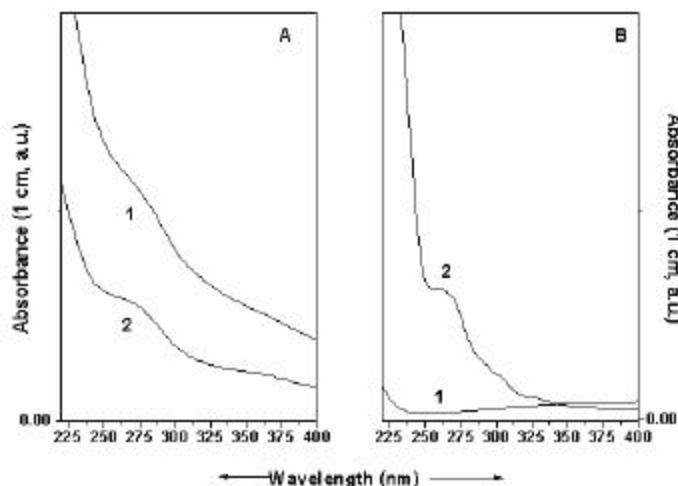


Fig. 6.2.2 : A) UV-vis spectra recorded from the aqueous phase before (curve 1) and after (curve 2) shaking a biphasic mixture of ssDNA1 + ssDNA2 molecules (10^{-6} M concentration of each oligonucleotide with ethidium bromide intercalator) in water and 10^{-4} M solution of ODA in hexane.

B) UV-vis spectra recorded from the hexane phase before (curve 1) and after (curve 2) shaking a biphasic mixture of ssDNA1 + ssDNA2 molecules (10^{-6} M concentration of each oligonucleotide with ethidium bromide intercalator) in water and 10^{-4} M solution of ODA in hexane .

The UV-vis data shown in Figs.6.2.1 and 6.2.2 clearly suggest that both pre-formed DNA duplex (Fig.6.2.1) as well as mixtures of ssDNA1 and ssDNA2 molecules (Fig.6.2.2) are transferred into hexane by electrostatic complexation with ODA molecules.

6.3. FLUORESCENCE STUDIES

It would be important to establish whether hybridization of the ssDNA1 and ssDNA2 molecules into double helical structures had occurred during the course of their phase transfer and if the double helical structure is retained after the phase transfer. As mentioned above, ethidium bromide is known to intercalate into the base pairs of DNA double helical structures and this process is readily detected by the enhanced fluorescence exhibited by this molecule on intercalation in DNA.⁸ Fig.6.3.A is a plot of the fluorescence spectra obtained from the hexane solutions of ODA complexed with DNA from the 1 : 1 (ssDNA-1 + ssDNA-2) solution (curve 1) and dsDNA12 solution (curve 2, pre-formed DNA duplexes of ssDNA1 and ssDNA2).

It is seen that in both cases, there is strong emission from the ethidium bromide intercalator at close to 570 nm indicating that (i) the double helical structure is indeed retained in the ODA-dsDNA12 hexane solution and more importantly, (ii) that not only have the single-stranded oligonucleotides ssDNA1 and ssDNA2 been transferred to the organic phase by complexation with ODA molecules, *they have hybridized into duplexes.*

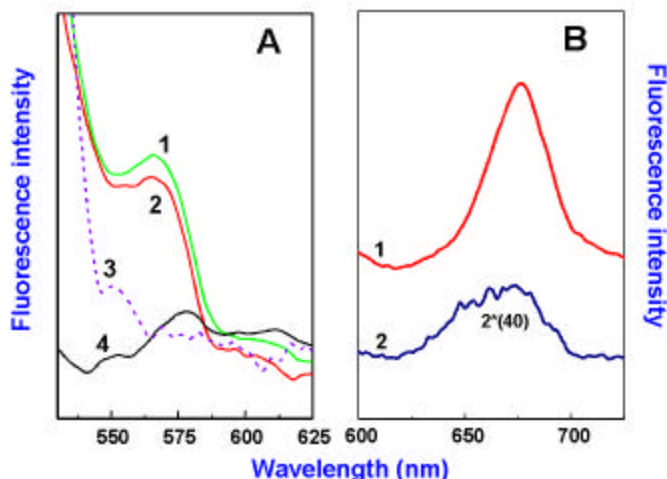


Fig.6.3. A) Fluorescence spectra recorded from the hexane phase after transfer of ssDNA1 and ssDNA2 molecules from an aqueous 1 : 1 mixture of the complementary oligonucleotides by complexation with ODA (curve 1) and pre-formed dsDNA12 molecules complexed with ODA (curve 2). The dashed curve corresponds to the fluorescence spectrum from a mixture of ssDNA-1-ODA and ssDNA-2-ODA separately phase transferred into hexane. (curve 3). Fluorescence spectra recorded from the hexane phase after transfer of ssDNA-1 and ssDNA-3 molecules from an aqueous 1 : 1 mixture of the non-complementary oligonucleotides by complexation with ODA is also shown as (curve 4).

B) Fluorescence spectra recorded from films of ssDNA(1+2)-ODA (curve 1) and dsDNA12-ODA (curve 2) complexes formed on quartz substrates by solvent evaporation (the hexane phase).

To the best of our knowledge, hybridization (and phase transfer) of complementary oligonucleotides at the liquid-liquid interface in the presence of an ionizable surfactant molecules has not been demonstrated so far. In all control experiments on the phase transfer of ssDNA-1 and ssDNA-3 mixtures (non-complementary oligonucleotides) in water by a similar process, no fluorescence was observed from the hexane phase (Fig.6.3.A, curve 4) even though presence of the single-stranded DNA molecules was indicated by UV-vis measurements. Fluorescence was also not observed from the hexane phase in a control experiment wherein only ethidium bromide was taken in the aqueous phase. Since both ODA and ethidium bromide are cationic at physiological pH, electrostatic complexation of these is unlikely to occur. Thus, the hybridization inferred by the fluorescence measurements shown in Fig.6.3.A (curve 1) is clearly due to recognition of the complementary base sequences and occurs only at the hexane-water interface. The cationic ODA molecules acting like counterions, screen the repulsive electrostatic interactions between the individual DNA strands thus facilitating the hybridization process. The formation of double helical structures of ssDNA-1 and ssDNA-2 does not occur in the bulk of the aqueous phase and these results clearly imply an interfacial process mediated by the cationic lipid molecules.

Of possible application potential in, for example gene sequencing, would be hybridization (and thus recognition) of complementary oligonucleotides by a sequential immobilization with ODA and phase transfer as briefly described in the experimental section.

To recollect, ssDNA-1 was first complexed with ODA and phase transferred following which the ssDNA1-ODA hexane solution was added to an aqueous solution of ssDNA2 + ethidium bromide intercalator and the biphasic mixture shaken vigorously. The fluorescence spectrum recorded from the hexane solution after this two-step process is shown as (dashed line in curve 3 in Fig.6.3.A). It is observed that there is no emission from ethidium bromide indicating clearly that hybridization has not occurred in this sequential complexation procedure. Apparently, once surrounded by a sheath of ODA molecules and made sufficiently hydrophobic, the single-stranded DNA molecules are unable to form double-helical structures with complementary oligonucleotides. This result throws some light on the nature of coordination of the ODA molecules to the DNA surface and indirectly indicates that the hybridization of ssDNA-1 and ssDNA-2 present simultaneously in solution during complexation with ODA occurs before complete hydrophobization of the individual strands is achieved.

An exciting aspect of the phase transfer of DNA molecules into an organic phase such as hexane is the possibility of depositing films of ODA-stabilized DNA by simple solvent evaporation. This process is used extensively in the formation of close-packed hexagonal arrays of hydrophobized colloidal particles such as gold and platinum.¹² The fluorescence spectrum obtained from a film of ssDNA(1+2)-ODA complexes on quartz is shown in Fig.6.3.B, curve 1 while the corresponding spectrum from the dsDNA12-ODA film is represented by curve 2 in Fig.6.3.B. Strong emission signals from ethidium bromide are observed in both the films with an emission at ca. 675 nm. While the strong emission clearly indicates the presence of the DNA molecules in the double helical structure and thus agrees with the solution-phase fluorescence measurements for the corresponding hexane phases (Fig.6.3.A), a large red shift in the emission wavelength is seen in the DNA-ODA films. This large red shift in the ethidium bromide emission wavelength is likely to be a consequence of the large increase in polarity of the intercalator environment in the film form. Such a red shift in the ethidium bromide emission wavelength on increase in the polarity of the intercalator environment has been observed in the literature.⁸ The fluorescence spectrum from the dsDNA12-ODA film in Fig.6.3.B has been multiplied by a factor of 40 (curve 2, Fig.6.3.B). This is a consequence of non-uniformity of the film during evaporation of hexane and is not related to a deterioration of the degree of hybridization of the dsDNA12 double helices. (The films formed as observed by the unaided eye were fairly patchy). This is borne out by the solution phase fluorescence measurements wherein it is observed that the fluorescence signals from both ssDNA(1+2)-ODA and dsDNA12-ODA complexes in hexane are of roughly the same intensity (compare curves 1 and 2, Fig.6.3.A).

6.4. UV-MELTING MEASUREMENTS

Films of ssDNA(1+2)-ODA and dsDNA12-ODA on quartz substrates were subjected to UV melting measurements and the data obtained is shown in Fig.6.4. (curve 1 : dsDNA12-ODA film; curve 2 : ssDNA(1+2)-ODA film).

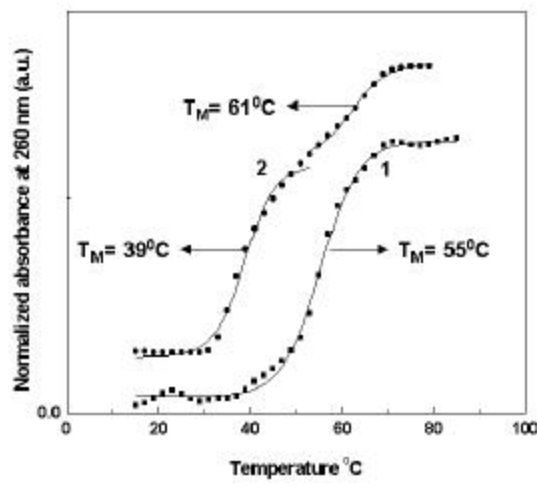


Figure 6.4. : UV-temperature plots of films of ssDNA(1+2)-ODA (curve 1) and dsDNA12-ODA complexes formed on quartz substrates by simple solution casting. The melting transitions obtained from sigmoidal fits to the data are indicated next to the respective curves.

It is seen that the pre-formed double helical DNA molecules complexed with ODA molecules show a single melting transition at 55 °C (curve 1, Fig.6.4.). Pattarkine and Ganesh have recently studied the interaction of the duplexes of dsDNA12 double helices with single-chain (CTAB) and double-chain (DOTAP) surfactant molecules in water as a function of varying lipid : DNA concentration ratio.^{6b} The T_M value of 55 °C observed for the dsDNA12-ODA complex is higher than the solution melting transition value of 41 °C indicating significant thermal stabilization of the duplex structure by the ODA molecules. The UV melting transition curve for the ssDNA(1+2)-ODA film was more complex and showed well-separated melting transition temperatures at 39 °C and 61 °C (curve 2, Fig.6.4.). Such two melting transition temperatures have been recently observed by Pattarkine and Ganesh as the lipid : DNA ratio was reduced below a critical value.^{6b} This was attributed to phase separation of lipid-free DNA double helical structures (lower T_M) and DNA double helices capped with a layer of surfactant molecules (higher T_M). In this study, DNA cannot exist in the organic phase without some degree of hydrophobization provided by the electrostatically complexed ODA molecules. The presence of two distinct melting transition temperatures may indicate two phase-transferred components

wherein the degree of complexation of the ssDNA(1+2) double helices with ODA molecules is different. It may also be possible that in some of the ssDNA(1+2)-ODA complexes, the hybridization of the complementary oligonucleotides into double helical structures is not complete and thus yields a lower melting transition temperature. The UV melting transition measurements shown in Fig.6.4 thus provide additional support to the formation of double helical structures in the ssDNA(1+2)-ODA films inferred earlier from fluorescence measurements (Fig.6.3) and also that the duplex structure is maintained after phase transfer of the dsDNA12 molecules.

6.5. FTIR STUDIES

The FTIR spectra recorded from solution-cast films of plain ODA (curve 1), dsDNA12-ODA (curve 2) and ssDNA(1+2)-ODA (curve 3) on Si (111) substrates are shown in Figs.6.5.A and 6.5.B in two different spectral windows. The features in Fig.6.5.A are important in identifying the DNA molecules and are in the range where the major resonances from the DNA bases, sugars and the phosphate backbone occur.^{13, 14}

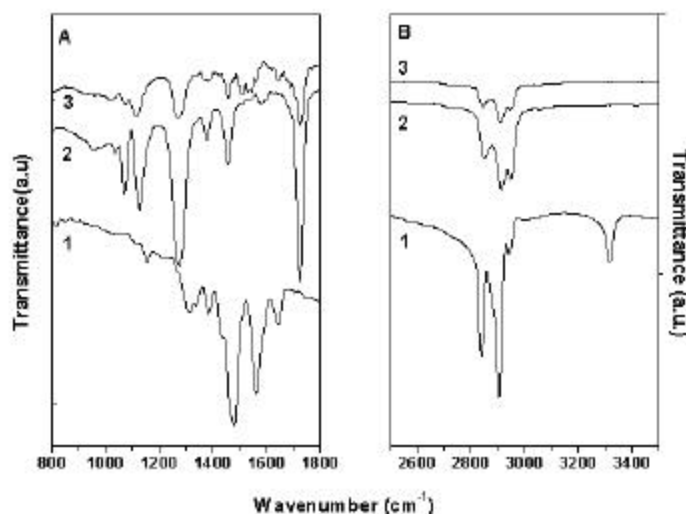


Figure 6.5. A) FTIR spectra recorded from films of ODA (curve 1), dsDNA12-ODA and ssDNA(1+2)-ODA formed by solution casting from hexane onto Si (111) substrates in the range of resonances from the DNA molecules.

B) FTIR spectra recorded from films of ODA (curve 1), dsDNA12-ODA and ssDNA(1+2)-ODA formed by solution casting from hexane onto Si (111) substrates showing the methylene (and methyl) vibrational modes from the ODA molecules.

A comparison of the different spectra shown in Fig.6.5.A shows that strong resonances occur in the dsDNA12-ODA and ssDNA(1+2)-ODA films at 1065 cm^{-1} , 1230 cm^{-1} and 1720 cm^{-1} .

These features are clearly absent in the bare ODA film (curve 1) and are therefore due to resonances occurring in the DNA molecules. The resonance at 1230 cm^{-1} is due to the backbone PO_2 antisymmetric stretching vibration while the absorption at 1720 cm^{-1} is due to mainly G-band resonances.¹³ The relatively high intensities of 1720 cm^{-1} peak as well as the resonance at 1065 cm^{-1} (due to the deoxyribose band) has been shown to be indicative of hybridization of the single-stranded DNA molecules into a Z-DNA double-helical conformation.¹⁴ Such a conformation is known to occur for double-helical DNA molecules in an environment of high ionic strength.¹⁴ In the case of the ssDNA(1+2)-ODA and dsDNA12-ODA composites of this study, the ODA molecules act like counterions and could thus lead to the Z-DNA double-helical conformation observed. This result provides support to the fluorescence data presented in Fig.6.3. where a highly polar environment for the intercalator, ethidium bromide, was inferred from the red shift in the emission wavelength.

The FTIR spectra for the ODA, dsDNA12-ODA and ssDNA(1+2)-ODA films in the range $2500 - 3500\text{ cm}^{-1}$ are shown in Fig.6.5.B. The resonances observed at 2850 , 2920 and 2960 cm^{-1} correspond to the methylene symmetric, antisymmetric and methyl antisymmetric vibrations respectively from the ODA molecules in the complex. In addition, a sharp resonance at 3330 cm^{-1} is seen in the case of the bare ODA film and is due to the N-H stretch vibrations.¹⁵ This feature vanishes on complexation of the ODA molecules with DNA and is similar to our earlier observations on electrostatic complexation of ODA molecules with negatively charged colloidal gold nanoparticles.^{15a} An interesting feature is the drastic reduction in intensity of the methylene antisymmetric and symmetric vibrational modes relative to that of the methyl vibrational modes. This indicates considerable orientational disorder in the DNA-ODA films, which is likely to be a consequence of electrostatic complexation with the cylindrical DNA double helical structures. The fact that the methylene symmetric and antisymmetric vibrational mode frequencies occur at 2850 and 2920 cm^{-1} indicates that the hydrocarbon chains in the ODA sheath are close-packed.¹⁶

6.6. CHEMICAL ANALYSIS FROM XPS

A chemical analysis of the ssDNA(1+2)-ODA film solution cast onto a Si (111) substrate was performed and the C 1s, N 1s and P 2p core levels were recorded. The C 1s and N 1s core levels are shown in Figs.6.6.1 A and B respectively. The C 1s core level could be stripped into two chemically distinct components at 285 eV and 288.2 eV binding energy (BE) by a non-linear least squares procedure. The peak at 285 eV (peak 1, Fig.6.6.1.A) arises due to electron emission from adventitious carbon (this level was used for alignment of the core level BEs) and the carbons in the hydrocarbon chains of ODA as well as the carbons in the bases and sugars of DNA. The peak at 288.5 eV BE is assigned to carbons co-ordinated to the

phosphates in the DNA backbone as well as the carbons co-ordinated to the amine group in ODA.

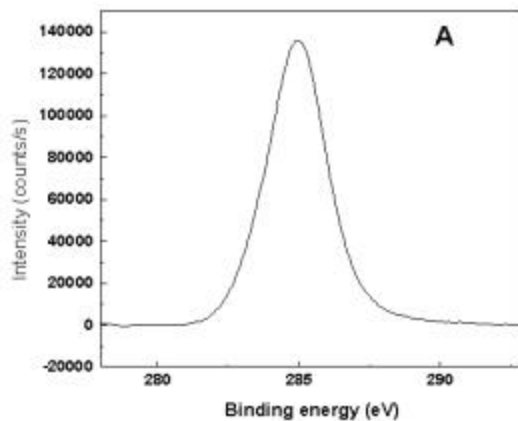


Fig. 6.6.1.A C 1s core level spectrum recorded from the ssDNA(1+2)-ODA film by solution casting onto Si (111) substrate. Two chemically distinct peaks have been resolved and are also shown in the figure.

The N 1s envelope consists of a single component centered at a BE of 399.7 eV (Fig.6.6.1B) and is due to electron emission from nitrogen atoms in the bases of DNA as well as from the amine groups in the ODA molecules.

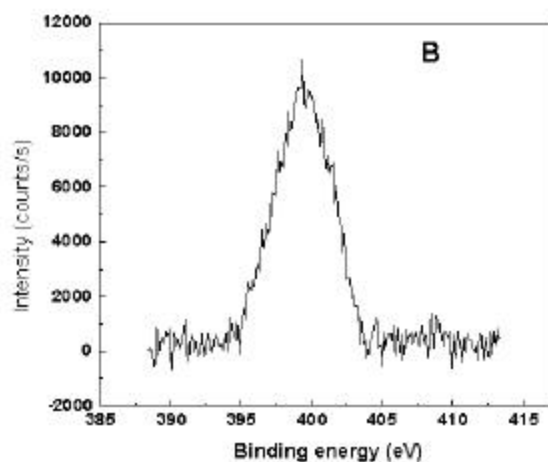


Fig. 6.6.1.B . N 1s core level spectrum recorded from the ssDNA(1+2)-ODA film by solution casting onto Si (111) substrate. One component is shown in the figure .

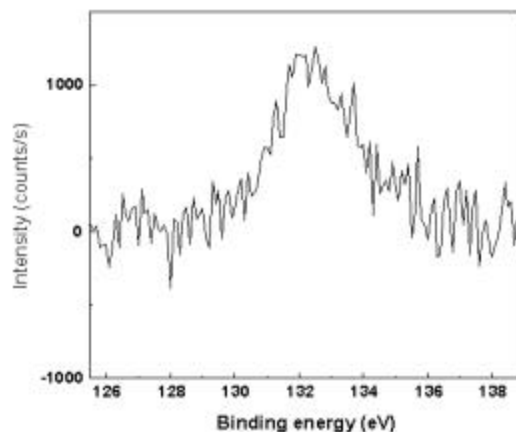


Fig.6.6.2 : P 2p core level spectrum recorded from the ssDNA(1+2)-ODA film by solution casting onto Si (111) substrate. The two spin-orbit components are shown in the figure.

The P 2p core level (due to electron emission from the DNA phosphate backbone) is shown in Fig.6.6.2. and has been stripped into the $2p_{3/2}$ and $2p_{1/2}$ spin-orbit components. The $2p_{3/2}$ BE has been measured to be 132.2 eV and is in fair agreement with earlier published XPS BE values of DNA molecules immobilized on self-assembled monolayer surfaces.¹⁷ The BE value of 136 eV quoted for the P 2p core level recorded from DNA films by these authors is for, we believe, (as already mentioned in chapter 4); the centroid of the P 2p envelope. The agreement between the BE of 132.2 eV of this study and that of Higashi *et al* would improve if the P 2p core level of Higashi *et al* were stripped into the two spin-orbit components as done in this study.

6.7. CONCLUSIONS

It has been shown that DNA molecules may be electrostatically complexed with cationic lipid molecules at the organic-water interface and furthermore, that the resulting hydrophobization of the DNA molecules enables their phase transfer into the organic phase by a simple two-phase shaking process. An important finding of this investigation is the surfactant facilitated hybridization (and consequent hydrophobization and phase transfer) of complementary single-stranded DNA molecules at the liquid-liquid interface under conditions where the hybridization to form double helical structures does not occur in the bulk of the aqueous phase. The hydrophobization of the DNA molecules by a sheath of electrostatically bound ODA molecules increases the thermal stability of the double helical structures. The DNA molecules may be conveniently cast in the form of thin films onto any solid support by simple solvent evaporation. This approach is expected to facilitate the generation of lipid-DNA complexes for possible application in gene-transfer systems etc.

6.8.REFERENCES

- (1) Blaese, R.M.; Culver, K.W. ; Miller, A.D.; Carter, S.; Fleisher, T.; Clerici, M.; Shearer, G. Chang, L.; Chiang, Y.; Tolstoshev, P.; Greenblatt, J.J.; Rosenberg, S.A.; Klein, H.; Berger, M.; Mullen, C.A.; Ramsey, W.J.; Muulen, L.; Morgan, R.A.; Anderson, W.A.; *Science*, **1995**, 270, 475.
- (2) Anderson, W.F. *Nature*, **1998**, 392, 25.
- (3) a) Hope, M.J.; Mui, B.; Ansell, S.; Ahkong, Q.F. *Mol.Memb.Biol.*, **1998**, 15, 1; (b) Miller, A.D. *Nature*, **1992**, 357, 244.
- (4) Felgner, P.L.; Gadek, T.R.; Holm, M.; Roman, M.; Wentz, M.; Northrop, J.P.; Ringold, M.; Danielsen, H. *Proc.Natl.Acad.Sci.U.S.A*, **1987**, 84, 7413.
- (5) a) Lasic, D.D.; *Trends Biotechnol.* **1998**, 16, 307; b) Radler, J.O.; Koltover, I.; Jamieson, A.; Salditt, T.; Safinya, C. R. *Langmuir* **1998**, 14, 4272; c) Radler, J.O.; Koltover, I.; Salditt, T.; Safinya, C. R. *Science* **1997**, 275, 810; d) Lasic, D.D.; Strey, H.; Stuart, M.C.A.; Podgornik, R.; Frederik, P.M. *J.Am.Chem.Soc.*, **1997**, 119, 83.
- (6) (a) Sergeev, V.G.; Pyshkina, O.A.; Lezov, A.V.; Melnikov, A.B.; Ryumtsev, E.I.; Zezin, A.B.; Kabanov, V.A. *Langmuir* **1999**, 15, 4434; (b) Pattarkine, M.V.; Ganesh, K.N. *Biochem.Biophys.Res.Comm.* **1999**, 263, 41; (c) Kuhn, P.S.; Barbosa, M.C.; Levin, Y. *Physica A*. **1999**, 269, 278; (d) Tanaka, K.; Okahata, Y. *J.Am.Chem.Soc.*, **1996**, 118, 10679.
- (7) Reimer, D.L.; Zhang, Y.; Kong, S.; Wheeler, J.J.; Graham, R.W.; Bally, M.B. *Biochemistry* **1995**, 34, 12877.
- (8) LePecq, J.B.; Paoletti, C. *J.Mol.Biol.* **1967**, 27, 87.
- (9) Shirley, D.A. *Phys.Rev.B.*, **1972**, 5, 4709.
- (10) Cantor, C.R. and Schimmel, P.R. *Biophysical Chemistry, Part II*, W.H. Freeman, New York (**1980**).
- (11) Cantor, C.R. and Schimmel, P.R. *Biophysical Chemistry, Part III*, W.H. Freeman, New York (**1980**).
- (12) a) Wang, Z.L. *Adv.Mater.*, **1998**, 10, 13; b) Vijaya Sarathy, K.; Kulkarni, G.U.; Rao, C.N.R. *J.Chem.Soc., Chem.Commun.*, **1997**, 537.
- (13) Neault, J.F. ;Tajmir-Riahi, H.A. *J.Phys.Chem.B.*, **1998**, 102, 1610.
- (14) Taillandier, E.; Liquier, J. *Methods in Enzymology*, **1992**, 211, 307.
- (15) a) Patil, V.; Malvankar, R.B. Sastry, M. *Langmuir*, **1999**, 15, 8197; b) Leff, D.V.; Brandt, L. Heath, J.R. *Langmuir*, **1996**, 12, 4723.
- (16) Hostetler, M.J.; Stokes, J.J.; Murray, R.W. *Langmuir*, **1996**, 12, 3605.
- (17) Higashi, N.; Takahashi, M.; Niwa, M. *Langmuir*, **1999**, 15, 111.

CHAPTER VII

CONCLUSIONS

A Concluderary remark on the salient features of the work described in the thesis is mentioned in this chapter.

7.1. SUMMARY OF THE WORK

With the advent of the discovery of the double helix structure of DNA, there has been no looking back in the progress of biomedical research and particularly, in the field of gene therapy. Success of gene therapy is largely dependent on the development of carrier system(s) capable of delivering genes into the target cells. Entrapment of DNA in cationic liposomes has important application in the development of non-viral DNA vectors in gene therapy. The immobilization of DNA in different matrixes and on planar supports is an exciting area of current research.

The objective of this thesis is to immobilize DNA (both single stranded and double stranded) and analogue of DNA (PNA) and look at the hybridization of single stranded DNA within thermally evaporated cationic lipid films and at the air-water interface with Langmuir monolayers. Hybridization and phase transfer of DNA molecules with cationic surfactant at liquid-liquid interface is also discussed in this thesis.

The immobilization of DNA is accomplished by simple immersion of a thermally evaporated octadecylamine film (ODA) in the DNA solution at close to physiological pH. The diffusion of the DNA molecules into the cationic lipid film is dominated by attractive electrostatic interaction between the negatively charged phosphate backbone of the DNA molecules and *in-situ* hybridization of the sequentially immobilized oligonucleotides is characterized by a host of techniques. In the case of double helical DNA structures, the extraction from solution and subsequent entrapment within the lipid matrix occurs without distortion to their double helical structure.

The immobilization analogues of DNA (namely PNA) in different matrixes has attracted wide attraction of researchers around the globe. Our work is based on the use of lipid monolayers and thermally evaporated lipid bilayers. We have demonstrated the sequential entrapment of single stranded DNA and complementary PNA molecules in thermally evaporated fatty amine films and shown evidence for their *in-situ* hybridisation. We also looked at the specificity of base pairing in the DNA-PNA complexes within the ODA matrix. Introduction of a single base pair mismatch in the DNA sequence leads to destabilization of DNA-PNA complex and a measurable lowering of the melting transition temperature. The sequential immobilization and hybridization of DNA-PNA molecules at the air-water interface with Langmuir monolayers is also accomplished. Complementary DNA and PNA sequences may be immobilized at the air-water interface with ODA Langmuir monolayers and furthermore, that facile hybridization of PNA and DNA single strands to yield PNA-DNA hybrids occurs at the interface was demonstrated.

We have also shown the hybridization of the complementary single-stranded DNA molecules at the air-water interface leading to the characteristic double-helical structure. We

have also looked at the effect of salt on the hybridization of single stranded oligonucleotides and pre-formed DNA duplexes at the air-water interface with cationic Langmuir monolayers. The hydrophobization of the DNA molecules is accomplished during vigorous shaking of a biphasic mixture of an aqueous solution of DNA and a hexane solution of the cationic lipid, octadecylamine (ODA). Electrostatic complexation of the DNA molecules with ODA at the liquid-liquid interface renders the DNA hydrophobic and results in their phase transfer into the organic phase. We have also shown that complementary single-stranded DNA molecules in the bulk aqueous phase hybridize to form double helical structures during electrostatic complexation with ODA at the liquid-liquid interface (and are thereafter transferred to the organic phase) under conditions where hybridization does not occur spontaneously in the bulk solution.

7.2. FUTURE PROSPECTS

The interesting aspect of our work is the ease of formation of DNA-LIPID composites and the retention of the double helical structure in the lipid films. The protocol is general and can be extended towards the immobilization of RNA, DNA-triplexes hormones and biological cells. This approach is expected to lead to a better understanding of DNA-lipid and DNA-drug interactions, especially in confined spaces. Application in gene-sequencing protocols may also be envisaged. This approach of complexing DNA molecules with the lipid monolayer in presence of salt is expected to lead to a better understanding of DNA-lipid and DNA-drug interactions, thereby finding applications as antisense/antigene therapeutic agents. The DNA-fatty lipid composite films would serve as model systems for understanding DNA-membrane interactions as well as in the study of DNA-drug/protein interactions. This approach also shows promise for the synthesis of patterned DNA films and consequent application in disease detection and genome sequencing.

Both the methodologies described in the thesis, for the formation of DNA-PNA-lipid films pave the way for use of PNA-DNA conjugates in various diagnostic and therapeutic applications. Furthermore, this approach is expected to lead to a better understanding of PNA-lipid and PNA-drug interactions. The possibility of depositing patterned lipid films and entrapping different PNA sequences in the different elements makes this approach promising for gene sequencing applications.